5-2013

Catalytic Decomposition of Nitrous Monopropellant for Hybrid Motor Ignition

Matthew D. Wilson

CATALYTIC DECOMPOSITION OF NITROUS OXIDE MONOPROPELLANT FOR HYBRID MOTOR IGNITION

by

Matthew Wilson

A thesis submitted in partial fulfillment
of the requirements for the degree

of

MASTER OF SCIENCE

in

Aerospace Engineering

Approved:

Dr. Stephen Whitmore Major Professor	Dr. David Geller Committee Member
Dr. Rees Fullmer Committee Member	Dr. Mark McLellan Vice President for Research and Dean of the School of Graduate Studies

UTAH STATE UNIVERSITY
Logan, Utah

2013

This page intentionally left blank

This page intentionally left blank

ABSTRACT

Catalytic Decomposition of Nitrous Oxide Monopropellant for Hybrid Motor Ignition

by

Matthew Wilson, Master of Science

Utah State University, 2013

Major Professor: Dr. Stephen Whitmore
Department: Mechanical and Aerospace Engineering

Nitrous oxide (N_2O) is an inexpensive and readily available non-toxic rocket motor oxidizer. It is the most commonly used oxidizer for hybrid bipropellant rocket systems, and several bipropellant liquid rocket designs have also used nitrous oxide. In liquid form, N_2O is highly stable, but in vapor form it has the potential to decompose exothermically, releasing up to 1865 Joules per gram of vapor as it dissociates into nitrogen and oxygen. Consequently, it has long been considered as a potential "green" replacement for existing highly toxic and dangerous monopropellants. This project investigates the feasibility of using the nitrous oxide decomposition reaction as a monopropellant energy source for igniting liquid bipropellant and hybrid rockets that already use nitrous oxide as the primary oxidizer. Because nitrous oxide is such a stable propellant, the energy barrier to dissociation is quite high; normal thermal decomposition of the vapor phase does not occur until temperatures are above 800 C. The use of a ruthenium catalyst decreases the activation energy for this reaction to allow rapid decomposition below 400 C. This research investigates the design for a prototype device that channels the energy of dissociation to ignite a laboratory scale hybrid rocket motor.

(129 pages)

PUBLIC ABSTRACT

Catalytic Decomposition of Nitrous Oxide Monopropellant for Hybrid Motor Ignition

by

Matthew Wilson, Master of Science

Utah State University, 2013

Nitrous oxide (N_2O), a commonly-used industrial gas, is also often used as a rocket motor oxidizer. It has been used in both hybrid rocket motors (using a solid fuel and a liquid oxidizer) and liquid rocket engines (using liquid fuel and oxidizer).

As a liquid form, nitrous oxide is highly stable, but in vapor form it can be decomposed, releasing large amounts of heat as it dissociates into nitrogen and oxygen. This project investigates using the energy from decomposing nitrous oxide to ignite a hybrid or liquid rocket. Such a system would be practical in rocket systems that already use nitrous oxide as the oxidizer.

Because nitrous oxide is so stable in liquid form, the necessary energy to begin the decomposition process is very high; without any other influences the decomposition of vapor nitrous oxide cannot occur until temperatures are above 800 C. However, a catalytic material can decrease the necessary energy for decomposition, and can begin nitrous oxide decomposition at temperatures near 400 C.

This research looks at the possibility of using a catalytic material made from ruthenium deposited on aluminum oxide to decompose nitrous oxide, and then to use the hot nitrogen and oxygen to ignite a hybrid rocket motor.

(129 pages)

CONTENTS

LIST OF TABLES

LIST OF FIGURES

NOMENCLATURE

$\Delta h_{f,N_2O}$ Heat of formation for nitrous oxide

$\Delta h_{f,N_2}$ Heat of formation for nitrogen

$\Delta h_{f,O_2}$ Heat of formation for oxygen

$\Delta H_{N_2/H_2}$ Heat of reaction for the nitrogen/hydrogen decomposition pathway of hydrazine

$\Delta H_{N_2/O_2}$ Heat of reaction for the nitrogen/oxygen decomposition pathway of nitrous oxide

$\Delta H_{NH_3/N_2}$ Heat of reaction for the ammonia/nitrogen decomposition pathway of hydrazine

$\Delta H_{NO/N_2}$ Heat of reaction for the nitric oxide/nitrogen decomposition pathway of nitrous oxide

$\dot{m}$ Mass flow rate through igniter

ρ Density of the working fluid

ρ_1 Density of the working fluid at orifice inlet

ρ_2 Density of the working fluid at orifice exit

τ_b Bubble formation time constant

τ_r Fluid residence time constant

A_t Orifice area for mass flux calculations

C_d Orifice subsonic discharge coefficient

C_d Discharge coefficient

E_a Activation energy for the decomposition reaction

$f_{N_2O}(T_e, P_e)$ Equation of state for nitrous oxide, as an explicit function of temperature and pressure

$f_{N_2}(T_e, P_e)$ Equation of state for nitrogen, as an explicit function of temperature and pressure

$f_{O_2}(T_e, P_e)$ Equation of state for nitrous oxide, as an explicit function of temperature and pressure

G_{HEM} Mass flux from homogenous equilibrium model

G_{NHNE} Non-homogeneous, non-equilbrium mass flux

G_{SPI} Mass flux from incompressible model

h_1	Enthalpy of the working fluid at orifice inlet
h_2	Enthalpy of the working fluid at orifice exit
h_{exit}	Specific enthalpy of igniter exit products
h_{STP}	Specific enthalpy of igniter exit products at standard temperature and pressure
h_{e,N_2O}	Specific enthalpy of nitrous oxide in the igniter exit products
h_{e,N_2}	Specific enthalpy of nitrogen in the igniter exit products
h_{e,O_2}	Specific enthalpy of oxygen in the igniter exit products
k	Non-equilibrium parameter
M_{N_2O}	Molecular weight of nitrous oxide
M_{N_2}	Molecular weight of atomic nitrogen
M_{O_2}	Molecular weight of atomic oxygen
P_1	Pressure of the working fluid at orifice inlet
P_2	Pressure of the working fluid at orifice exit
P_e	Decomposition reactor exit pressure
P_v	Vapor pressure of the working fluid, used in orifice flow calculations
T	Temperature of the working fluid
T_e	Temperature of igniter exit products
W_E	Power output of Estes 1/2A3-4T black powder engines
W_{N_2O}	Power output of catalytic nitrous oxide igniter
w_{N_2O}	Mass fraction of nitrous oxide in the igniter exit products
w_{N_2}	Mass fraction of nitrogen in the igniter exit products
w_{O_2}	Mass fraction of oxygen in the igniter exit products
y	Mass fraction of the nitrous oxide that has been decomposed

CHAPTER 1
INTRODUCTION

1.1 Research Motivation

The recent emergence of commercial spaceflight, both for space tourism and satellite communications, has renewed interest in more cost-effective space propulsion methods. A recent study (2003) by the European Space Agency European Space Research and Technology Center (ESA/ESTEC) has identified two essential elements to achieving low cost space access:

1. Reduced production, operational, and transport costs due to lower propellant toxicity and explosion hazards; and

2. Reduced costs due to an overall reduction in subsystems complexity and overall systems interface complexity. [1, 2]

This research focuses on a reduced hazard, lowered complexity ignition subsystem for an upper stage booster system, emphasizing a focus on the key design elements identified in the 2003 ESA/ESTEC study.

Incorporating the first ESA/ESTEC design element – a reduction in propellant hazard and toxicity – into a booster stage comes at significant cost. As the propellant materials become less energetic, they also become increasingly difficult to ignite. The proposed ignition method includes the ESA/ESTEC design elements, while providing reusable and "on demand" ignition. On demand ignition becomes critically important for a variety of propulsion system applications, primarily clustered rockets where an unfired thruster can cause uncontrollable disturbances, upper stage boosters needing in-flight ignition and reignition, and space propulsion where propellants can be cold-soaked or superchilled.

Current propellant combustion ignition is achieved by one of five methods.

- One or multiple pyrotechnic charges, also known as "squib" igniters, can be used for single start ignition. Pyrotechnic igniters are most frequently used to ignite solid-propellant rocket motors. As well as being unsuitable for multiple ignitions, squib igniters are also susceptible to the Hazards of Electromagnetic Radiation to Ordnance (HERO) [3], and large pyrotechnic igniters present a significant operations hazard.

- Plasma torches ignite the combustion reactants with a directed flow of plasma, and have been effectively used for gas turbine engines and supersonic combustion ramjets for ground test articles [4]. However, these devices are bulky and require a significant power input, and are generally ill-suited for space-propulsion applications. Although plasma torches provide a very high temperature source, they produce a low mass flow and the total overall available enthalpy is low. SpaceX originally considered a torch-igniter for the Merlin Engine, but down-selected to pyrophoric ignition instead due to torch-ignition complexity and reduced complexity [5].

- Pyrophoric ignition features hypergolic bi-propellants like Triethylaluminum-Triethylborane (TEA-TEB). Historically, most LOX/RP bi-propellant engines, such as the Saturn V F-1, have used TEA-TEB as the ignition source. Pyrophoric ignition does offer very simple design solutions and can be used for multiple restarts, but this class of propellants presents the extreme disadvantage of being highly toxic and difficult to work with during ground processing; all commonly used pyrophoric fluids spontaneously explode upon contact with even a low oxygen environment.

- Electric spark plugs with bi-propellant oxidizer and fuel injectors is a common method of ignition for bi-propellant engines, including the J-2 and RL10A-4-2 engines [6, 7]. However, like bi-propellant engines themselves, spark igniters are complex and require precise tuning for reliable performance. Poorly tuned bipropellant igniters can lead to motor "hard starts" with the potential to produce a significant initial pressure surge and injector back flow.

- Finally, catalytically dissociated monopropellants are often used as self-starters for monopropellant engines. Hydrazine is by far the most prevalent propellant in this category, and like pyrophoric ignition, simple designs featuring multiple restarts have reached a high state of technology readiness. Multiple design have been successfully flown on spacecraft. Like pyrophoric propellants, hydrazine is extremely toxic, and requires great care in ground processing. Although procedures are in place to allow hydrazine to be managed within tightly controlled government-operated test ranges, environmental restrictions associated with toxic propellant transport, storage, servicing, and clean up of accidental releases are rapidly making the use of this hazardous propellant less desirable. Consequently, both government and commercial organizations are increasingly willing to accept a slightly reduced system performance in exchange for a significant increase in overall system safety and "environemtnal friendliness." Thus the development of safer alternatives to hydrazine is being hotly pursued in the aerospace community.

1.2 Nitrous Oxide

This research investigates the possibility of using nitrous oxide (N_2O) as an alternative to current ignition methods, specifically phyrophoric ignition fluids, or toxic monopropellants such as hydrazine. Nitrous oxide is a relatively inexpensive and widely available green propellant, and is the oxidizer of choice for most low-cost hybrid and liquid propulsion systems. In liquid form, it is classified as non-explosive and non-flammable by the U.S. Occupational Safety and Health Administration (OSHA) [8]. Although it is impossible to force a dissociation reaction of nitrous oxide in its liquid form, in vapor form it can be dissociated in a highly exothermic reaction, producing as much as $1865\,\mathrm{J/g}$ [9, 10]. Because of this highly exothermic decomposition, N_2O has been considered as a potential green monopropellant alternative to the highly toxic hydrazine monopropellant [11]. If such a nitrous oxide-based monopropellant system can be designed and shown to be effective, then it offers an ignition method with significantly reduced mass, volume, and complexity for those systems that already use N_2O as the primary oxidizer. For bipropellant systems that

would traditionally use a sparker ignition system, a nitrous oxide monopropellant igniter would elimitate the fuel flow path, and reduce the igniter complexity to that of a monopropellant feed system. As an alternative to current monopropellant systems that use fluids such as TEA-TEB or hydrazine, N_2O has the distinct advantage of being significantly less hazardous and more environmentally friendly.

An additional benefit of a nitrous oxide monopropellant is the high level of storability: this propellant can be loaded into the propulsion system long before the engine is ever fired. This makes N_2O ideal for in-space propulsion, where the system must remain inert and viable for extended periods of time. Nitrous oxide also has a very high vapor pressure near room temperature, above 5000 kPa at 20 C. Although not generally desirable, this high vapor pressure makes simple self-pressurizing systems possible.

However, nitrous oxide decomposition does have several significant drawbacks:

- Exhaust gas temperatures can reach as high as 1600 C, compared to the typical 1100 C of hydrazine decomposition. Not only does this higher temperature require more exotic case materials to withstand the heat, but it dramatically reduces the number of possible catalysts available for nitrous oxide decomposition. Many catalysts that would work for hydrazine simply vaporize away in the hotter environment, making catalyst selection a significant issue.

- The exothermic decomposition of nitrous oxide produces molecular nitrogen, molecular oxygen, and nitric oxide (NO); these molecules have a high molecular weight, and this results in a significantly lower specific impuse when compared to hydrazine. Even with the 500 C higher dissociation temperature of N_2O, the specific impulse of a nitrous oxide dissociation monopropellant is less than that of hydrazine - 180 s for nitrous oxide, compared to the 220 s for hydrazine. Thus with this significantly lower performance, and the recent introduction of ionic liquid propellants such as Ammonium Dinitramide (ADN) [12, 13] and Hydroxylamine Nitrate (HAN) [14, 15] that offer significantly higher I_{SP}'s around 230 s, nitrous oxide decomposition only becomes practical for bipropellant and hybrid systems that already use N_2O as the

primary oxidizer. The reduced monopropellant performance is much less significant for a system employing N_2O decomposition for ignition, as the exhaust gases are fed directly into the larger engine to initiate combustion and constitute a minor portion fo the overall propellant consumption.

- Perhaps the most significant difficulty with nitrous oxide decomposition is the high activation energy (E_a). The high stability of N_2O that gives it excellent safety and storage properties also mandates a high activation energy for the decomposition reaction, 5700 J/g for thermal decomposition [16,17]. This high activation energy requires the N_2O vapor to be heated to a minimum of 800 C to initiate thermal decomposition, with even higher temperatures required for rapid decomposition. Elevated pressures can decrease this temperature, but feasible line pressures dictate a minimum temperature of at least 600 C. Aside from the obvious difficulties associated with heating the system to 600 C or above by an external energy source, thermal decomposition strongly favors the endothermic decomposition reaction

$$N_2O \rightarrow NO + {}^1/_2N_2 \qquad \Delta H_{NO/N_2} = +19.17^{kJ}/_{kg} \tag{1.1}$$

as opposed to the desired exothermic decomposition reaction

$$N_2O \rightarrow N_2 + {}^1/_2O_2 \qquad \Delta H_{N_2/O_2} = -1865^{kJ}/_{kg} \tag{1.2}$$

This is illustrated in Fig. 1.1.

- Catalytic decomposition attempts to decrease the necessary activation energy for the desired exothermic reaction by passing the gaseous nitrous oxide over a carrier material impregnated with transition metals, such as Ir, Ru, Rh, Ni, Zr, Cu, or Co. By using catalytic decomposition, the reaction temperature of nitrous oxide can be decreased to as low as 250 C. This reaction pathway still requires preaheating the reaction chamber, but 250 C can be achieved more easily than the significantly higher temperatures required for thermal decomposition. In addition, catalytic decomposition strongly

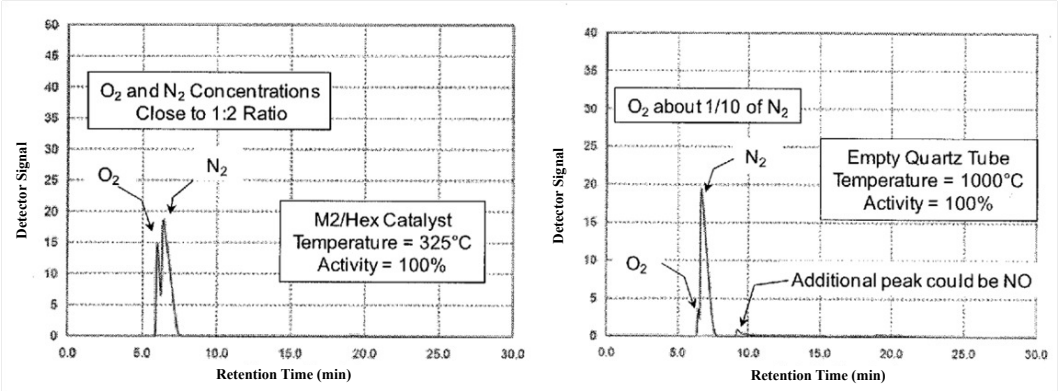

(a) (b)

Fig. 1.1: Representative (a) catalytic and (b) thermal product compositions.

favors the exothermic N_2–O_2 reaction, improving the sustainability and efficiency of the reaction. For these reasons, this research investigated catalytic methods for reducing E_a so that the dissociation reaction can be triggered at the significantly lower temperature and require a significantly lower external energy input.

1.3 Hybrid Motor Ignition

At Utah State University (USU), several graduate students have been involved with the construction, assembly, and firing of hybrid motors for several years. Due to their low cost and excellent safety aspects, hybrid motors are ideal for undergraduate and graduate level university research. In contrast to traditional solid- or liquid-propelled rocket systems, hybrid rockets store the liquid or gaseous oxidizer separately from the solid fuel grain and present little-to-no risk of explosion during storage or transport. Hybrid propellants become energetic only within the combustion chamber. As a testament to the benign nature of hybrids, a plexiglass and gaseous oxygen hybrid demonstration model design developed by the United Technology Center has been fired over 50,000 times by various organizations without ever experiencing a single hazardous failure [18].

To date the vast majority of hybrid rocket motors, including those tested at USU,

are ignited by small pyrotechnic charges. Although reliable and inexpensive, pyrotechnic charges are one-shot devices, and achieving multiple fuel grain "restarts" require hours of motor disassembly and reassembly to replace the pyrotechnic grains. In-situ restarts are not possible. Development of an alternative ignition method capable of restarting hybrid motors without disassembly is of great interest to the hybrid rocket community.

This research will focus on the design, development, and testing of a monopropellant nitrous oxide igniter. The igniter was designed for use on an existing 98 mm hybrid rocket motor being used at USU, with almost no modification to the motor design. The successful ignition of this motor desmostrates the feasibility of the monopropellant N_2O igniter concept. Details of the hybrid motor and igniter design are presented in sections 4.2 and 5.4.

CHAPTER 2
BACKGROUND AND PREVIOUS WORK

2.1 Rocket System Classifications

There are four types of chemically propelled rocket engines: monopropellant, liquid bipropellant, solid, and hybrid. Figure 2.1 shows these main engine types. Monopropellant engines either employ a cold gas in a "blow down" system that expels cold gas to provide impulse, or employ a dissociable liquid like hydrazine or hydrogen peroxide. Bipropellant liquid engines mix and burn highly volatile oxidizer and fuel components in the combustion chamber before being expelled through the nozzle. Solid rocket motors use a propellant grain that binds both the oxidizer and fuel in a hydrocarbon binder, and typically have an internal volume that becomes the combustion chamber. A hybrid rocket motor, sometimes referred to as a solid-liquid rocket motor, stores the liquid or gaseous oxidizer separately from the solid fuel surrounding the combustion chamber. A comparison of some of the advantages and disadvantages of each rocket type is shown in Table 2.1.

Table 2.1: Comparison of properties between chemical propulsion types.

Factor	Monopropellant	Bipropellant	Solid	Hybrid
Throttle and Commanded Shutdown Capability	Yes	Yes	No	Yes
Possibly Non-toxic Combustion Exhaust	Yes	Yes	No	Yes
Transport, Storage and Handling Properties	Fair	Fair	Poor	Good
Manufacturing Cost	Moderate–High	Moderate–High	Moderate	Low
Easily Scalable	No	No	Yes	Yes
Specific Impulse (I_{sp})	Low	High	Moderate	Low
Propellant Safety	Varies	Varies	Poor	Excellent

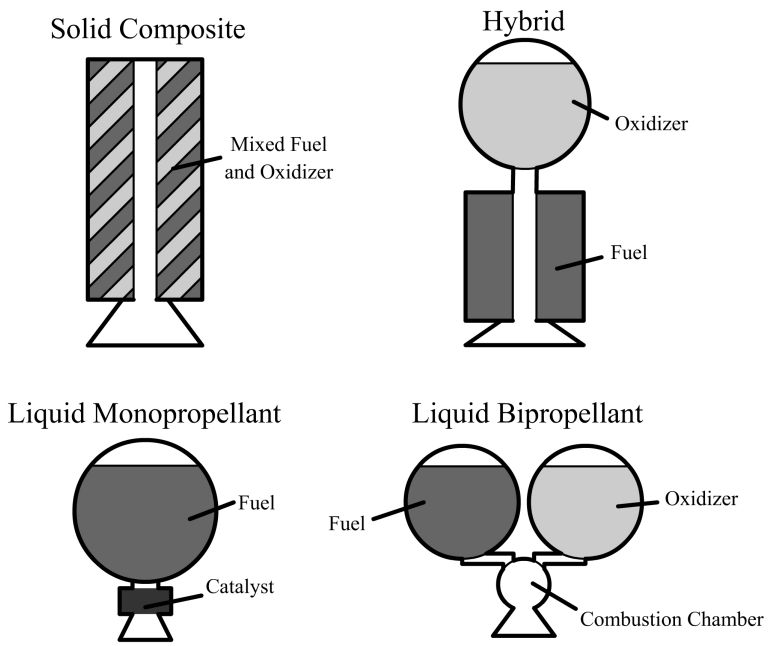

Fig. 2.1: Types of chemical rocket engines.

2.1.1 Monopropellant Propulsion Systems

Monopropellant rockets are most frequently used for space propulsion or reaction control applications where simplicity and reliability are more important than performance. The simplest style of monopropellant thruster employs a compressed gas with a pressure regulator and a control valve. Cold gas thrusters generally have low I_{sp} – less than 70 s– and cannot provide the ΔV for orbital maneuvering or launch systems, and consequently are only used for attitude control applications.

"Warm gas" monopropellant rockets offer a significant improvement in performance when compared to cold-gas systems, and still retains very simple design features. Hydrazine (N_2H_4) is by far the most commonly used monopropellant for primary spacecraft propulsion systems and attitude control thrusters [19] [20]. Hydrazine thrusters are simple, versatile, and dependable, although hydrazine has a low vapor pressure and requires a "top pressurant" for rocketry use. Figure 2.2 shows a typical arrangement with a pressurant tank, propellant tank, electric solenoid or pneumatic valve, catalyst bed, post-combustion chamber, and exit

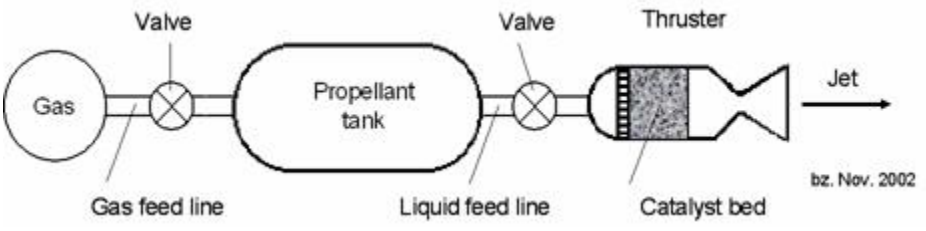

Fig. 2.2: Key components of a liquid bipropellant engine.

nozzle.

The industry standard catalyst material is Aerojet S-405, previously known as Shell-405. Although hydrazine decomposition using the S-405 catalyst can be performed with no additional heat input to the catalyst, typical designs pre-heat the catalyst bed to insure a more reliable ignition and a consistent burn profile. In preheated configurations, a vacuum specific impulse near 240 s can be achieved, depending on the level of ammonia decomposition [19]. Hydrazine is attractive as a monopropellant because of its high hydrogen content; when passed through the S-405 catalyst the decomposition produces ammonia (NH_3), nitrogen (N_2), and hydrogen (H_2) gas according to the simple reaction models

$$3N_2H_4 \rightarrow 4NH_3 + N_2 \qquad \Delta H_{NH_3/N_2} = -15.2^{\mathrm{kJ}}/_{\mathrm{kg}} \tag{2.1}$$

$$4NH_3 \rightarrow 2N_2 + 6H_2 \qquad \Delta H_{N_2/H_2} = +8.35^{\mathrm{kJ}}/_{\mathrm{kg}} \tag{2.2}$$

The primary reaction, Eq. 2.1, is highly exothermic and produces up to 15.2 kJ/kg of propellant dissociated. The associated gaseous products can reach temperatures of approximately 1365 C. At these temperatures the ammonia gas product is unstable and dissociates through equation 2.2 to produce nitrogen and hydrogen gas. This secondary reaction is endothermic and removes approximately 8.35 kJ/kg of heat from the overall reaction. The catalyst structure also affects the percentage of the NH_3 that is dissociated in the reaction. In a well-tuned combustion chamber, a total reaction with approximately $35 - 50\%$ am-

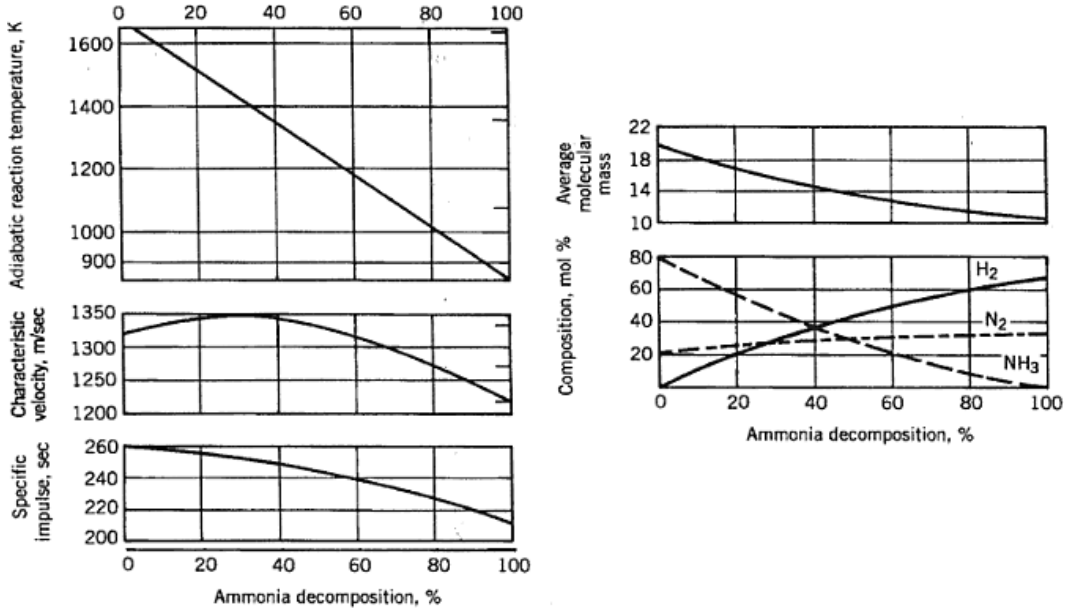

Fig. 2.3: Hydrazine performace as a function of ammonia decomposition fraction.

monia dissociation is possible. Figure 2.3 shows the predicted performance of a hydrazine thruster as a function of ammonia dissociation. The graph shown specific impulse values for an infinitely expanded nozzle in a vacuum; real nozzles can achieve specific impulses approximately $10 - 15\%$ lower than the plotted values, approximately 220 s for vacuum conditions.

Unfortunately, hydrazine is a powerful reducing agent that poses serious environmental and health concerns. Hydrazine is extremely destructive to living tissues, and is a known carcinogen. Exposure produces a variety of adverse systemic effects including damage to liver, kidneys, nervous system, and red blood cells [21]. In addition to these biological and toxicological impacts, hydrazine presents a level of environmental danger for the spacecraft and launch vehicle. Liquid hydrazine is capable of detonation if heated rapidly. Vapor and solid hydrazine are both capable of detonation given extreme shock, such as the nearby explosion of a linear charge or blasting cap. Linear charges and explosive bolts are common in large launch vehicles. Solid hydrazine buildup, possibly augmented by frozen oxygen, detonated by a linear charge in an adapter ring is suspected in the failure of a Atlas-Centaur

upper stage [22].

Most significantly, hydrazine has a high vapor pressure at room temperature, approximately 1000 kPa (145 psia). For many applications a high storage vapor pressure is a good propellant feature because it offers the option of delivering the propellant to the combustion chamber using only its natural vapor pressure and offers a potential for further reduction of the system simplicity [23]. Unfortunately, because of this higher vapor pressure, hydrazine fumes significantly at room temperature and presents a high risk as a respiratory hazard. All hydrazine servicing operations must be performed with the use of Self Contained Atmospheric Protective Ensemble (SCAPE) suits.

Although procedures are in place to allow toxic propellants to be managed safely on tightly controlled military and NASA-owned flight experiments, the toxicity and explosion potential requires extreme handling precautions. Increasingly, infrastructure requirements associated with toxic propellant transport, storage, servicing, and clean up of accidental releases are becoming cost prohibitive. As space flight operations continue to shift from government–run organizations to private companies and universities operating away from government-owned test reservations, servicing payloads requiring hydrazine as a propellant becomes operationally infeasible. The necessity of extreme handling precautions makes hydrazine unfavorable for secondary payloads.

Following the recommendations from the ESA/ESTEC study, the European Space Agency and the US Department of Defense (DoD) have recently begun development of less toxic, less hazardous replacement options for hydrazine. A useful monopropellant replacement for hydrazine must be chemically and thermally stable, for good storage properties, but must easily decompose and have good combustion properties. Cryogenic or high freezing point propellants requiring temperature control are not appropriate space propulsion applications. Although mass-specific impulse is important, volume-specific impulse (density impulse) is an even more important consideration, and a high propellant storage density is preferred. Most importantly the propellant must be sufficiently stable to allow technicians and engineers to safely work with the propellant.

Hydrogen Peroxide (H_2O_2) is sometimes used as an oxidizing agent for bipropellant systems, and is currently being proposed as a "less toxic" alternative to hydrazine [24]. Unfortunately, H_2O_2 offers a significantly lower overall performance than hydrazine with vacuum I_{sp} slightly below 170 s. More importantly propulsion-grade solutions of H_2O_2 have an even higher room temperature vapor pressure than hydrazine, approximately 1200 kPa (175 psia). Thus, while not as toxic as hydrazine, peroxide still presents a significant respiratory hazard. Propellant grade peroxide solutions are also unstable and present a moderate explosion risk [25]. The reduced performance, coupled with the still significant objective and health hazards, do not favor hydrogen peroxide as a "green" alternative to hydrazine.

For most of the past decade the US Department of Defense (DoD) and the Swedish Space Corporation (SSC) subsidiary ECological Advanced Propulsion Systems (ECAPS) have been pursuing green-propellant alternatives based on aqueous solutions of ionic liquids. Ionic liquids are water-soluble substances that normally exist in solid form at room temperature, but melt below the boiling point of water. When dissolved in water these materials exhibit very strong ion-to-ion interactions. Two of the currently most promising ionic liquid replacement options for hydrazine are Ammonium Dinitramide (ADN) [12, 13] and hydroxyl-ammonium nitrate salt NH_3OHNO_3 (HAN) [14, 15, 26].

ADN melts at approximately $90-93$ C, and HAN melts at approximately $44-45$ C. In solid form both ADN and HAN are highly energetic salts with both reducing and oxidizing components, and as such the solid materials are unstable and potentially explosive. Thus, for propellant applications both ADN and HAN are used as concentrated aqueous solutions to order to limit the explosive potential.

In typical applications, a fuel component such as methanol is added to the solution to increase the propellant performance. Since these HAN and ADN solutions include both oxidizer and fuel components, they are more correctly referred to as "propellant blends" than as monopropellants. Because these propellants are mixed in aqueous solutions, they possess a very low vapor pressure at room temperature, and do not present a shock or respiratory hazard, allowing simpler handling procedures than those for hydrazine. Thus servicing

operations can be performed without the use of SCAPE suits. This low vapor pressure is one of the primary reasons that these propellants are considered to be significantly less hazardous than either hydrazine or peroxide.

The Swedish Space Corporation and the Swedish Defence Research Organization developed the ADN liquid propellant blend. The blend is composed of an ionic aqueous solution (10% water) of ADN (65%) with methanol (20%) as a fuel, and ammonia (5%) as the solution stabilizer. The High Performance Green Propellant (HPGP) is marketed under the product name LMP-103S by ECAPS. Moog Space and Defense Group and Alliant Techsystems (ATK) have partnered with ECAPS to make LMP-103S available to the US spacecraft market [27]. LMP-103S propellant blend is catalytically decomposed to produce water vapor and approximately2000 $^{\mathrm{kJ}}/_{\mathrm{kg}}$ of heat.

In August 2011, ECAPS announced the results of a year-long series of in-space tests of a 1 N thruster implemented on the Prisma spacecraft platform, comparing their HPGP to hydrazine. The comparisons claimed that HPGP delivered equivalent–to-superior performance. ECAPS has claimed that their 1 N thruster has achieved a TRL level of 7.0 following this spaceflight demonstration [28–30]. The opportunity to fly the HPGP system served as means to flight demonstrate the new propulsion technology, but also served as a demonstration of how to incorporate system level aspects to the spacecraft level design. Implementation of the 1 N HPGP propulsion system solved issues with respect to five main system level interfaces namely, thermal, power, shock, vibration, and plume effects. ECAPS reported a mean in-space I_{sp} exceeding 220 s for the Prisma flight experiment.

The Naval Ordinance Station, Indian Head, MD developed a number of HAN-based liquid monopropellants for use in artillery guns for the US Army [31]. Three of these formulations were designated as LP1846, LP1845 and LP1898 where concentrated HAN is mixed as an aqueous solution with tri-ethanol-ammonium nitrate (TEAN, $(OHCH_2CH_2)_3NHNO_3$) or diethyl-hydroxyl-ammonium nitrate (DEHAN, $(CH_3CH_2)_2NHOHNO_3$) [26, 32–34]. In these formulations HAN serves as the oxidizing agent, the TEAN/DEHAN components act as fuel, and water is the solvent and buffering agent. The fuel-rich components are

added in the blend to achieve higher energy release and higher flame temperature. Of these propellant formulations LP1846 was the most highly developed and tested. Aerojet Corporation of Redmond Washington (Formerly the PRIMEX Corporation) conducted alternative development activities where the fuel components of LP1846 were replaced with Glycine ($C_2H_5NO_2$) [35]. The Aerojet HAN-glycine (HANGLY26) formulation emphasized compatibility with existing hydrazine (S-405®) catalyst beds and was design to have a low combustion temperature, less than 1100 C. HANGLY26 decomposes with an exhaust temperature similar to hydrazine, but produces exhaust products with a significantly higher molecular weight, thus HANGLY26 has a lower I_{sp} than hydrazine (190 s). Because of its significantly greater density, HANGLY26 does have greater volumetric impulse efficiency than hydrazine. In this formulation sufficient water was added to keep the combustion temperature below 1100 C. This approach was selected to allow an up-front focus on propellant and thruster development rather than a lengthy catalyst development program [36]. Higher performing propellants that replace the glycine fuel component with methanol are under development. One formulation, designated as HAN 269MEO, has achieved a vacuum I_{sp} near 270 s. Catalytic ignition remains the method of choice for both ADN and HAN-based propellant formulations. Unfortunately, because of the high water content, both ADN and HAN-based propellants stored as aqueous ionic liquid solutions are notoriously hard to ignite. Development of a room-temperature catalyst capable of withstanding combustion temperatures exceeding 1300 C remains a major challenge, and unfortunately, the "holy grail" of a durable, highly active catalyst that can decompose water/ionic liquid/propellant blends at low temperatures, but can survive at high temperatures in an acidic and oxidizing environment has yet to be achieved.

2.1.2 Liquid Bipropellant Propulsion Systems

Although bipropellant liquid engines have sometimes been used for spacecraft propulsion and attitude control systems, liquid systems are primarily used in launch vehicle first and second stages due to their excellent I_{sp}'s (the space shuttle main engines can achieve 452 s) and very high thrust-to-weight ratios. For launch vehicles, where high power and high

efficiency are imperative, liquid bipropellant engines are the ideal solution, and will likely remain so for the forseeable future. Liquid systems also have the ability for reliable start, stop, and restart, and have the ability to throttle, making them ideal for orbital transfer operations. Liquid rocket engines are the core of many launch vehicle systems, including the five F-1 engines of the Saturn V first stage, the three Space Shuttle Main Engines (SSMEs), and the nine Merlin engines of the Falcon 9.

Although a variety of oxidizer/fuel combinations have been used, the most commonly used liquid propellant combinations are liquid oxygen / liquid hydrogen (LOX/LH2) and liquid oxygen/ kerosene (LOX/RP-1). Hypergolic combinations, such as monomethylhydrazine (MMH) and nitrogen tetroxide (N_2O_4) are frequently used in reaction control systems.

Although simple in concept – with two liquid propellants flowing into the combustion chamber and igniting – in reality bipropellant engines are by far the most complex chemical combustion engines available. Figure 2.4 shows two idealized liquid bipropellant engines, a pump-fed system and a pressure-fed system. Both designs have oxidizer and fuel tanks and valves, a combustion chamber, and a convergent-divergent nozzle. The pump-fed system includes a gas generator and turbine to power the pumps, whereas the pressure fed system has top-pressurization tanks for both fuel and oxidizer.

As an example of the complexity of a real bipropellant engine, Figure 2.5 shows the plumbing schematic of the J-2 engine. Key points of complexity are the oxidizer and fuel turbopumps (cryogenic turbopumps for liquid oxygen or liquid hydrogen), the gas generation cycle (for startup and turbopump power), and the heat exchangers, both on the bell of the nozzle and the oxidizer turbopump. Because of this complexity, and the use of fuels that are either cryogenic (around 20 K for LH2) or extremely toxic, liquid rocket engines are expensive to operate, with high design, fabrication, and operational costs [37] [38].

2.1.3 Solid Propellant Propulsion Systems

Solid propellant motors are one of the most conceptually simple forms of rocket engines, being comprised of a single solid containing mixed oxidizer and fuel. This solid composite

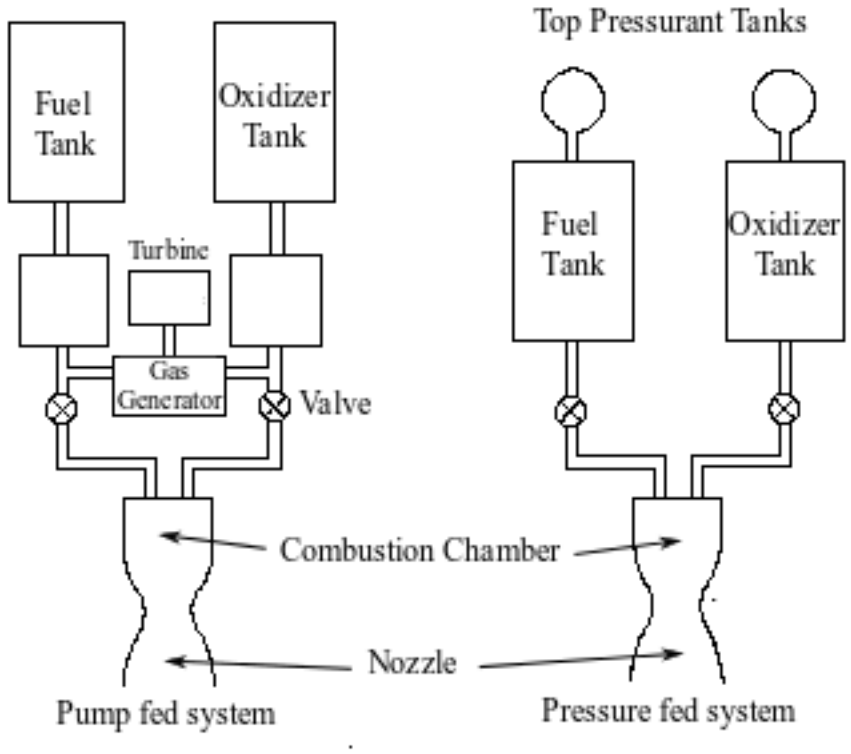

Fig. 2.4: Key components of a liquid bipropellant engine.

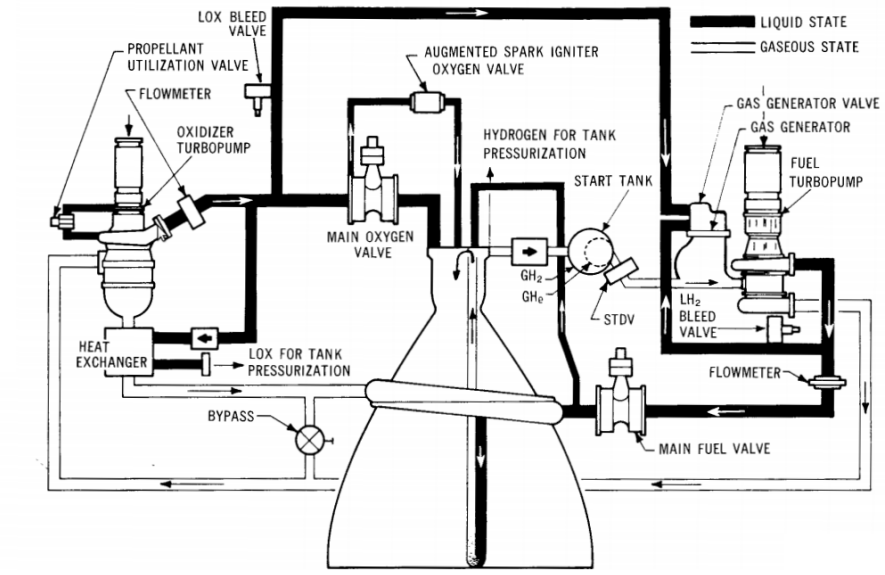

Fig. 2.5: Functional schematic of the Saturn-IVB J-2 engine.

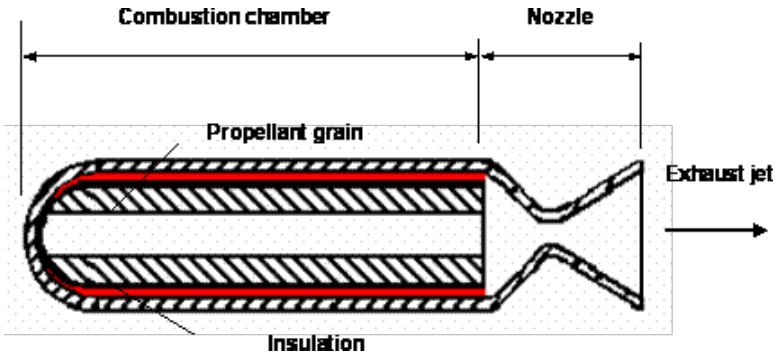

Fig. 2.6: Schematic of a solid rocket motor.

is encased within a pressure vessel, with some form of internal port geometry functioning as the combustion chamber, and a sonic nozzle as the product exit. Figure 2.6 shows the main components of a solid rocket motor, including the grain, combustion chamber, and nozzle.

Solid rocket motors are the oldest types of rocket engines, with black powder rockets being used in fireworks and military applications as far back as the 13th century. Although modern low-power hobby rockets frequently use black powder, larger rockets typically use a more energetic mixture, such as ammonium perchlorate composite propellant (APCP). APCP is a castable material, comprised of an elastomer binder (which also functions as the fuel) with various additives mixed in. Additives are usually ammonium perchlorate (AP), powdered aluminum (AL), and various burn catalysts.

Although not as efficient as liquid engines, solid propellant motors are often used in launch vehicles due to their high power; many LVs are either augmented by solids, or have the option of using "strap-on" solids to increase payload capacity. Solid rocket motors can provide very high levels of thrust for the initial liftoff; the space shuttle Solid Rocket Boosters (SRBs) each provided 2.8 Mlbf at space shuttle launch, or about 83% of the total liftoff thrust [39].

Solid motors are one-shot use; once lit solid rocket motors cannot be throttled or shut down until all of the fuel has been consumed. However, a solid motor can be designed to have a varying thrust profile by carefully shaping the initial fuel grain combustion port,

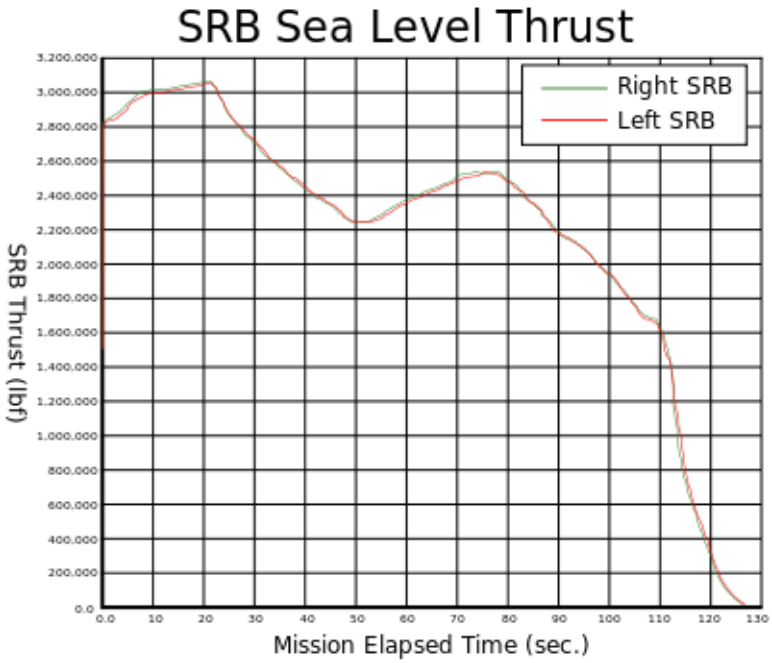

Fig. 2.7: Thrust profile of the Space Shuttle Solid Rocket Boosters.

and this technique is used on all launch vehicle motors to provide an optimized thrust profile for the LV. Figure 2.7 shows the tailored thrust profile of the space shuttle SRBs, demonstrating the high initial thrust, the throttle down for the maximum dynamic pressure region, followed by the ramp up before burnout.

Because the fuel and oxidizer are stored in a single solid, waiting for a small amount of activation energy to start the uncontrollable combustion process, solid rocket motors present a significant objective hazard

during storage, transport, and servicing. Solid rockets are particularly susceptible to stray electrical currents and radiation, known as hazards of electromagnetic radiation to ordinance (HERO) [3].

2.1.4 Hybrid Propulsion Systems

Hybrid motors are the most recently developed variant of the chemical propulsion types, and a growing number of companies are designing, fabricating, and testing hybrid rocket

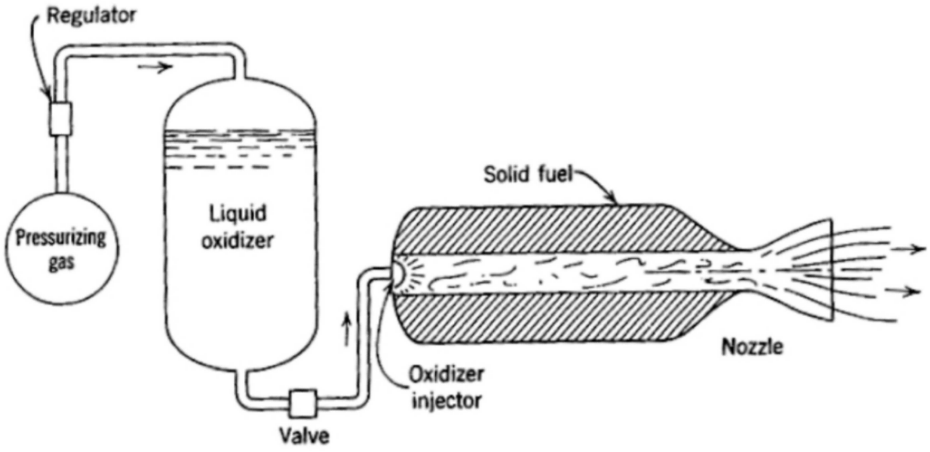

Fig. 2.8: Hybrid rocket motor configuration.

systems. Figure 2.8 shows a typical hybrid motor configuration, including the pressurization and oxidizer tanks, fuel grain and combustion port, and the nozzle. As with the solid, the combustion chamber is a port within a solid fuel grain, although the oxidizer is injected at the forward end instead of being contained within the grain. Hybrids can also use a gaseous oxidizer, eliminating the need for a second pressurization tank. However due to the higher volumetric efficiency of using a liquid-phase oxidizer, this gaseous design is atypical.

In a hybrid rocket motor, liquid or gaseous oxidizer is stored in a tank separated by a valve from the solid fuel residing in the combustion chamber. The solid fuel also typically provides insulation for the walls of the combustion chamber. This arrangement segregates the fuel from the oxidizer until the valve is opened, and the reaction rate of the solid fuel and oxidizer is limited by oxidizer flow and the convection-based pyrolysis of the solid fuel grain. This is markedly different from the behavior of liquid bipropellant engines where the reaction rate is limited by flow rate, diffusion, and kinetics, or the behavior of solid rocket motors, where the reaction rate is limited by kinetics and heat transfer. Also unlike solid-propelled rockets, where fuel grain flaws and age-induced cracks present a significant safety issue, hybrid rockets exhibit a relative insusceptibility to grain flaws.

In contrast to traditional solid or liquid motors, hybrid rocket motors separate the liquid oxidizer from the solid fuel and present a low risk of explosion while burning. The vast majority of hybrid rocket propellants are inherently safe to store, transport, and service [40]. While hybrid systems based upon low-risk propellants generally deliver lower I_{sp} than conventional bi-propellant liquid rockets and offer lower volumetric efficiency than solid rockets of the same thrust level, the inherent design safety can potentially lead to an overall reduction in system operating costs.

Other advantages of hybrid rockets when compared to solid rocket systems include the capability for in-flight restart, throttling, easy ground handling, and relative insusceptibility to grain flaws. Hybrid systems offer greater performance than cold-gas, monopropellant, or solid rocket systems and can have a higher density-specific impulse than liquid bipropellant engines [20].

Despite the advantages listed above, hybrid motor systems are not without technical difficulties and operational shortcomings. Hybrid motors have traditionally suffered from three primary deficiencies:

1. Hybrid propellant systems have lower I_{sp} than conventional bi-propellant liquid rockets and lower volumetric efficiency than solid rockets of the comparable thrust levels

2. Hybrid systems tend to have low fuel regession rates, resulting in typical designs having a significantly long aspect ratio, where the motor length is often 10 times the major cross section diameter.

3. Because of the previously mentioned high N_2O activation energy, hybrid rocket motors that employ nitrous oxide as the oxidizer are notoriously hard to ignite. This naturally leads to the popular choice of pyrotechnic igniters, which provide an excess of energy to begin the combustion process. Sample ignition methods for hybrid motors, as well as all of the discussed chemical rocket systems, will be discussed in section 2.2.

2.2 Rocket System Ignition

As mentioned in section 1.1, there are five currently-used technologies for combustion

igntion: pyrotechnic charges, plasma torch, electric spark, pyrophoric ignition, or catalytically dissociated monopropellants. However, not all ignition methods can be used for all types of chemical rockets, and each classification of motor has one or two ideal methods that provide an ideal match to the propulsion system. Ignition methods for each chemical rocket type are discussed in detail below, with several case studies of pre-existing combustor/igniter designs.

2.2.1 Monopropellant Ignition Systems

Many monopropellant systems do not have or need a separate ignition system, as they are all either cold gas systems, which have no combustion to ignite; or warm gas catalytically decomposed systems, where all of the propellant is decomposed through a catalyst bed.

However, the majority of propellant catalysis, especially hydrazine decomposition over the standard industry catalyst S-405®, perform best at elevated temperatures, typically over 350 C. Hydrazine monopropellant systems can start with a cold catalyst bed, using the slower decomposition at initial temperatures to warm up the catalyst bed, until the higher catalyst temperatures are reached. However, typical designs pre-heat the catalyst bed to insure more reliable ignition and consistent burn profile.

2.2.2 Liquid Bipropellant Ignition Systems

The current state-of-the-art for the ignition of liquid bipropellant rocket systems is based upon spark-ignition of the fuel/oxidizer feed streams. Immediate ignition within the engine is essential, as failure to ignite within milliseconds can cause excess liquid propellant to pool in the chamber. When a delayed ignition does occur, this pooled propellant vaporizes and combusts rapidly, causing a "hard start" that can catastrophically rupture the combustion chamber, or fatigue the internal components to where a restart is impossible. Because of this, ignition timing and igniter flame stability are critical issues, and current large bipropellant booster ignition systems are extremely complex, requiring significant system-specific tuning for proper function. Two examples of liquid engine ignition systems are discussed: The igniter for the J-2 engine of the Saturn-IVB upper stage, and

the ignition system for the RL10A-4-2 engine of the Altas V/Centaur Common-Core. Both of these liquid propulsion systems were designed for upper-stage lifting vehicles, and can provide a large portion of the ΔV for LEO insertion as well as significant ΔV for in-space maneuvering. The Centaur Common-Core is currently the only operational large booster in the United States space arsenal that is capable of in-space restart.

2.2.2.1 Saturn-IVB (J-2) Ignition

The first ignition system discussed is the augmented spark igniter (ASI) of the J-2 engine in the Saturn-IVB second stage. This engine was used to power the second stage of the Saturn V series of launch vehicles, most popularly known from the Apollo moon missions. A schematic of the J-2 engine was shown in Fig. 2.5. The engine uses liquid oxygen (LOX) as the oxidizing fluid, liquid hydrogen (LH2) as the fuel, and has a small cryogenic helium tank for LOX tank pressurization. (Gaseous hydrogen tapped from after the heat exchanger pressurizes the LH2 tank.)

The ASI, shown in Fig 2.9, is mounted to the injector face, and ignites primary combustion by two smaller fuel and oxidizer lines and two spark igniters. The ASI has an internally mounted ignition monitor, to ensure immediate ignition without any hard start. The spark igniter operated continuously during entire engine firing and was capable of multiple re-ignitions under both vacuum and ambient pressure conditions.

For the Saturn 1B design, the booster ignition was accomplished by a combination of spark ignition in the ASI and a gas generation cycle (lit via a separate spark ignition) [6,41]. Start sequence was initiated by supplying energy to two spark plugs in the gas generator and two in the augmented propellant spark igniter. The engine mounted gaseous hydrogen (GH2) "blow-down" start tank provided the initial drive for the engine turbopumps prior to gas generator ignition. Following the spark activation, two solenoid valves were actuated; one for helium control, and one for ignition phase control. Helium was routed to hold the propellant bleed valves closed and purged the thrust chamber liquid oxygen dome control pressure, the LOX pump seal, and the gas generator oxidizer passage. Additionally, the main fuel and ASI oxidizer valves were opened, creating an ignition flame in the ASI chamber

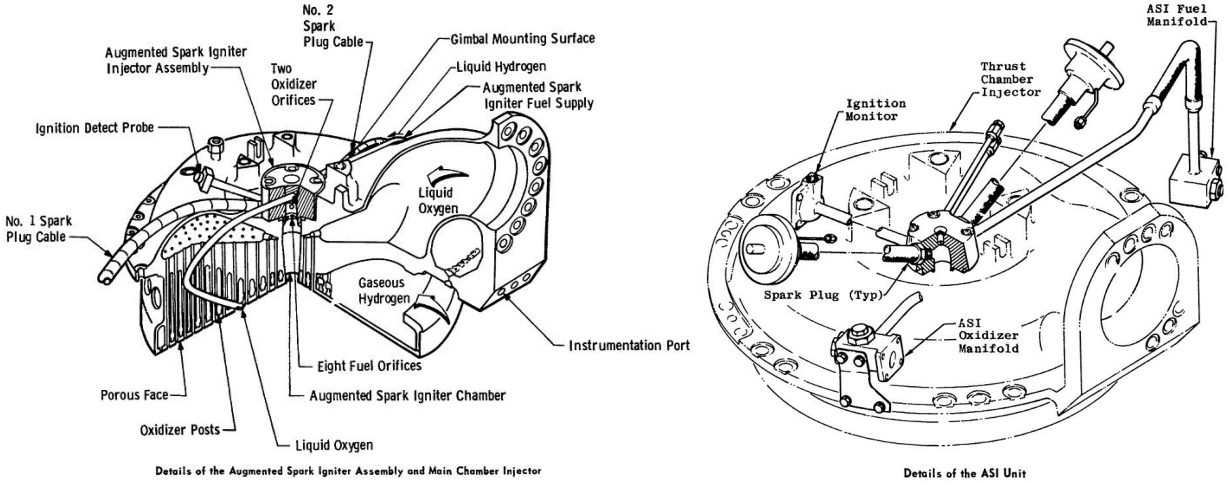

(a) (b)

Fig. 2.9: Augmented Spark Ignition (ASI) assembly for the J-2 motor. (a) shows how the ASI sits within the injection face, and (b) gives a view of the components that create the ASI.

that passed through the center of the thrust chamber injector, with proper ignition being determined by the internally mounted ignition monitor.

After an ignition delay of 1-8 seconds (depending on engine configuration and engine restart) to condition the thrust chamber for start, the start tank valve was opened to initiate turbine spin. Slightly less than half a second later, the start tank valve closed, and the mainstage solenoid actuated. Concurrently, the helium purges of gas generator and thrust chamber end, the gas generation cycle began to power the turbopumps, the main oxidizer valve opened 14°, and the oxygen turbine valve began to gradually open, ensuring a smooth transition to full engine ignition. Energy in the spark plugs was cut off and the engine was operating at rated thrust. During the initial phase of engine operation, the (GH2) start tank was re-pressurized by tapping off a controlled mixture of liquid hydrogen from the thrust chamber fuel inlet manifold and warmer hydrogen from the thrust chamber fuel injection manifold just before entering the injector.

Clearly, this ignition sequence is extremely complex, although the majority of the complexity comes from the careful choreography of tank pressurization, gas generation, and

turbopump power.

2.2.2.2 Centaur Common-Core (RL10A-4-2) Ignition

The second liquid engine ignition system studied is the RL10A-4-2 engine for the Atlas V upper stage. This second stage is known as the Centaur Common Core. Like the J-2 engine, the RL10A-4-2 is a LOX/LH2 engine, although the RL10 uses gaseous hydrogen (GH2) and gaseous oxygen (GOX) for spark ignition and turbopump initiation. Although the majority of pre-Centaur second stages also used an RL10A-4 engine with a single Direct Spark Ignition system, the Common-Core's RL10A-4-2 incorporated a Dual-Direct Spark Ignition (DDSI) system, to improve system reliability [7]. Figure 2.10 shows the DDSI system "grey box" design. The DDSI spark plugs are embedded in the center of the injector. During ignition, GOX is supplied to the region of the spark plug from the injector manifold through a GOX igniter shuttle valve. Fuel is supplied from flow paths in the injector and flows to the igniter region. The fuel and oxygen local to the spark provide the initial ignition to light the chamber at the low pressure, cold conditions of space. The GOX valve closes after start from increasing system pressures to prevent high temperatures around the igniter spark plug. To insure survivability and allow the restart capability, the spark plug is cooled by GH2 during steady state.

2.2.3 Solid Propellant Ignition Systems

All solid motors are ignited by pyrotechnic igniters. Pyrotechnic igniters consist of an electrical resistance element, surrounded by a pyrogen, a more volatile solid mixture of fuel and oxidizer, which will ignite when exposed to the high temperatures from the resistive element. Current is passed through the element, the heat ignites the pyrogen, and the burning pyrogen ignites the main motor. As an example, the ignition system for the Space Shuttle Solid Rocket Boosters (SRBs) will be described.

2.2.3.1 Space Shuttle Reusable Solid Rocket Motor Ignition

The space shuttle SRBs – like most solid motors – is pyrotechnically ignited, however

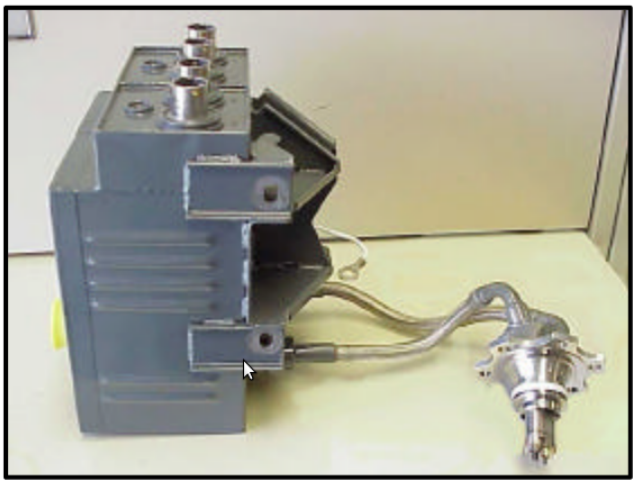

Fig. 2.10: RL10A-4-2 Dual-Direct Spark Ignition (DDSI), prior to installation.

the ignition sequence involves more than the simple resistive element / pyrogen / solid fuel discussed in the introduction to this section. A pyrogenic initiator sits in the forward end of each solid motor, as shown in Fig. 2.11 [42].

SRB ignition can occur only when a manual lock pin from each SRB safe and arm device has been removed by the ground crew during prelaunch activities. At T-minus 5 min, the space shuttle orbiter sends the arm command, firing the NASA Standard Detonators (NSDs) that rotate the safe and arm device to the arm position.

A PIC single-channel capacitor discharge device controls the firing of each pyrotechnic device. Three signals must be present simultaneously for the PIC to generate the pyro firing output. These signals – arm, fire-one and fire-two – originate in the orbiter general-purpose computers and are transmitted to the PICs. The arm signal charges the PIC capacitor to 40 Volts (minimum of 20 Volts). These solid rocket motor ignition commands are only issued when the three SSMEs are at or above 90-percent rated thrust, no SSME fail and/or SRB ignition PIC low voltage is indicated, and there are no holds from the Launch Processing System (LPS).

At T minus zero, the two SRBs are ignited by sending of the fire-two command (arm and fire-one being set high by during pre-launch and SSME firing), under command of the

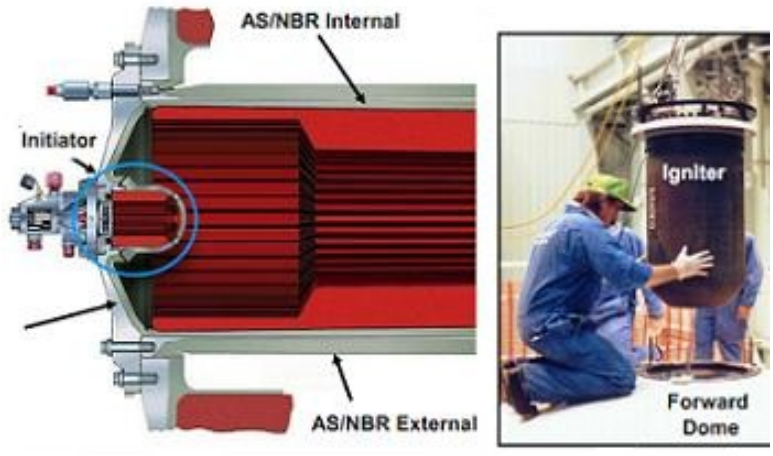

Fig. 2.11: Pyrogenic igniter for the space shuttle solid rocket boosters.

four onboard computers. The fire two command causse the redundant NSDs to fire through a thin barrier seal down a flame tunnel within the initiator. This ignites a pyro booster charge, which is retained in the safe and arm device behind a perforated plate. The booster charge ignites the propellant in the igniter initiator; combustion products of this propellant ignite the solid rocket motor initiator, which fires down the length of the solid rocket motor igniting the solid rocket motor propellant.

2.2.4 Hybrid Bipropellant Ignition Systems

The potential for starting, stopping, and restarting hybrids has been known since their inception, and has often been touted as a key selling point of hybrid motors. Re-ignition is of less interest for launch or endo-atmospheric vehicles, where coasting times will be of short duration and the motor will remain sufficiently hot to restart on its own, but any form of hybrid used for on-orbit station keeping or orbital maneuvers would need an efficient and reliable method for restarting a cold motor. However, there has been almost no investigation into practical methods for in-flight restart. Even the conventional methods for single ignition of hybrids, namely secondary hypergolics [43], small solid propellant igniters [44], and propane-sparker systems [45] were developed and patented between 1964

and 1970. The idea of using a pyrotechnic valve to initiate oxidizer flow and ignite the motor [46] is relatively recent, as it was patented in 1995, but this is the extent of the current technology. None of these methods combine both simplicity and reignition capability. A hypergolic ignition system defeats the safety advantage of nitrous oxide, solid propellant igniters are not reusable, propane sparker systems require a secondary tank and piping path for propane and significantly increases risk, and a pyrotechnic valve is a one-use ignition method.

2.3 Nitrous Oxide Decomposition

The majority of research and development into nitrous oxide decomposition catalysis has targeted the reduction of greenhouse gas emissions [47–52]. Studied catalysts include sintered Ni/Co/Cu oxide pellets and porous ceramic supports with Rhodium or Ruthenium doping. Although this research is informative, the emphasis on the environmental elimination of N_2O focuses the research towards low molar concentrations of nitrous oxide; typically below 5 mol% N_2O, and on how other gases influence nitrous oxide formation and destruction. For propulsion applications, where flows are 100 mol%, these studies are of limited utility.

Multiple researchers have attempted to dissociate N_2O vapor using the industry standard S-405® catalyst bet (catbed) previously developed for hydrazine [11, 53, 54]. This catbed is composed of alumina pellets impregnated with iridium. The catalytic material was originally commercially developed under the brand name Shell-405® by the Shell Chemical Division of Shell Oil Company, Houston, TX [55]. In 2002 commercial production shifted from Shell Chemical to the Aerospace Corporation, Redmond WA. The product is now commercially available as Aerojet S-405 [56]. Unfortunately, the high dissociation temperatures for nitrous oxide – as high as 1600 C – renders the S-405 catbed ineffective after a single use [57, 58].

Thus, if nitrous oxide is to become practical as a monopropellant option, catalyst development is a key research area. The desired product is a highly active catalyst that can decompose N_2O at reasonably low temperatures, but can survive at high temperatures in an

acidic and oxidizing environment. Developing a catalyst bed that works at low temperatures eliminates the need for a high-power external power source. Developing a rugged catalyst that survives for extend burn periods, will allow for multiple ignitions of the primary rocket system. The primary design criteria for these advanced catalytic materials are:

- Structural integrity of the carrier material over the complete temperature range (e.g. no shrinkage)
- Large surface area of the carrier to allow active (catalytic) material to be absorbed in sufficient quantities
- Thermal stability of the active material (high melting point, no evaporation or diffusion under the conditions in the reactor)
- Ability to decompose the propellant at low temperatures so as to require little or no preheating of the catalytic material.

There are several papers published on propulsive nitrous oxide decomposition with catalysts other than Shell-405®. Reaction Systems, LLC has pursued nitrous oxide decomposition for the purpose of scramjet ignition, developing a new catalyst material as well as a regeneratively-cooled N_2O heat exchanger and reactor [59, 60]. Zhu et al. worked on a similar catalyst for high concentrations of nitrous oxide, and list space propulsion as a prime example [61]. Both of the catalysts proposed for N_2O propulsion are based upon a new category of materials called hexa-aluminates [52, 59, 61]. These catalysts are ideal for propulsion by decomposition; they are both active at low temperatures near the 300 C mark, yet still thermally stable at the high temperatures possible in full decomposition. This catalyst research provides a basis for the research activities to be discussed in the following sections.

CHAPTER 3
OBJECTIVES

3.1 Thesis Statement

The primary objective of the research is to demonstrate the feasibility of using nitrous oxide as a green monopropellant ignition fluid for hybrid and liquid rocket systems, especially those that already employ nitrous oxide as the primary oxidizer. Analytical and experimental methods are used to demonstrate this feasibility.

3.2 Research Objectives

There are four primary objectives of the research, each one being a logical step towards the final goal of demonstrating a nitrous oxide igniter's feasibility.

1. Investigate several possible active catalyst materials, focusing especially on those that are commercially available. Select a viable catalytic material, and perform in-house tests to understand the catalytic activity.

2. Develop a one-dimensional simulation of an igniter system. The purpose of the simulation algorithm is to better understand igniter operation, and to provide a feasible method for sizing and choosing igniter components.

3. Using the working simulator, design an igniter flow path and size a prototype igniter for ignition of a Chimaera 98 mm hybrid motor. Build the prototype igniter, and perform tests to demonstrate its ability to energetically decompose nitrous oxide.

4. Incorporate the final igniter in an existing Chimaera motor assembly, and ignite the hybrid motor via the decomposition igniter. In this way, the feasibility of this novel green monopropellant for hybrid motor ignition can been experimentally demonstrated.

CHAPTER 4

EXPERIMENTAL APPARATUS

4.1 Activity Test Apparatus

To gather the necessary information on the catalyst activity, a simple packed bed reactor was designed and assembled. Figure 4.1 shows a simplified diagram of the test setup. The entire system is mounted on a wheeled cart to facilitate movement of the test setup into and out of Utah State University's (USU) on-campus Jet Engine Test Cell. The system setup can be seen in Figure 4.2.

Gaseous nitrous oxide is used as the reactant, and inert carbon dioxide (CO_2) is used as purge and preheat flow. Both solenoids are binary control, so the flow is either fully nitrous oxide or fully carbon dioxide. Because N_2O and CO_2 have very similar thermodynamics and transport properties, the shared needle valve allows for one choking point to produce nearly identical flow rates for both fluids. Thus any measurable changes in the system as the flow is switched from inert gas to reactant are solely due to the decomposition of nitrous oxide.

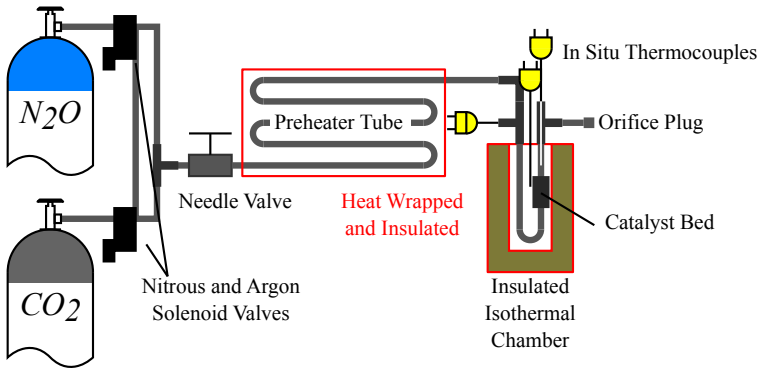

Fig. 4.1: Basic diagram of catalyst test setup.

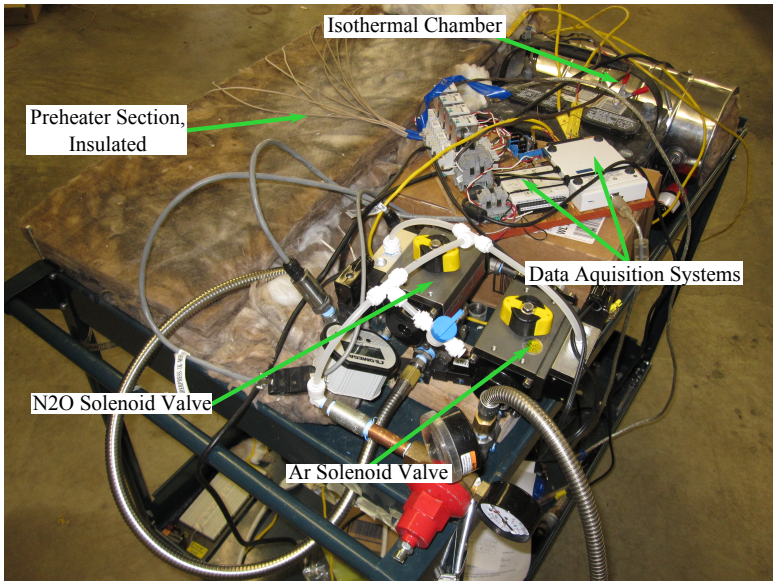

Fig. 4.2: Activity testing setup.

The flow then goes through 10 feet (3.05 m) of thin-walled stainless steel tubing that has been tightly wrapped with heating tape and insulated. This plumbing section preheats the fluid to the desired test temperature, which is measured by a thermocouple downstream of the preheater section. After this first thermocouple, the tubing enters a well insulated pipe, designed to function as an isothermal chamber. The isothermal chamber is oriented horizontally, to mitigate thermal stratification in the enclosed air. There is a second thermocouple in the chamber, along with an immersion heating element. Within the isothermal chamber, there is a 4 inch (10.16 cm) length of 0.68 inch ID x 0.75 inch OD (1.73 cm x 1.9 cm) tubing, which serves as the catalyst chamber. The catalyst chamber holds 15 g of catalyst. Size 20 stainless steel mesh in both ends keeps the catalyst pellets in place. Directly after the reactor section, the plumbing exits the isothermal chamber, and a thermocouple extends down this length of plumbing to measure the flow temperature immediately downstream of the reactor chamber. The flow system is capped with an interchangeable orifice plug.

The upstream needle valve setting and the downstream orifice size both control the reactor pressure and flow rate. Using a variety of orifices and needle valve settings allows

for a wide range of operating conditions to be tested. Decomposition percentage can be calculated from the flow temperatures upstream and downstream of the reactor, although it is worth noting that the thermal mass of the reactor and catalyst also influences this measurement. Both the preheater and the isothermal chamber have separate PID control systems, to keep the preheater section and isothermal chamber at the desired temperatures.

4.2 98 mm Hybrid Test Motor

The hybrid ignition part of the research is accomplised with a 98 mm Chimaera hybrid motor. The hybrid motor is a commercially available Cesaroni 98 mm solid-rocket motor that has been modified by replacing the original forward motor cap with a custom-designed motor cap with a single port oxidizer injector. A threaded pressure transducer port was installed in the motor injector cap to allow for chamber pressure measurements. The stock nozzle holder was replaced by a custom nozzle holder with a nozzle that had a larger throat diameter than the stock nozzle holder could support. To reduce run-to-run variability due to nozzle erosion, nozzles fabricated from a single piece of high-density graphite replaced the original manufacturer-supplied phenolic nozzle.

The nozzle has a 4.2:1 expansion ratio and has a designed throat diameter of 1.7 cm. Two Estes "mini A" class 10-gram solid rocket motors are inserted into the injector cap as igniters. Electronic matches burned by a 12 volt DC signal ignite these small motors. The igniters must be replaced after each test firing. Additional advantages provided by this configuration are a ready-made flight-weight motor and the ability to rapidly reload between motor tests.

HTPB fuel grains are cast using the commercially available Sartomer Poly bd® R-45M polybutadiene resin and PAPI 94® MDI curative. Sartomer R-45M has a polymerization factor of approximately 50 and a molecular weight of 2800 kg/kg-mol [62]. PAPI 94 is a polymethylene polyphenylisocyanate produced by Dow® Plastics Inc [63]. The formulation contains methylene diphenylene diisocyanate (MDI) in proprietary proportions. The curative has an average molecular weight of 290 kg/kg-mol. The nitrogen, carbon, oxygen (N-C-O) bonds in the MDI react with the hydroxyl (OH) terminations in the polybutadiene

resin to cure the fuel grain.

For most tests, carbon black was added to the mixture to insure opaqueness and prevent radiative heating of the fuel grain and motor case liners. HTPB/MDI/carbon black mass proportions were set at 87%/ 12.5%/ 0.5%, respectively. Past experience has determined that these proportions assure adequate fuel grain cure and material hardness. The resin and curative were mixed in a commercial paint mixer that was sealed and fitted so that the fuel mixture could be placed under a vacuum during the mixing process. A commercial H-VAC vacuum pump was used to remove gas bubbles created in the fuel grain during the mixing process. The de-gassed mixture was cast in cardboard sleeves with a 2.67 cm OD polyvinyl chloride (PVC) pipe used as a mandrel. Before casting, the mandrel was coated with Ease Release® 400 mold release agent to insure proper release after the fuel grain cured.

Each fuel grain is approximately 57.15 cm in length, 8.26 cm in diameter, the initial fuel port diameter is 2.67 cm, and post combustion chambers are 5.66 cm in diameter and 1.27 cm deep. The mean density of the HTPB fuel grains used for these tests was approximately 966 kg/m^3, and the cast fuel grains had a mean mass of 2.50 kg. Fig. 4.3 presents a schematic of the test motor.

All previous tests of the 98 mm-diameter hybrid rocket motor used in this project were ignited by two small "squib" pyrotechnics, made from commercially-available hobby rocket 1/2A3-4T Estes solid rocket motors with the recover charge removed. Each 1/2A3-4T engines has 3.50 g of black powder, and burns for approximately 1 second. The igniter locations within the 98 mm motor can be seen in Fig.4.3, internal to the forward chamber enclosure. Figure 4.4 shows the Estes igniters in place, as well as the installed electric resistance igniters.

Firing is accomplished by passing ~ 9 A of current through each resistive igniter. The resistive elements are covered in an AP/nitrocellulose mixture (a form of solid propellant, with both oxidizer and fuel), which ignites, providing enough energy within the chamber of the Estes motors to ignite them. The 98 mm hybrid ignition sequence consists of one of Estes igniter being fired 0.2 s before primary oxidizer flow, and the second Estes igniter

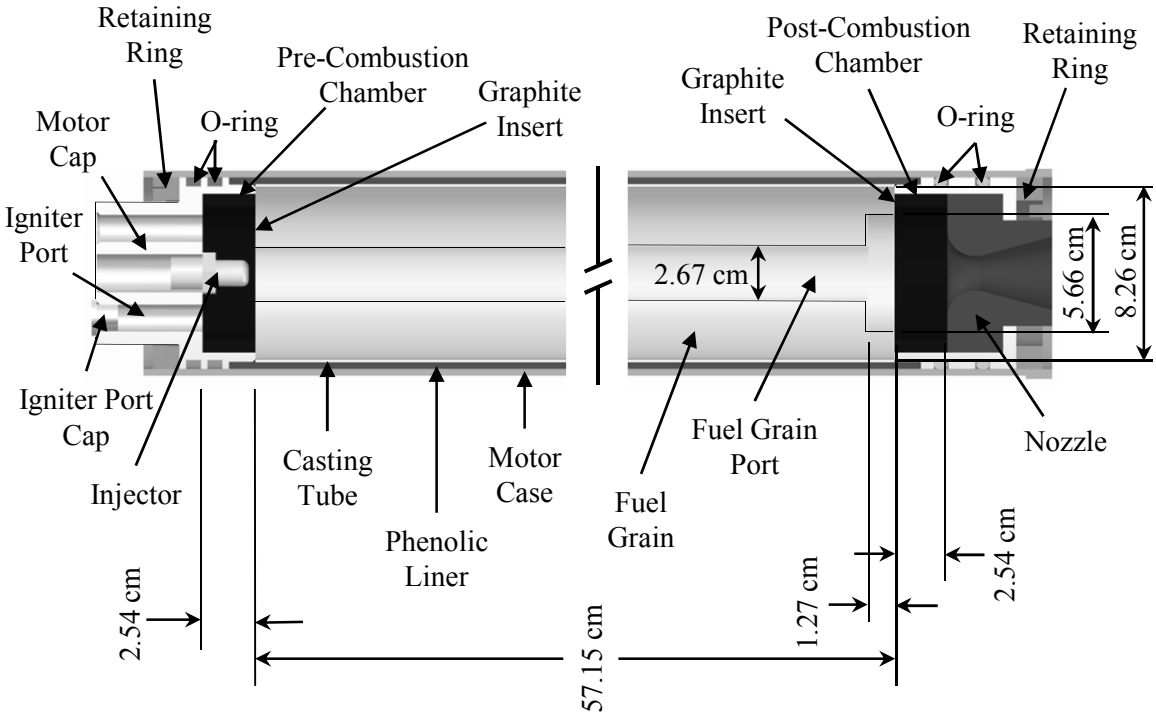

Fig. 4.3: Test motor schematic.

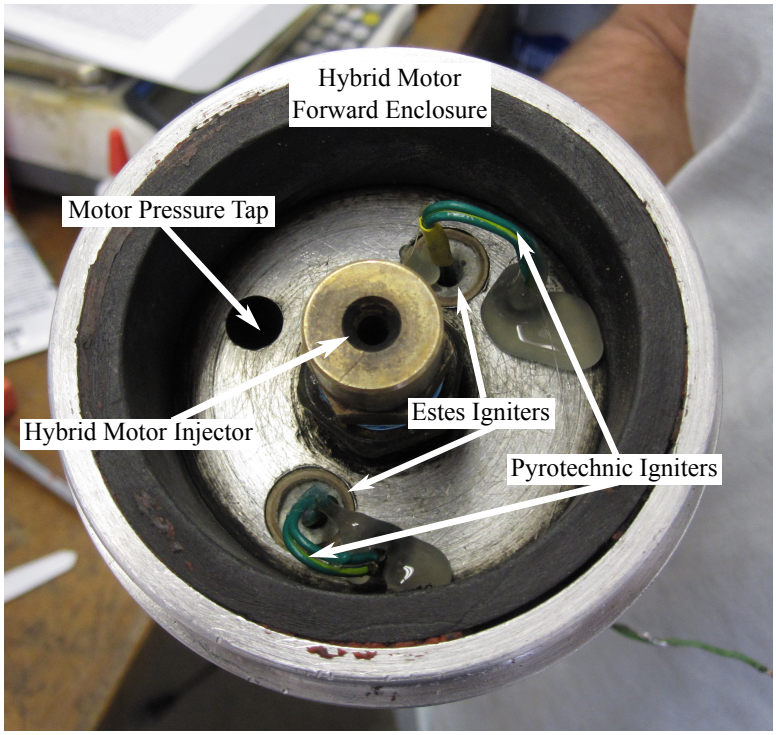

Fig. 4.4: Estes igniters in the Chimaera 98 mm motor forward encosure.

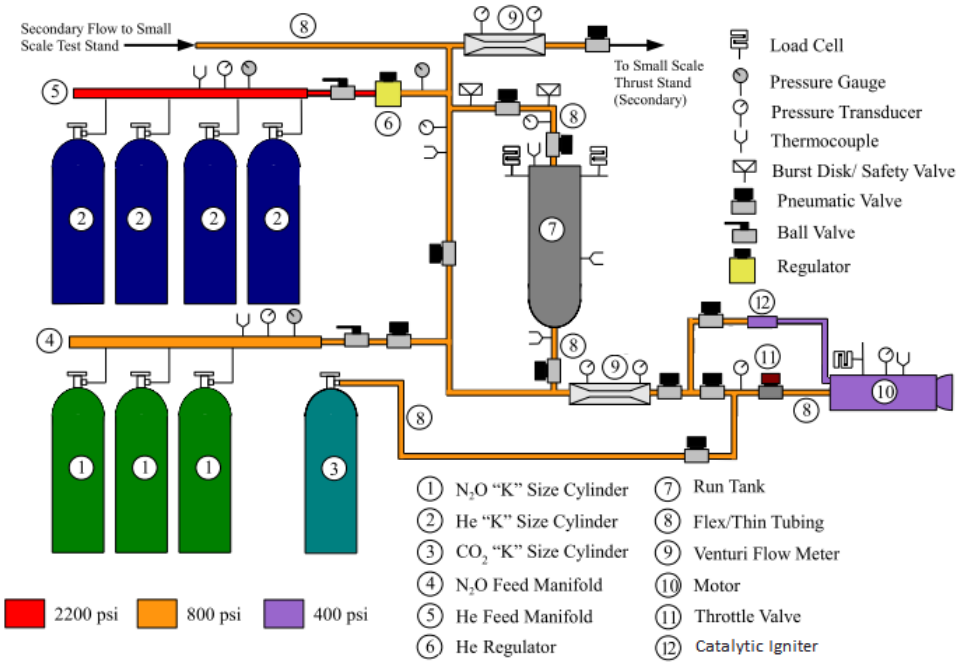

Fig. 4.5: Plumbing and instrumentation diagram for "MoNSTeR Cart" test stand and propellant supply system.

firing 0.3 s after oxidizer flow. This ignition sequence is highly reliable, and resulted in very few ignition failures.

4.3 Hybrid Motor Test Apparatus

The 98 mm hybrid motors have traditionally been tested on the Utah State University (USU) campus. USU has a fully functioning jet engine test cell (JETC) on campus, and all of the hybrid motor firings performed associated with this research were performed in the JETC. The Mobile Nitrous oxide Supply and Testing Resource (MoNSTeR) cart was custom built for hybrid rocket research at USU, and features an oxidizer delivery system, a modular thrust balance platform, and all of the associated system piping, instrumentation, and hardware required for hybrid rocket testing. Figure 4.5 shows the Piping and Instrumentation Diagram (P&ID) for the MoNSTeR cart oxidizer delivery system, in the configuration to be used for catalytic ignition tests.

4.3.1 MoNSTeR Cart Piping System

To allow sufficient mass flow rates with minimal line losses, a predetermined mass of N_2O oxidizer, nominally 500 g/s of burn time, was delivered to a closely coupled "run tank" from a series of "K" sized industrial pressure cylinders. Helium (He) top pressure, set by a manual regulator, was used to keep the nitrous oxide above saturation pressure for the entire run and insured a single-phase liquied flow up to the motor and igniter injectors for the expected range of ambient temperatures. The He "top pressure" was set by a manual regulator and was maintained near 5650 kPa for throttling tests. The design motor chamber pressure was 2760 kPa. A pneumatic run valve upstream of the throttle valve was triggered by an electronic solenoid valve, and was automatically controlled by the instrumentation software.

Oxidizer mass flow was sensed by two vertical Omegadyne® LCCD-100 (445 N) load cells mounted on the run tank, and by an inline Venturi flow meter mounted in the oxidizer feed-line just ahead of the run valve. Differential Venturi flow meter pressure was measured using twin Omegadyne® PX409-1.0KA5V (0-6900 kPa) absolute pressure transducers. Axial load was sensed by an Omegadyne® LCCD-500 (2225 N) load cell and chamber pressure was sensed using an Omegadyne® PX409-1.0KA5V (0-6900 kPa) absolute pressure transducer mounted to the motor cap. An Omegadyne® Type-K thermocouple was mounted at the aft-end of the motor case to sense motor case temperature and thermal soak-back following the end of the burn. All instrumentation was excited using a 10 VDC power source. The output response for the load cells is 3 mV/Volt, and 0-5VDC for the pressure transducers.

The motors were mounted in a thrust balance on the MoNSTeR cart. A motor mounting bracket in the thrust balance is supported on the sides by five ball and clevis joint linkages, two in the vertical and three in the horizontal direction. Motion is constrained in the vertical and horizontal directions and rotations are constrained about all three principal axes by the linkages. The axial load cell is attached between the fore end of the motor mounting bracket and a rigid thrust beam using ball and clevis joints on either side. Linkages and

the axial load cell were aligned to within 0.2° of the principal axes using precision squares and inclinometers.

4.3.2 MoNSTeR Cart Instrumentation

A National Instruments data acquisition (DAQ) system manages motor fire, igniter fire, and log test data. An NI-compact DAQ® 9174[1] (cDAQ) 4-slot bus controller with multiple analog input (16-bit), analog output, digital output, and thermocouple modules (24-bit) manages the measurements and valve control. Operators and experimenters are remotely located in a secure control room separated from the test area. Communications to the test stand are managed by an operator-controlled computer via universal serial bus (USB) using amplified extension cables. General control and measurement functions are controlled by a LabVIEW® virtual instrument (VI) hosted on the control computer.

[1] http://sine.ni.com/nips/cds/view/p/lang/en/nid/207535

CHAPTER 5
RESULTS AND DISCUSSION

5.1 Catalyst Selection

As mentioned in section 2.3, there are several different types of catalysts that have been tested, and the choice of catalyst that performs best with nitrous oxide is a key part of the research. Initially, the hexa-aluminate catalyst used by Zhu et al. was evaluated [61]. However, given the resources available within the project budget, after several attempts the catalyst could not be successfully synthesized, and an alternative catalyst was chosen. Following an extensive trade study, the alternative catalyst bed was constructed from ruthenium deposited on alumina pellets. This catalyst, although having somewhat less desirable catalysis characteristics, has the distinct advantage of being commercially available, as well as a history of being successfully used previously for high molar fraction N_2O decomposition.

5.1.1 Ruthenium on Alumina

The selected catalyst consists of pre-prepared 0.5 wt% Ruthenium on alumina pellets[1]. Zeng and Pang [51] used a similar catalyst for their research, and also experimented with relatively high N_2O molar fractions, up to 28 mol%, and reported catalytic activities of $48000\,{}^{\mu\mathrm{mol}}/_{\mathrm{g\,h}}$ at 400 C [51]. Figure 5.1 shows the results of multiple catalyst tests, using a flow of 28 mol% N_2O in He over Ru-loaded alumina pellets. The catalyst loadings varied between 0.0 and 0.26 wt%, with an optimal catalyst loading of slightly under 0.2 wt%. An interesting phenomenon is the very sharp rise in conversion percent over a relatively narrow temperature band. This is the range in which a nitrous oxide igniter should function, where the maximum amount of conversion can be reached with a minimum of preheating.

Figure 5.2a shows a pile of unused catalyst pellets. The pellets are micro-porous cylinders 3.2 mm in diameter and 3.5 mm in length, and have a packed density of approximately

[1] Sigma-Aldrich product listing 206172 ALDRICH

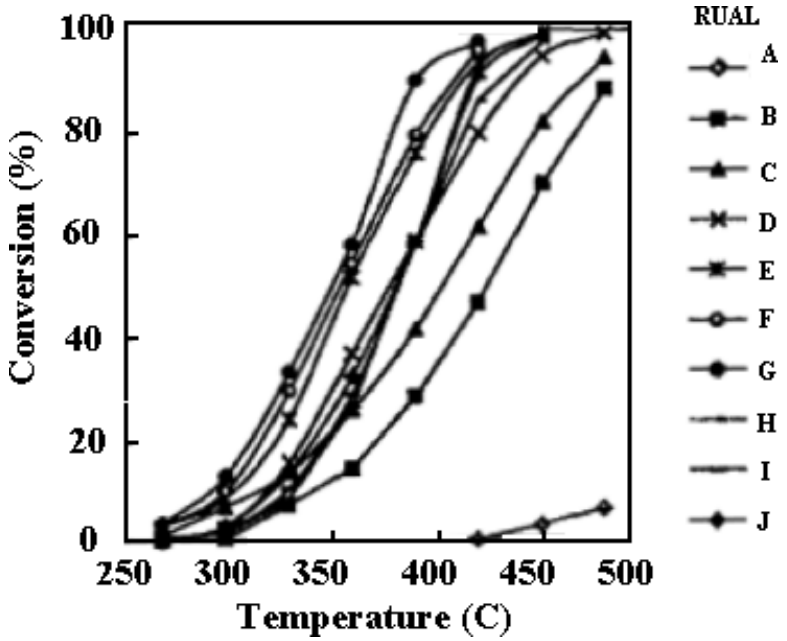

Fig. 5.1: Conversion percent vs temperature over Ru-loaded alumina. Different curves correspond to varying Ru loadings between 0.0 and 0.26 wt%. Figure created and published by Zeng and Pang [51].

0.6 g/cm^3.

5.1.2 Catalyst Characterization

Before a reliably operating igniter can be built, the decomposition characteristics of the catalyst must be better understood. Most importantly, the limiting factor for the decomposition must be known. The reaction can be limited by:

- Pure kinetics, where the reaction is limited by the speed at which the physical catalyst can absorb, combine, and release oxygen,
- Pore diffusion, where the reaction is limited by the diffusion of reactants and products into and out of the microscopic catalyst pores,
- Boundary layer diffusion, where the fluid flow outside of the catalyst cannot move the products and reactants toward and away from the surface.

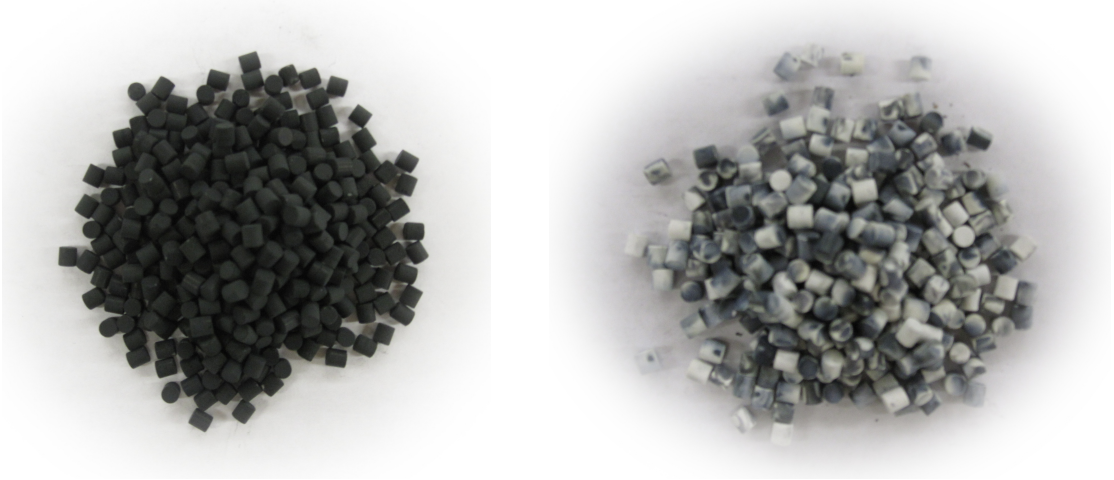

(a) Ruthenium on Alumina catalyst pellets, as received and before any use.

(b) Ruthenium on alumina pellets, after overheating and losing Ru to vaporization.

Fig. 5.2: Ruthenium alumina catalyst.

Which of these modes dominates determines how the system should be scaled up to the final igniter design. A secondary test objective is the measurement of the critical onset temperature where the reaction changes from slow partial decomposition to rapid complete decomposition. Figure 5.1 shows an example of this event. Finally, catalyst testing is necessary to determine the maximum usable temperature of the catalyst. Since the Ru is deposited on the surface instead of being incorporated into the structure, at higher temperatures the Ru will vaporize off of the surface, leaving a destroyed catalyst. Figure 5.2b shows an example of a depleted catalyst bed.

5.1.3 Characterization Test Procedure

After system safety and functionality tests, the CO_2 flow is turned on, and the needle valve set to give the desired pressure. Once the needle valve has been set, the test cell is evacuated and the system controlled remotely using a LabVIEW interface. The heater control systems are turned on and the system is brought up to temperature. Based upon the data from Zeng shown in Fig. 5.1, the initial temperature for the system was chosen

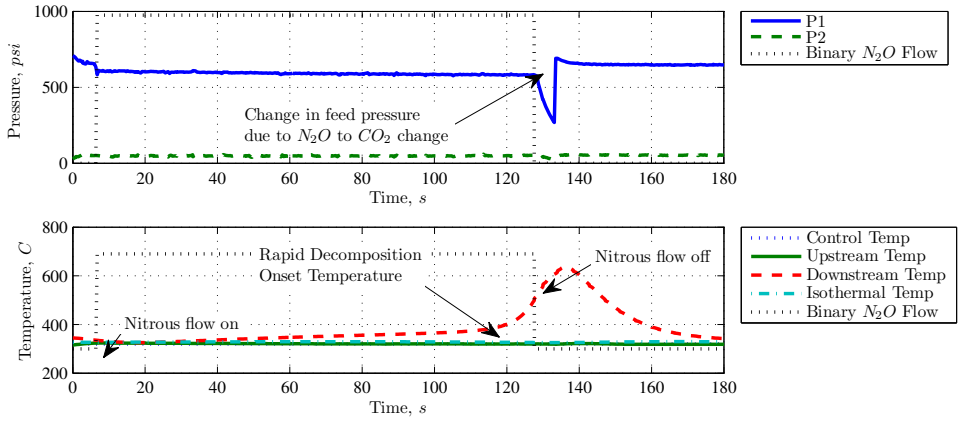

Fig. 5.3: A representative catalyst activity test.

to be 325 C. Testing does not progress until both the preheater and isothermal chamber temperatures are constant.

Once the system is stable at the initial temperature, the LabVIEW script begins saving data, and the flow is switched to nitrous oxide. As nitrous oxide begins flowing through the system, the exit temperature begins to rise, due to the low, but non-zero, reaction rate. As the catalyst bed continues to heat, eventually a critical temperature is reached, and the reaction rate begins to increase. The exit temperature rises significantly, and the N_2O flow is quickly turned off, to prevent damage to the catalyst.

Data from an example test are shown in Fig. 5.3. The critical reaction temperature can be clearly seen, around 400 C. The lower reaction rate before this temperature can be seen by the slower temperature climb early, and the fast reaction can be seen in the few seconds before the nitrous flow is shut off. Of special interest is the high rise in reactor exit temperature after the flow is switched to CO_2. This temperature rise is caused by the combined thermal mass of the stainless steel fittings and walls that compose the catalyst reactor, and the thermal mass of the catalyst pellets.

The needle valve was then reset for a different chamber pressure, and the test was repeated. Chamber pressures ranged from 50 to 350 psi; higher pressures were not tested

as a safety feature.

The full range of testing was repeated with multiple exit orifices. Collectively, three separate orifices were examined, with diameters of 0.063, 0.047, and 0.023 inch (1.6, 1.19, and 0.58 mm). This orifice set fully captured the system characteristics for mass flow rates of 0.7 g/s to 2.5 g/s.

5.1.4 Catalyst Bed Upper Temperature

After the necessary reaction rate data had been gathered, a series of tests was performed to establish an upper limit for the catalyst material. The peak temperature from decomposition was incrementally increased, and the catalyst examined after each test.

The destructive catalyst tests established an absolute maximum temperature of approximately 900 C for the Rh on alumina catalyst. At both 700 and 800 C, visible whitening occurred in patches on the catalyst pellet faces and edges directly facing into the fluid flow. However, the visual color change did not noticeably affect catalyst performance until a peak temperature over 900 C was reached. Beyond this temperature, the catalyst demonstrated significantly lower total decomposition rates, indicative that there was not enough Ruthenium left to react with the nitrous oxide. Based on these results, a hard limit of 900 C was imposed on the catalyst pellets, with a desired temperature around 800 C or lower.

5.1.5 Dissociation Onset Temperature

The dissociation onset temperature was defined as the point where the rate of temperature increase (in Kelvin per second) exceeded a threshold value. Figures 5.4 and 5.5 both show the onset temperature at which the heating rates exceed the specified values, shown here for 3, 5, and 8 K/s. Depending on the definition for critical heating rate, the onset temperatures range from 340 C to 460 C . Higher pressures have lower onset temps, between 340 C and 380 C. To ensure that the reaction rate is well within the higher range at the beginning of the ignition sequence, an initial igniter temperature of 400 C was chosen.

Figures 5.4 and 5.5 reveal a clear correlation between nitrous oxide pressure and onset temperature, and very little if any correlation between nitrous oxide flow rate and onset

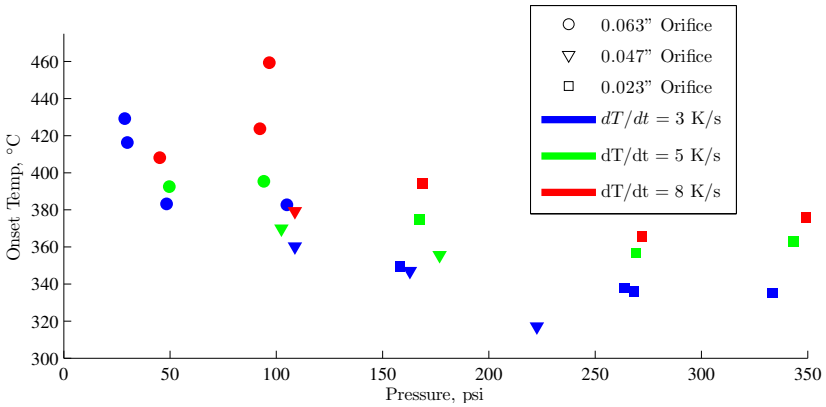

Fig. 5.4: Onset temperature vs. pressure, for a range of cutoff reaction rates.

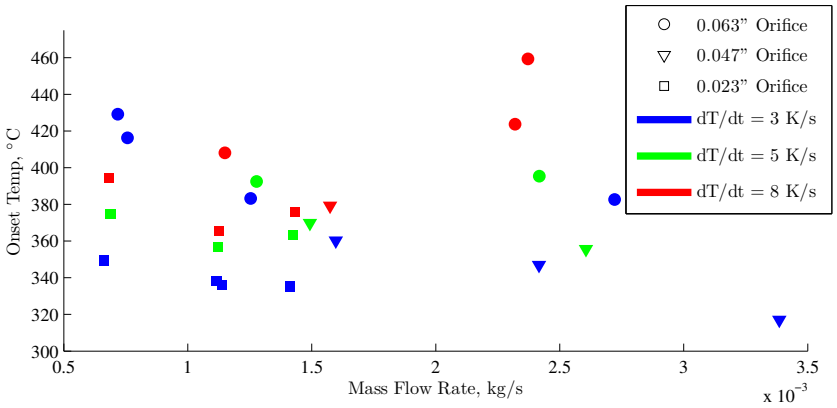

Fig. 5.5: Onset temperature vs. mass flow rate, for a range of cutoff reaction rates.

temperature. Based of these results, the onset temperature is primarily influenced by reactor pressure. The result implies that the limiting factor in N_2O decomposition is the rate kinetics, and the mass of catalyst in the chamber should scale directly with mass flow rate.

5.2 Reactor Design

With a catalytic material that is understood, and the necessary flow conditions for high activity known, the focus of the research turns to the igniter design. The key aspects of this design are discussed in this section, including the decomposition model developed for igniter sizing.

5.2.1 Flow Path Design

Proper design of the igniter flowpath is critical for the successful completion of the research objectives. The chosen design is a system that uses regenerative cooling of the catalyst bed, and the matching regenerative heating of the preheat section, to deal with the majority of the steady-state energy requirements. Electrical heating elements will still be necessary to bring the catalyst bed up to the decomposition temperature. The necessary heat transfer rates for this type of system will be discussed in section 5.2.2.

Reaction Systems, LLC [60] suggested a double-annular design for their scramjet igniter, as shown in Fig. 5.6. This allows for both liquid nitrous oxide preheating, as it flows through the outer annulus, and catalyst cooling, as the flow turns and moves through the inner tube where the catalyst is deposited on the walls. The configuration is similar to an opposing flow heat exchanger, using some of the decomposition energy to vaporize and preheat the nitrous oxide. However, this double annular design requires a reactor with a length to diameter (L/D) ratio of around 30. For rocket system applications, this is a very inconvenient form factor. As mentioned earlier, it is also designed for a wall-deposited catalyst, instead of the packed bed pellet chamber that this research needs.

The final igniter flow path design used in this research consists of a preheat section of tubing first wrapped around the reactor, then traveling through the catalyst bed before flowing through the decomposition catalyst. The key parameter influencing the size of this

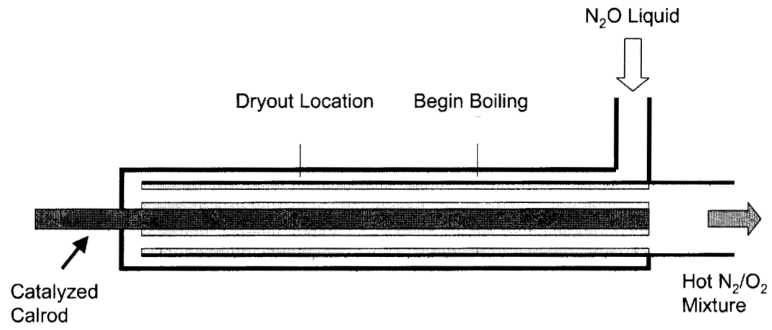

Fig. 5.6: Double-annular scramjet ignition design used by Reaction Systems, LLC.

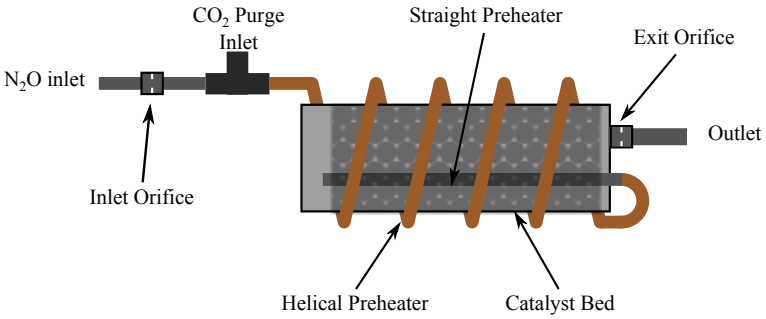

Fig. 5.7: Nitrous oxide flow path used in the igniter design.

preheat section is the heat transfer rate between the preheater and the catalyst bed. Figure 5.7 shows the flowpath for the final igniter.

5.2.2 Thermal Fluid Modeling

In order to ensure that the 98 mm hybrid motor would properly ignite, the igniter was sized to match the power output and total enthalpy output of the two miniature Estes 1/2A3-4T solid-propellant motors previously discussed in section 4.2. The 1/2A3-4T motors have 3.50 g of black powder each, and burn for approximately 1 second. Since the energy density of black powder is $\sim 3\,^{\mathrm{MJ}}/_{\mathrm{kg}}$ [64], the power output of two Estes motors (W_E) is

approximated as

$$W_E \approx 2\left(\frac{3.50\text{g} \cdot 3\,^{\text{MJ}}/_{\text{kg}}}{1\text{s}}\right) = 21\text{kW} \tag{5.1}$$

This is the minimum desired input to the motor from the decomposition reactor. For the purposes of this analysis, the power output from a decomposing flow of nitrous oxide (W_{N_2O}) is calculated as the difference in enthalpy between the dissociation products at the exit conditions (h_{exit}) and the exit products at standard temperature and pressure (h_{STP}).

$$W_{N_2O} = \dot{m}\left(h_{\text{exit}} - h_{\text{STP}}\right) \tag{5.2}$$

where $\dot{m}$ is the massflow through the igniter.

The exit flow is multi-component, being composed of nitrous oxide, nitrogen, and oxygen. The exit flow is assumed to be chemically non-reacting and composed of ideal gases, thus the power output becomes:

$$W_{N_2O} = \dot{m}\left[w_{N_2O}\left(h_{e,N_2O} - \Delta h_{f,N_2O}\right) + w_{N_2}\left(h_{e,N_2} - \Delta h_{f,N_2}\right) + w_{O_2}\left(h_{e,O_2} - \Delta h_{f,O_2}\right)\right] \tag{5.3}$$

where w_{N_2O}, w_{N_2}, and w_{O_2} are the partial mass fractions of nitrous oxide, nitrogen, and oxygen, respectively, and the enthalpies of the dissociation products are h_{e,N_2O}, h_{e,N_2}, and h_{e,O_2}. The enthalpies of formation of nitrous oxide, nitrogen and oxygen are $\Delta h_{f,N_2O}$, $\Delta h_{f,N_2}$, and $\Delta h_{f,O_2}$, which are by definition h_{STP} for the decomposition products. The mass fractions of nitrous oxide, oxygen, and nitrogen are calculated as:

$$w_{N_2O} = 1 - y \qquad w_{N_2} = y \cdot \frac{M_{N_2}}{M_{N_2O}} \qquad w_{O_2} = y \cdot \frac{M_{O_2}}{M_{N_2O}}$$

where y is the fraction of nitrous oxide that has decomposed, and M_{N_2O}, M_{N_2}, and M_{O_2} are the molar weights of nitrous oxide, nitrogen, and oxygen.

Substituting y into Eq. 5.3 gives

$$W_{N_2O} = \dot{m}\left[(1-y)\left(h_{e,N_2O} - \Delta h_{f,N_2O}\right) + y\frac{M_{N_2}}{M_{N_2O}}\left(h_{e,N_2} - \Delta h_{f,N_2}\right) + y\frac{M_{O_2}}{M_{N_2O}}\left(h_{e,O_2} - \Delta h_{f,O_2}\right)\right] \tag{5.4}$$

The final enthalpies cannot be explicitly solved for. Instead, the set of equations

$$(1-y)\,h_{e,N_2O} + y\frac{M_{N_2}}{M_{N_2O}}h_{e,N_2} + y\frac{M_{O_2}}{M_{N_2O}}h_{e,O_2} = y\cdot\Delta h_{f,N_2O} + h_{i,N_2O} \tag{5.5}$$

and

$$\begin{aligned} h_{e,N_2O} &= f_{N_2O}\left(T_e, P_e\right) \\ h_{e,N_2} &= f_{N_2}\left(T_e, P_e\right) \\ h_{e,O_2} &= f_{O_2}\left(T_e, P_e\right) \end{aligned} \tag{5.6}$$

must be simultaneously solved for the unknowns h_{e,N_2O}, h_{e,N_2}, h_{e,O_2}, and the exit temperature T_e. The N_2O inlet enthalpy h_{i,N_2O}, the decomposition fraction y, and the exit pressure P_e are the operating conditions that must be known. The equations of state for the fluids, $f_{N_2O}\left(T_e, P_e\right)$, $f_{N_2}\left(T_e, P_e\right)$, and $f_{O_2}\left(T_e, P_e\right)$, are inherent properties of the fluids, and empirical formulae must be used.

The reactor bed was designed to have an internal pressure that was approximately 700 kPa above the 98 mm motor chamber pressure, to prevent backflow of hybrid combustion products. Previous tests of the 98 mm-diameter motor demonstrated that at the nominal thrust level of 800 N, the operational chamber pressure was near 2800 kPa ($\sim$ 400 psi), thus a reactor pressure of 3500 kPa (510 psi) was chosen.

A modified version of the non-homogeneous non-equilibrium (NHNE) model developed by Dyer et al. at Stanford University was used for the inlet orifice size calculation [65]. Because the nitrous oxide flow through this orifice is multiphase, standard choking area calculations cannot be used. This model uses a weighted average of the homogeneous equilibrium (HEM) mass flux (G_{HEM}),

$$G_{HEM} = \frac{\dot{m}}{A_t} = \rho_2 \sqrt{2\left(h_1 - h_2\right)} \tag{5.7}$$

and the incompressible (SPI) mass flux (G_{SPI}),

$$G_{SPI} = \frac{\dot{m}}{A_t} = \sqrt{2\rho_1\left(P_1 - P_2\right)} \tag{5.8}$$

to compute a single mass flux using a weighted "non equilibrium parameter" k,

$$k = \frac{\tau_b}{\tau_r} = \sqrt{\frac{P_1 - P_2}{P_v - P_2}} \tag{5.9}$$

where τ_b is the bubble formation time constant, and τ_r is the fluid residence time constant.

The two-phase mass flux, G_{NHNE}, is calculated as a weighted average of the incompressible and HEM mass fluxes,

$$G_{NHNE} = C_d\left(\frac{1}{1+k}G_{HEM} + \left(1 - \frac{1}{1+k}\right)G_{SPI}\right) \tag{5.10}$$

where C_d is the subsonic discharge coefficient of the orifice.

In these relations h_1, P_1, and ρ_1 are the enthalpy, pressure, and density of the fluid at the orifice inlet; h_2, P_2, and ρ_2 are the enthalpy, pressure, and density of the fluid at the orifice exit, and P_v is the vapor pressure of the working fluid. This same relationship, with different pressure drops and initial qualities, applies to both the expansion orifice positioned before the coolant channels and the injector orifice that sprays into the combustion chamber.

The parameter k is the inverse square root of the cavitation number and expresses the ratio of the difference between the upstream total pressure and the downstream pressure, and the vapor pressure and the downstream pressure. Small values for k demonstrate a high degree of cavitation in the flow and an increase in fluid quality in the orifice. When k is large, the incompressible SPI model is weighted heavily. When k is small, the two-phase HEM model is weighted heavily. The combined model of Eq. (5.10) allows for two-phase flow effects that plateau the mass flux as the downstream pressure is lowered. This is consistent with observed two-phase mass flow properties.

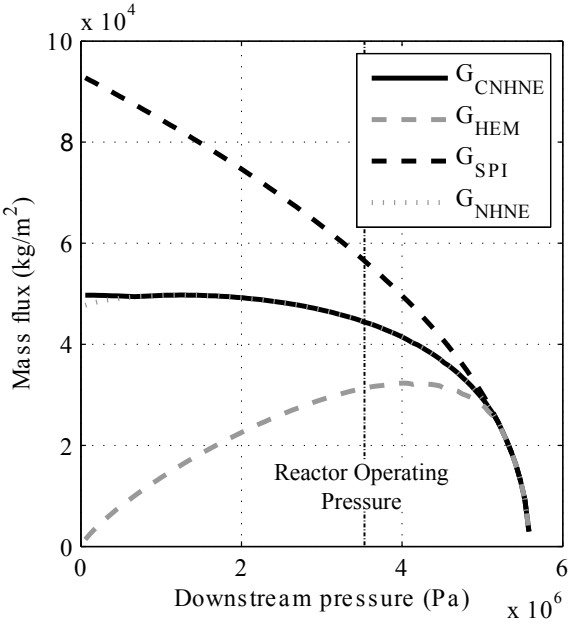

Fig. 5.8: Mass fluxes predicted by the SPI model, the HEM, the NHNE model, and the CNHNE model for nitrous oxide with various downstream pressures and an upstream pressure of 5.58 MPa (809 psi) and temperature of 295 K .

The model proposed by Dyer was modified and extended to allow choking mass flow. For very small exit pressures, the mass fluxes predicted by the NHNE model decrease with decreasing exit pressure, a trend unlikely to exist in reality. Thus, a model was used that uses the maximum flow rate predicted by NHNE model for any downstream pressure between the upstream pressure and the exit pressure. Figure 5.8 shows mass fluxes predicted by the SPI model, the HEM , the NHNE model, and the choked NHEM model (CNHNE) for nitrous oxide that is slightly sub-cooled upstream of the injector. The design operating pressure of the reactor is shown at 3500 kPa. Although the fluid moving through the orifice is not choked, the sensitivity of the mass flux to downstream pressure variation is low. The pressure drop across the inlet orifice is high enough to prevent backflow and pressure instabilities from forming.

The fluid flow exiting from the reactor is fully gaseous and the NHNE model reduces to the HEM model; the HEM model is equivalent to standard orifice choking correlations.

Table 5.1: Predicted states and orifices for 3.53 MPa (512 psi) reactor pressure, 86 kPa (12 psi) motor chamber pressure, and 15 g/s mass flow.

	$T\,(°C)$	$P\,(\text{MPa})$	$h\,(\text{kJ/kg})$	$D\,(\text{mm})$
Initial Properties	20.0	5.03	214.8	
First Choke Point				0.352
Igniter Inflow	4.86	3.53	214.8	
End of Catalyst Bed	957.8	3.23	2079.3	
Second Choke Point				1.167
Igniter Outflow	958.5	0.86	2079.3	

Equations 5.3 - 5.10 were combined into a numerically solved algorithm written in MATLAB. This numerical model is described in detail in Appendix A. The equations of state in Eq. 5.6 were approximated by the Helmholtz free energy models developed by Lemmon and Span [66] and Span and Wagner [67, 68]. These equations give the properties of the desired fluids throughout the range of interest as explicit functions of the temperature T and density ρ.

The numerical model takes the initial nitrous oxide properties, calculated for a saturated liquid at 20 C, the desired chamber pressure and exit pressure, and the desired mass flow rate, and calculates the flow properties at key points, both orifice sizes, and the output power. For the first iteration of the algorithm, the mass flow through the igniter is chosen as 15 g/s, which is approximately 5% of the nominal mass flow rate of the 98 mm hybrid test motor. The exit orifice is sized to be choked at ambient test conditions – approximately 86 kPa (12.5 psi) at the test altitude – since the unlit motor will not have any chamber pressure built up. Once the hybrid motor reaches its full pressure, the exit orifice will no longer be choked and the flow rate through the igniter only serves to keep combustion products from flowing back into the catalyst chamber. As the motor chambr pressure builds the massflow throught he reactor drops off significantly. Tables 5.1 and 5.2 show the model predictions for the specified conditions.

The selected massflow of 15 g/s provides 24.26 kWto the combustion chamber, and exceeds the output power of the two Estes 1/2A3-4T by more than 15 %.

Table 5.2: Power comparisons for 3.53 MPa (512 psi) reactor pressure, 86 kPa (12 psi) motor chamber pressure, and 15 g/s mass flow.

Vaporization and Preheat Power	−9.49 kW
Decomposition Power	27.97 kW
Power to Hybrid Chamber	24.26 kW

5.3 Igniter Prototype Testing Apparatus and Procedures

The igniter prototype testing apparatus and procedures are presented in this section. The igniter prototype designs and evalution will be presented in section 5.4.

5.3.1 Igniter Prototype Test Apparatus

The data collection methodology was nearly identical for all prototypes. Nitrous oxide inlet, pre-catalyst, and exit temperatures were measured, as well as igniter case temperature and catalyst bed pressure. After some of the tests showed signs of thermal damage to the stainless steel catalyst bed walls, an additional thermocouple was added after the bulk of the catalyst and before the exit choke point. This thermocouple met with limited success, as the highly oxidizing environment and the high temperatures destroyed several Type-K thermocouples.

The flow rate of nitrous oxide through the system was also measured with two pressure transducers mounted in a venturi flowmeter on the MoNSTeR cart. The venturi has a thermocouple mounted on the plumbing exit, and so the mass flow rate of the nitrous oxide can be readily calculated. A schematic of the system is shown in Fig. 5.9.

5.3.2 Igniter Prototype Test Procedures

The LabVIEW instrumentation control and data aquisition software (the VI) was written to have the capability for both igniter testing and full hybrid ignition, so that the same control software used for the prototype evaluation can be used for the full hybrid motor tests. For each test, a similar testing procedure was followed. A brief summary of the test flow is presented here, with the full details contained in the testing checklists.

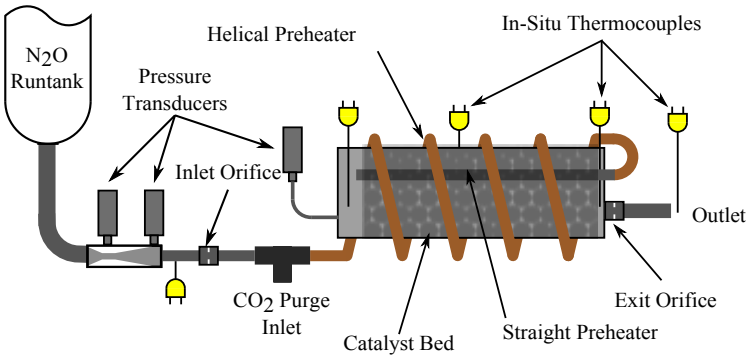

Fig. 5.9: Schematic of the igniter prototype testing system.

1. The reactor is assembled, mounted on the MoNSTeR cart, and the MoNSTeR cart wheeled into the JETC and bolted into the thrust plate. All electrical connections are made, and the plumbing and wiring is inspected to ensure proper functionality. The test computer is powered on, and the data aquisition system is verified to be running and capturing real data.

2. The high-temperature heating elements surrounding the igniter reactor are used to preheat the catalyst bed to the desired temperature. The LabVIEW VI uses a simple on-off controller for the heating elements, which gives a variation in the catalyst bed temperature of less than 1 C.

3. Once the igniter has reached a steady-state temperature, the nitrous oxide and carbon dioxide bottles are opened, and the plumbing system is prefilled with liquid N_2O. The test cell is evacuated in preparation of reactor firing.

4. Following a countdown, the test sequence is initiated. After a 5 second delay, the igniter valve opens, and nitrous oxide begins flowing through the igniter reactor. The inlet, pre-catalyst, post-catalyst, and exit flow temperatures are logged, as well as the catalyst chamber pressure. Failsafes are written into the controlling program so that if an excessive temperature or pressure occurs, the system immediately goes into

purge, shutting down the nitrous oxide flow and opening the carbon dioxide purge valve. The test instructor also has the option to initiate purge at his discretion.

5. If no catastropic failure occurs, the test proceeds for a pre-determined amount of run time, and initiates purge at the end. The system is allowed to cool, the MoNSTeR cart is wheeled back into the hybrid project lab, and disassembly of the igniter for system evaluation can begin.

For each prototype test, the test instructor followed a testing checklist; a document with detailed step-by-step instruction on how to perform the test. The full checklist is included in Appendix B.

5.4 Igniter Prototype Designs and Evaluation

The design parameters calculated in section 5.2.2 were used as the baseline for the development of several reactor bed prototypes. The reactor bed design was performed incrementally, and the "lessons learned" from each series of evaluation tests were applied to guide the design evolution. This section details this design evolution. Table 5.3 presents a summary of the prototypes and the lessons learned from the testing of each design prototype.

Table 5.3: Prototype reactors, dates of testing, and test results.

Name	Catalyst Volume	Date of Final Test	Result
Two-inch Diameter	125.0 cm^3	8/22/12	Catastrophic Failure
One-inch Diameter External Helix	50.0 cm^3	10/11/12	Insufficient Regenerative Heating
One-inch Diameter Internal Graphite	40.5 cm^3	10/24/12	Insufficient Thermal Mass
One-inch Diameter External Preheater	50.0 cm^3	11/07/12	Successful Firing

5.4.1 Two-Inch Diameter Igniter

The igniter is very similar to a shell and tube heat exchanger, with a few modifications. The shell side is downstream of the tube side, and is filled with catalytic pellets to decompose the nitrous oxide. The shell and tube design serves to preheat the liquid nitrous oxide to 400 C, as well as to cool the decomposing nitrous oxide and catalyst bed. Figure 5.10 shows a model of the final system.

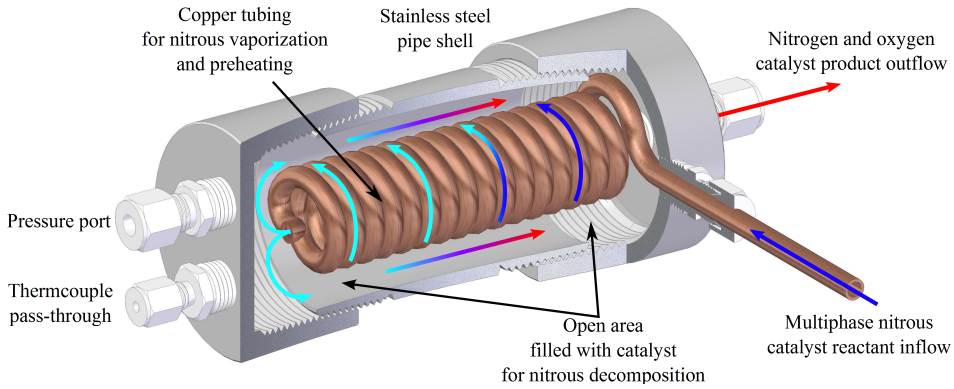

Fig. 5.10: Design of the 2-inch igniter prototype, showing the modified shell and tube heat exchanger.

The shell of the igniter is made from off-the-shelf 2-inch (5.08 cm) stainless steel pipe fittings to minimize cost and necessary machining. The aft pipe cap is drilled and tapped with a 1/4 inch (0.635 cm) NPT hole in the side, serving as the fluid entrance, and a second 1/4 inch (0.635 cm) NPT hole in the center of the base, as the fluid exit. The forward pipe cap has two 1/4 inch (0.635 cm) NPT holes in the base for a thermocouple pass-through and pressure tap. The inner tube path is copper tubing, similar to that used for refrigeration systems. There is an aluminum oxide disc in the base of the aft pipe cap, with a precisely ground choking orifice. Not pictured is a second orifice plate upstream of the copper tubing, dropping the inlet pressure from saturation to the desired 3.53 MPa (512 psi). The shell is filled with 75 g of catalyst pellets and 800 g of copper-coated BBs before being assembled,

and the full assembly is wrapped in high temperature heating tape and insulated. The catalyst chamber has a mixture of active catalyst pellets and BBs for several reasons: first, by lowering the density of catalytic material the decomposition rate will be lower, allowing for better regenerative cooling by the nitrous oxide flow through the helical coils, and second, to provide some thermal mass for the initial startup transient, to assist in fully vaporizing the nitrous oxide before the higher temperatures – and therefore higher regenerative heating – can occur.

The igniter prototype is shown in Fig. 5.11. The decision was made to add an additional helix of the copper inlet tubing around the outside of the catalyst bed, to further enhance heat transfer from the catalyst bed. The catalyst bed and plumbing is wrapped in heating tape (not shown), and the assembly surrounded by high-temperature insulation.

The prototype igniter was fired once, on August 22, 2012. The test was not successful, as can be seen in the images in Fig. 5.12. Figure 5.13 shows the data collected from this test. Approximately 10 seconds into the test, the chamber pressure began to oscillate erratically, and at 50 seconds past nitrous oxide flow, the chamber pressure jumped, and sparks began flying out of the decomposition reactor. The test was terminated, and the system purged with carbon dioxide. In Fig. 5.12 (a), the reactor shortly after the test is shown. The aft end of the catalyst bed had overheated, and was visibly glowing. Figure 5.12 (b) shows the interior of the catalyst bed, after reactor disassembly. The internal components of the reactor had fused into a single solid.

After a careful review of the design and testing data, a numerical error was found in the scaling calculations for the igniter, driving the design to an igniter prototype with double the desired amount of catalyts. This increase in catalyst created higher internal motor temperatures, melting the copper from the internal tubing helix and the BB coating. The reactor and the catalyst pellets could not be salvaged.

5.4.2 One-Inch Diameter with Helical Heat Path

Once the igniter was redesigned with the smaller catalyst bed, the second prototype reactor was built. The decrease in catalyst volume leads to a change to off-the-shelf 1-inch

(a) (b)

Fig. 5.11: The 2-inch igniter, assembled prior to testing.

(a) (b)

Fig. 5.12: The 2-inch igniter, showing details of the failure.

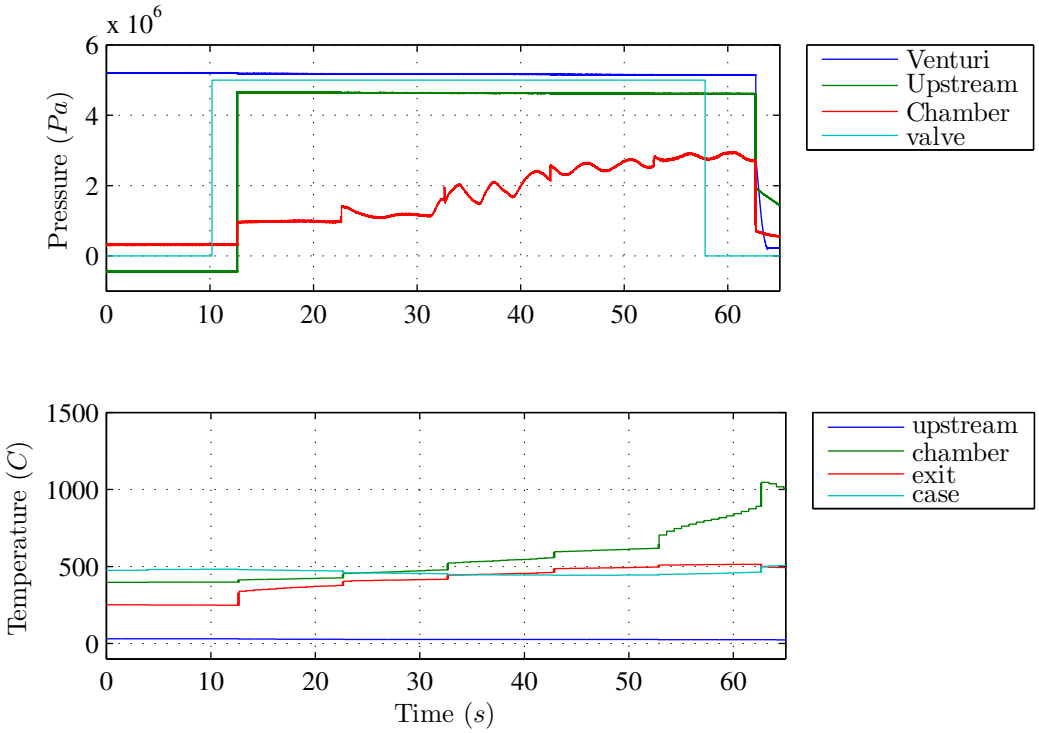

Fig. 5.13: Temperature and pressure for 2-inch prototype test.

(2.54 cm) stainless steel pipe fittings, and as a result, there is no room on the inside for the helical tubing seen in the 2-inch prototype. Also, the decision was made to eliminate copper from inside the catalyst chamber, to prevent another catastrophic failure. Instead, the fluid moves through an external copper helical tube, then into a thin-walled stainless steel tube going through the catalyst chamber, as seen in 5.14. The copper-clad BBs were replaced with stainless steel ball bearings. Figure 5.15 shows the fully assembled prototype reactor. Sub-figure (b) shows the heating tape, as wrapped.

Several tests were performed with the prototype reactor, and all displayed a similar behavior. Figure 5.16 shows a representative test. As can be seen, decomposition did occur in a controlled manner, with an exit flow that gradually increases in temperature. However, the temperature of the nitrous oxide prior to the catalyst bed steadily drops as the exit stream temperature increases. This result indicates that there was insufficient heat transfer

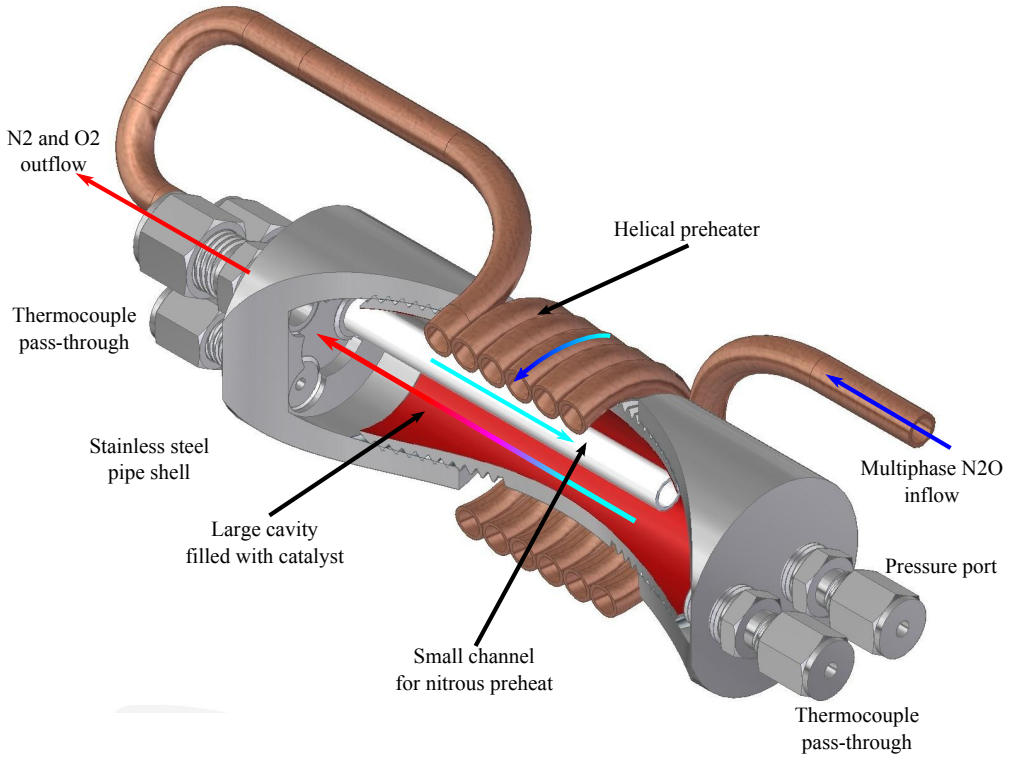

Fig. 5.14: Design of the 1-inch igniter prototype, showing the modified shell and tube heat exchanger.

between the catalyst and the preheater for sustained regenerative decomposition.

Another minor point of failure can be seen in Figure 5.17b. The exit temperatures within the catalyst bed were high enough to not only vaporize the Ruthenium from the alumina pellets, but also to melt the stainless steel mesh containment mesh, effectively gluing the bottom layer of catalyst pellets to the inside of the reactor, and potentially plugging the exit orifice.

The conclusion was that much of the energy required for the nitrous oxide preheat came from the thermal mass of the system, and of the outer stainless steel case, without sufficient regenerative heat transfer.

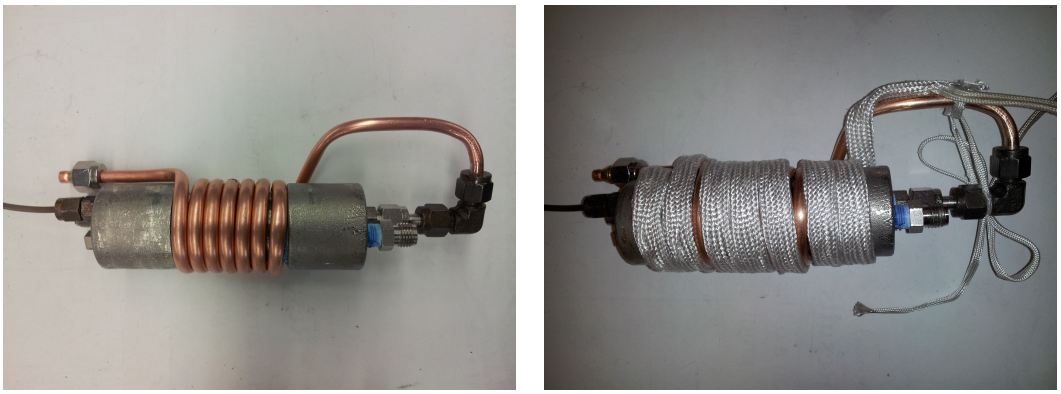

(a) (b)

Fig. 5.15: The 1-inch igniter with external helical copper tubing, assembled prior to testing.

5.4.3 One-Inch Diameter with Graphite Insert

To improve the regenerative heat transfer, a graphite heat exchanger was designed and built to replace the single packed bed of catalyst particles. Instead of a single volume filled with a mix of catalyst pellets and stainless steel spheres, a series of machined graphite pieces split the catalyst bed into four cylindrical chambers, with five small preheater channels running counter-parallel to them. A conceptual drawing of the channels, and the flow path through them, is shown in Fig. 5.18.

Graphite has a much higher thermal conductivity than does stainless steel (81 $^{W}/_{m \cdot K}$ and 16 $^{W}/_{m \cdot K}$, respectively), which aids in the regenerative heat transfer and should improve the regenerative heating of the liquid nitrous oxide. The final machined pieces, and the assembly created by gluing them together with furnace cement,[2] are shown in Fig. 5.19.

Tests with the graphite insert prototype did not perform as expected. Figure 5.20 shows the chamber pressure and temperatures for a representative test. No decomposition occurs, because the initial nitrous oxide stream cannot be heated to acceptable levels. Unfortunately, although graphite has a much higher thermal conductivity than does stainless steel, it also possesses a much lower heat capacitance. The igniter does not have enough thermal mass to transition through the startup transient and preheat the nitrous oxide

[2]Rutlant 2000F Fire Cement, McMaster part number 7573A65

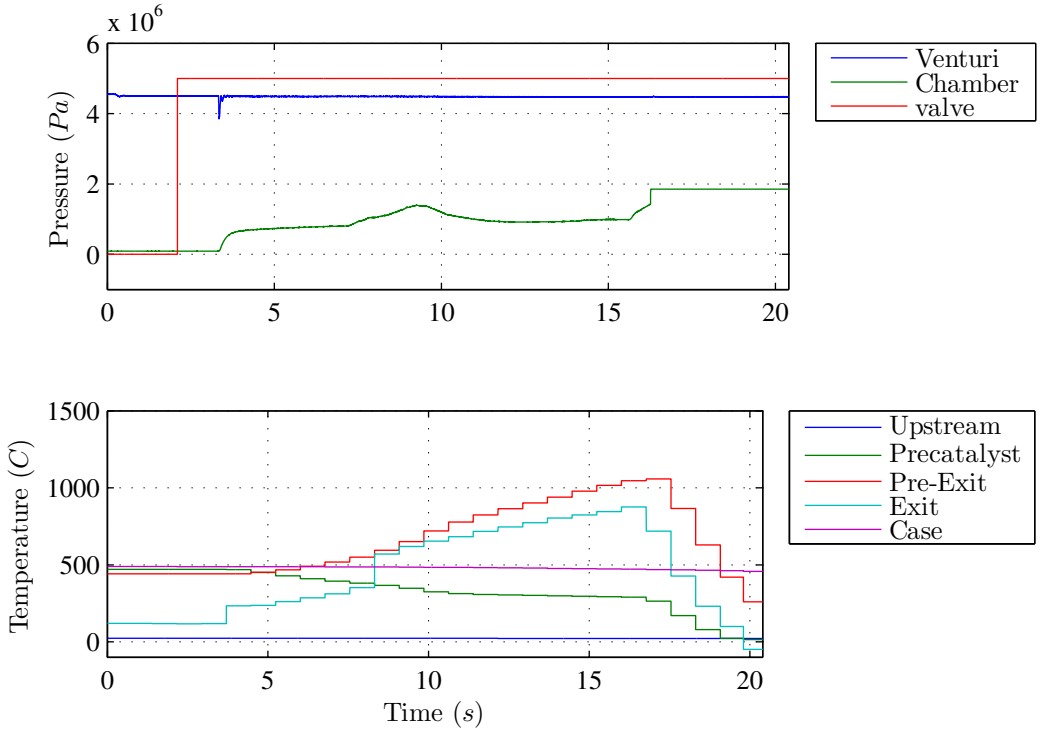

Fig. 5.16: Temperature and pressure for 1-inch helical prototype test.

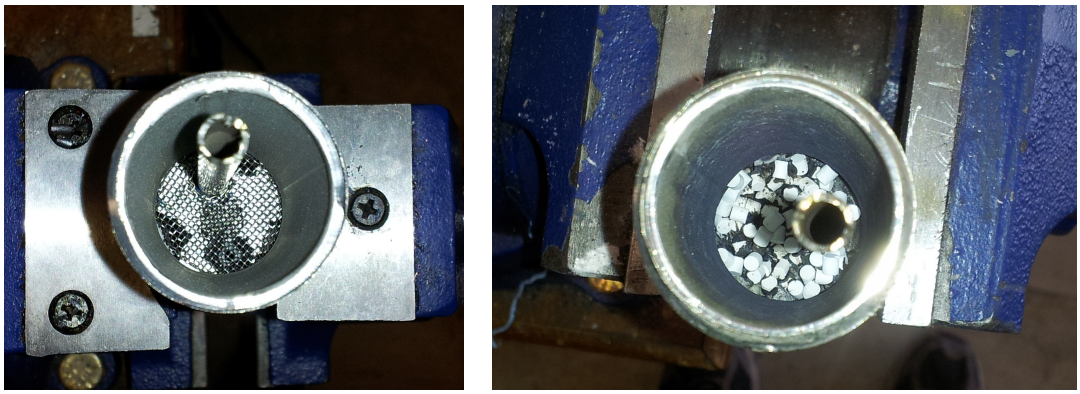

(a) (b)

Fig. 5.17: The 1-inch igniter, showing (a) the internal aft end prior to testing, and (b) the internal aft end after testing.

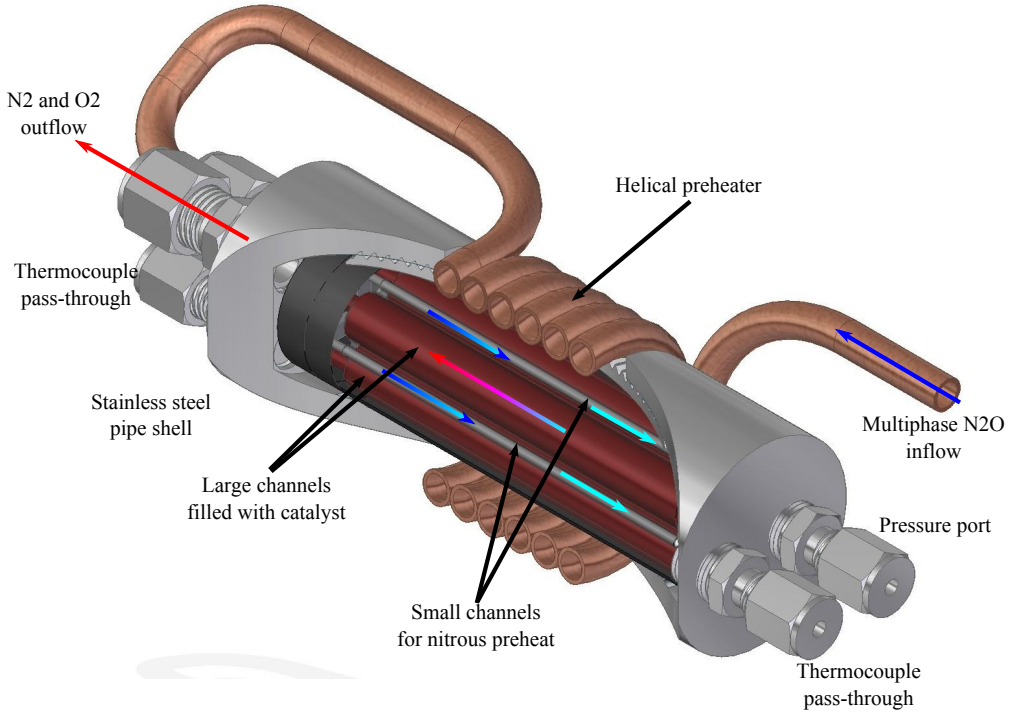

Fig. 5.18: Conceptual view of the internal channels for the graphite heat exchanger.

before decomposition occurs.

5.4.4 One-Inch Diameter with Separate Preheater

As a result of the previous test with the machined graphite heat exchanger, it was determined that a truly regenerative nitrous oxide igniter required a manufacturing method beyond that available for this research. To approximate the effect of a fully regenerative preheater section, a thermal mass bed was inserted into the flow line before the catalyst bed. This new preheater section contained a volume filled with the stainless steel ball bearings and was wrapped with flexible heater elements. The heater elements remained on for the duration of the tests, allowing the N_2O to be preheated by a method other than the regenerative cooling of the catalyst chamber. A schematic of the system is shown in Fig. 5.21.

The tests with the preheater performed significantly better than any of the previous

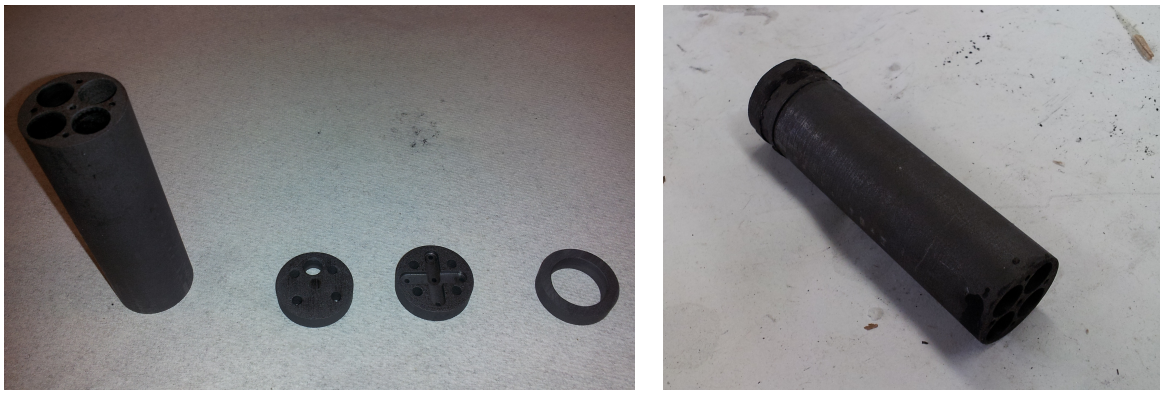

(a) (b)

Fig. 5.19: The graphite heat exchanger, (a) as machined and (b) assembled with furnace cement

prototype reactors. Figure 5.22 shows the data collected from this test. As can be seen, the temperature rise demonstrated a markedly different behavior from the previous tests. Both the Pre-Exit and Exit thermocouples melted due to the much higher decomposition product temperatures.

This design evolution provided sufficient energy output to attempt the ignition of a hybrid motor. The packed bed reactor and separate preheater is the final igniter used to ignite the Chimaera 98 mm hybrid motor, discussed next.

5.5 Hybrid Motor Ignition

The final objective of the research, the ignition of the Chimaera 98 mm hybrid motor, will now be discussed. The ignition of a hybrid motor is significantly more dangerous than the testing of the prototype reactor, thus several pre-hybrid tests were performed, to validate the reactor and hybrid motor assembly. Table 5.4 presents the milestone tests in this section.

5.5.1 Test Objectives

The primary test objective is to demonstrate the ignition of a hybrid motor using the

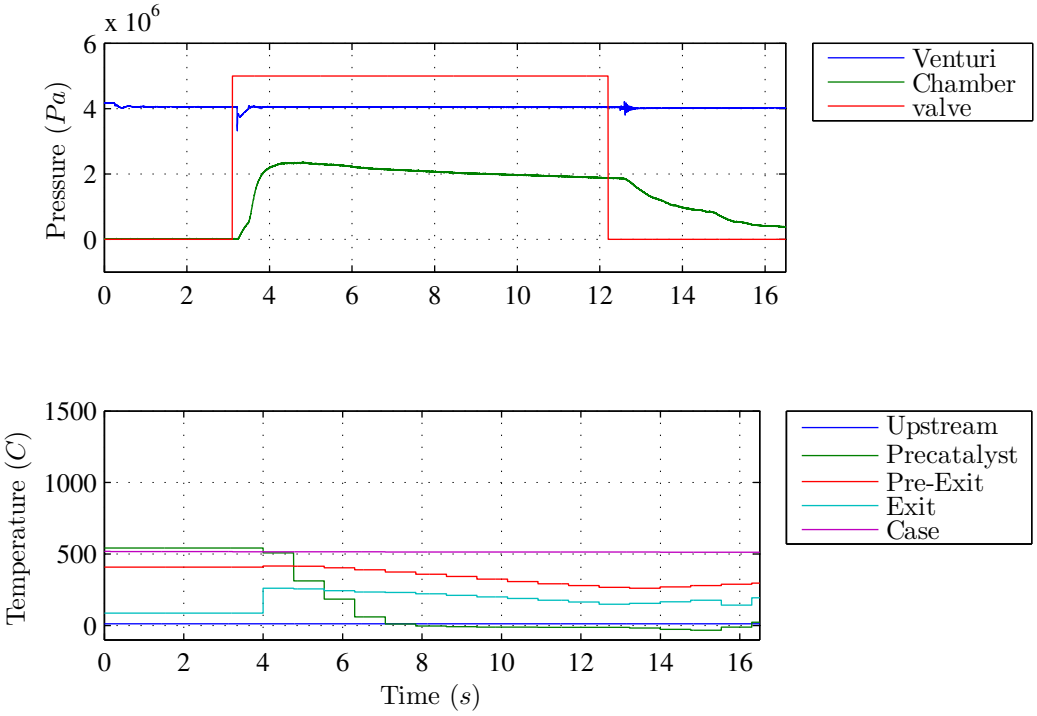

Fig. 5.20: Temperature and pressure for 1-inch graphite insert prototype test.

decomposition energy of nitrous oxide. The final prototype igniter from section 5.4 will be used to ignite a Chimaera hybrid motor, replacing the pyrotechnic igniters currently used. Hybrid motor and decomposition igniter start-up transients will be studied, and the hybrid motor burn profile with the catalytic decomposition igniter is compared to that of a pyrotechnically lit hybrid burn.

5.5.2 Test Hazards and Mitigations

Although hybrid motors are considered very safe, there is still the possibility of a catastrophic failure that can cause large amounts of damage, both to the test setup and to the testing enclosure. Combining a separate catalytic reactor with this type of system only serves to increase the risk of failure, and a list of hazards and mitigations has been compiled, as shown in Table 5.5.

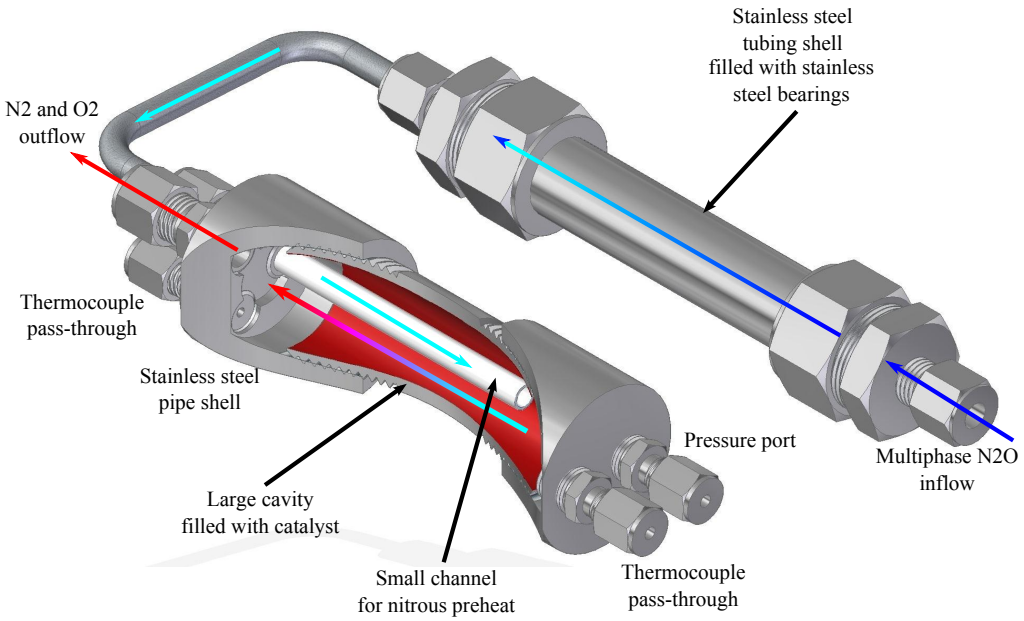

Fig. 5.21: Conceptual view of the internal channels for the graphite heat exchanger.

Table 5.4: Prototype reactors, dates of testing, and test results.

Test Purpose	Date of Conclusive Test	Result
Verification of Reactor / Hybrid Connection	11/7/12	Catastrophic Failure
Verification of Reactor / Hybrid Connection	11/30/12	Successful
Final Hybrid Ignition	12/14/12	Successful

It is possible that the decomposition igniter can accidentally ignite or decompose any free-floating nitrous oxide. Especially during system purges or failed ignition, there is the possibility of large amounts of nitrous oxide vapor to be present within the test cell. The chances of such a failure were deemed very low, but the possibility is still there. Such an event can be avoided by strict attention to a predetermined testing checklist, and by following standard procedures. Both of these were done for the hybrid motor ignitions, and the testing checklists can be found in Appendix B.

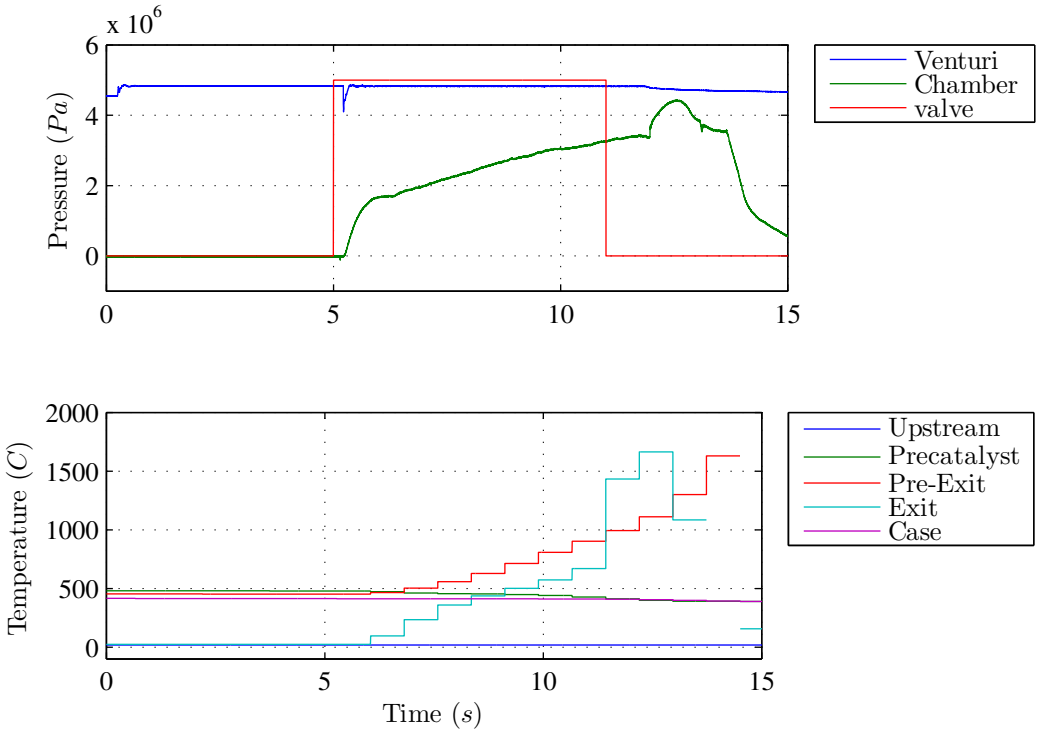

Fig. 5.22: Temperature and pressure for 1-inch Helical prototype test.

There is the possibility of the hybrid motor exploding. The explosion of a hybrid rocket motor is less dangerous than a similar failure in a liquid or solid propellant system, as an explosion of the hybrid system is motivated solely by the chamber pressure, not by any explosive potential of the propellants. Still, a hybrid explosion would be very severe, and must be avoided. Hybrids are not naturally inclined to such failure paths; although "plugging" the nozzle, either by a failed part upstream or a fractured fuel grain will cause an extreme motor overpressure. Another possibility is for the hybrid motor to experience "chugging," where the dynamics of the injection set up a destabilizing oscillation of the chamber pressure. The plugged nozzle risk is mitigated by ensuring that no parts of the decomposition igniter can disconnect and plug the hybrid nozzle, and the likelihood of chugging is reduced by ensuring that both the main motor injector and the igniter flow stream are both choked or nearly choked.

Table 5.5: Hazards and mitigations for the final igniter test.

Hazard	Severity	Likelihood	Mitigation
Hybrid motor explodes	High	Moderate	No additional components capable of plugging motor nozzle, igniter exit choke point
Hybrid motor leaks	High	High	Thorough testing and redesign of the igniter / hybrid connection
Accidental nitrous oxide ignition	Moderate	Low	Proper use of checklists and procedures

The most likely failure path is a "leaking" of the hybrid motor. In a plumbing system, a small leak would not be catastrophic, but in a hybrid motor where the contained gases are hot combustion products, a leak would be disastrous. In effect, the leak becomes another nozzle for the hybrid motor, and can erode away both the motor case and anything the leak is pointed at. The use of a separate catalytic igniter requires a plumbing connection from the exit of the igniter into the hybrid motor, and this connection will be carrying the extremely hot decomposition products through it. To deal with this possibility, several forward enclosure tests were performed with the decomposition reactor firing through the connecting plumbing and into a hybrid motor chamber.

5.5.3 Forward Motor Enclosure Test

The plumbing connection between the igniter and the hybrid motor was of utmost concern. The hot decomposition products from the igniter will be flowing through this narrow tubing for approximately 10 seconds prior to motor firing, and the connection must not leak for the duration of the motor test. There was also concern about plumbing these hot products through the aluminum forward enclosure, and any damage that might be incurred. To test the possibilities without the risks associated with a full hybrid motor test, several forward motor enclosure tests were performed, to qualitatively observe the effects on the associated plumbing.

The procedures for these tests were identical to those for the prototype igniters, with

the only difference being that the reactor was mounted in the proper position for hybrid ignition, including being attached to a hybrid motor case with fuel grain. The main oxidizer flow was disabled, and the exit nozzle of the hybrid motor was removed for these tests, as the primary purpose is to ensure the reliability of the igniter / hybrid plumbing. A minor secondary benefit of these tests is the use of the actual fuel grain within the motor case. If the decomposition igniter is capable of igniting a hybrid motor, the pyrolyzation of the HTPB fuel grain should be readily seen, and this can serve as an indicator of how likely a hybrid motor ignition will be, as well as the exit flow temperature and approximate reactor firing time for ignition.

The hot decomposition products from the reactor began to pyrolyze the fuel, as expected. However, several seconds after pyrolization began, the stainless steel connection tube between the reactor and the hybrid motor disintegrated, causing an immediate test shutdown. A camera was aimed at the exit of the motor for the duration of the test, and Fig. 5.23 shows several example video stills.

In (a), the pyrolyzation of the HTPB fuel grain can clearly be seen, as a faint flame exiting the fuel port along with large amounts of unburned hydrocarbon. The image in (b) is noticeably brighter than (a), due to the failure of the connection tube and the resulting flame coming out near the front end of the motor (off-image). By (c), the catastrophic failure is well under way, and (d) is the aftermath, showing a smoky test cell and the last vestiges of flame from the fuel grain.

Figure 5.24 shows the forward enclosure and the igniter reactor exit after the failed test. The stainless steel pipe fitting comprising the aft end of the reactor has been destroyed by the hot decomposition products passing through it. The proposed solution to the problem is a water-cooled copper connection pipe, with an aluminum oxide inner tube. The copper heat exchanger is shown in Fig. 5.25. A standard water faucet is used as a source of water, which flows through the larger copper pipe over the smaller pipe, soldered in place. The flow rate of the water from the faucet was experimentally measured as $2.5\,{}^{\mathrm{Gal}}/_{\mathrm{min}}$, or $158\,{}^{\mathrm{g}}/_{\mathrm{s}}$. Thus, the cooling effectiveness of the water is

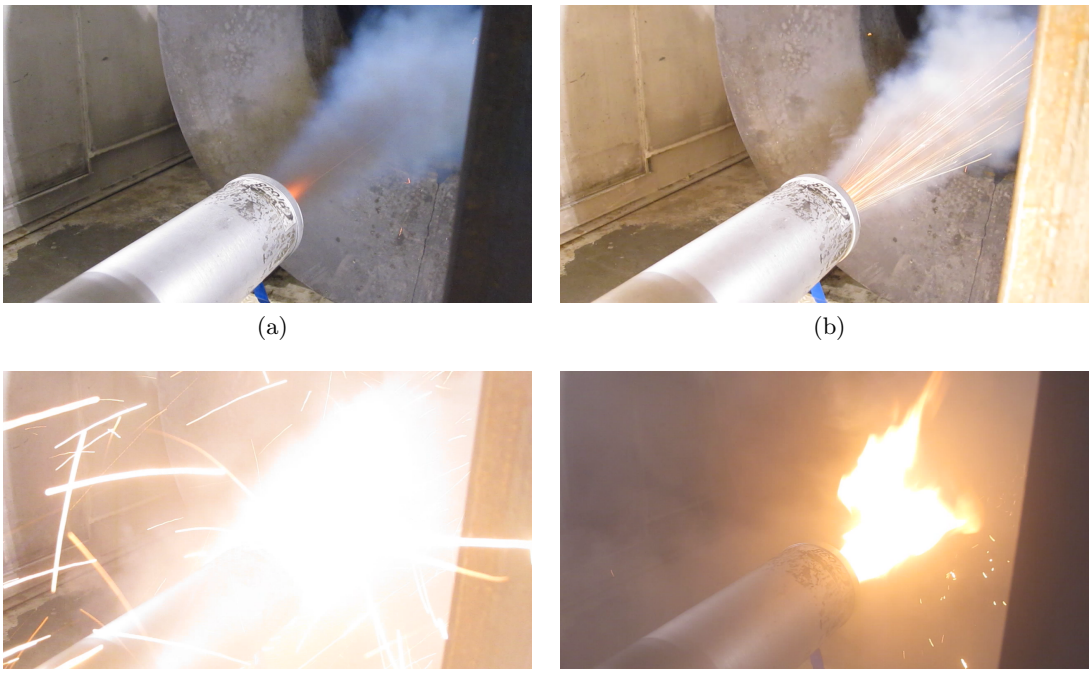

(a) (b)

(c) (d)

Fig. 5.23: Screen captures from the forward enclosure test.

$$158\,\mathrm{g/s} \cdot 4.184\,\mathrm{J/g{\cdot}K} = 660\,\mathrm{W/C} \tag{5.11}$$

For the full decomposition igniter power of 27.97 kW, the water flow would be able to absorb the full power from the reactor with a temperature rise of 41 C. In application the temperature rise will be much less than this, as the purpose of the water cooler is to prevent the destruction of the igniter exit tubing over the length of the burn.

A second forward enclosure test using the water cooled interconnect successfully transfered the decomposition products to the motor chamber, with no damage to the interconnecting pipe or hybrid motor forward enclosure. After a careful examination of all components, the conclusion was reached that the system posed minimal additional hazard to the Chimaera 98 mm hybrid system, and an ignition via nitrous oxide decomposition could be attempted.

(a) (b)

Fig. 5.24: Forward enclosure and decomposition igniter after the failed forward enclosure test.

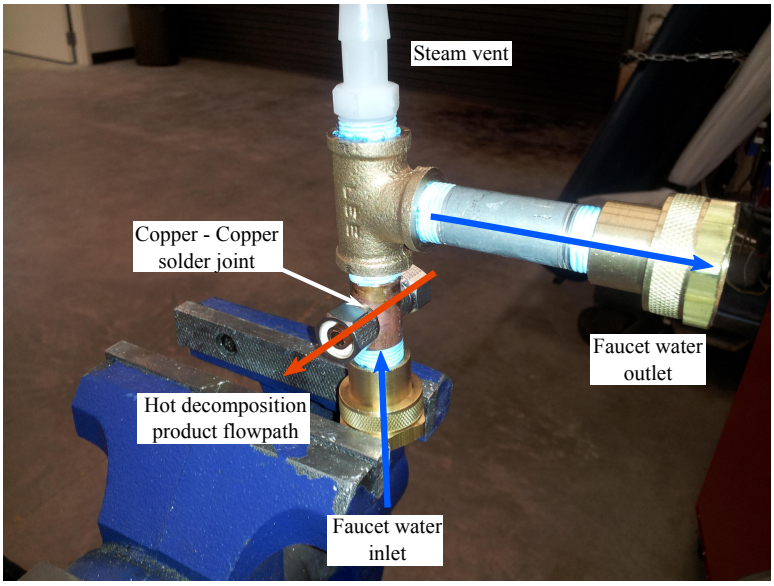

Fig. 5.25: The proposed solution to the igniter / hybrid connection.

5.5.4 Test Procedures

The full hybrid testing procedures are similar to those used for the testing of the prototype reactors. The same LabVIEW VI was written to handle both igniter tests and full hybrid tests. A summary of the testing procedures is as follows:

1. The hybrid motor and igniter reactor are assembled and mounted on the MoNSTeR cart. All plumbing fittings between them and the MoNSTeR cart are made, and the MoNSTeR cart and NiBBLeR cart wheeled into the JETC and bolted into the thrust plate. All electrical connections are made, and the plumbing and wiring is inspected to ensure proper functionality. The test computer is powered on, and the data aquisition system is verified to be running and capturing real data.

2. The high-temperature heating elements surrounding the igniter reactor are used to preheat the catalyst bed to the desired temperature.

3. Once the igniter has reached a steady-state temperature, the nitrous oxide, nitrogen top pressurant, and carbon dioxide bottles are opened, and the plumbing system is prefilled with liquid N_2O. The test cell is evacuated in preparation of reactor firing.

4. Following a countdown, the test sequence is initiated. After a 5 second delay, the igniter valve opens, and nitrous oxide begins flowing through the igniter reactor. All of the reactor chamber temperatures and pressures are recorded, as well as the standard data for the hybrid motor, including the thrust levels, chamber pressure, and flow rates.

5. Main oxidizer flow for the hybrid motor can be initiated in two ways. First, the exit temperature of the igniter reactor is measured using a type K large bead thermocouple threaded through the motor nozzle and to the top of the fuel grain; if this thermocouple goes out of range, the thermocouple has been destroyed by the hot exhaust temperatures, and the main motor starts. Second, if for any reason pyrolysis of the fuel grain is occuring and the thermocouple ignition did not work, the test instructor can manually initiate the main oxidizer flow and begin the hybrid motor test.

6. After the main oxidizer valve opens, the test proceeds for 2.5 seconds. This is sufficient to demonstrate the ignition capabilities of the decomposition reactor. Longer burn times are not beneficial for the purpose of this test, and have the potential to make a catastrophic failure worse. At the end of the motor burn, the system proceeds as for a standard Chimaera hybrid motor test: the main oxidizer valve closes, the feed lines are purged of nitrous oxide, and the motor chamber is purged with CO_2.

For the full hybrid test the test instructor followed a testing checklist, included in Appendix B.

5.5.5 Test Results

On December 13, 2012, the final hybrid motor ignition test occured, and the test data for the burn is shown in Fig. 5.26. After the initial 5 second delay, followed by an additional 5 seconds for igniter ramp-up, the hybrid motor was ignited via the thermocouple trigger, and fired successfully for 2.5 seconds. The hybrid motor chamber pressure behaved similarly to an Estes-ignited Chimaera motor. It is of note that the igniter chamber pressure was in fact lower than that of the hybrid motor during the igniter ramp-up. The igniter massflow is also slightly higher than was expected. This data is consistent with an exit orifice that is oversized, possibly as a result of nozzle erosion during the forward enclosure tests.

Figure 5.27 shows several screen captures from the video of the final test, showing the progression from fuel pyrolysis, to a small flame identical to that of the forward enclosure tests, followed immediately by main oxidizer flow and hybrid ignition.The time delay between open flame and hybrid ignition was exceptionally short; a single frame of the test video shows the small flame caused by the decomposition igniter.

The start-up transient of the Chimaera motor lit by decomposition was compared to a start-up transient of a nominal Estes lit 98 mm test; focused views of the period of interest in the chamber pressure profiles are shown in Fig. 5.28b. The time scale is referenced to the opening of the main motor valve. The beginning of HTPB pyrolysis can be seen in 5.28a approximately 0.5 seconds before main valve opening as a small pressure increase. From

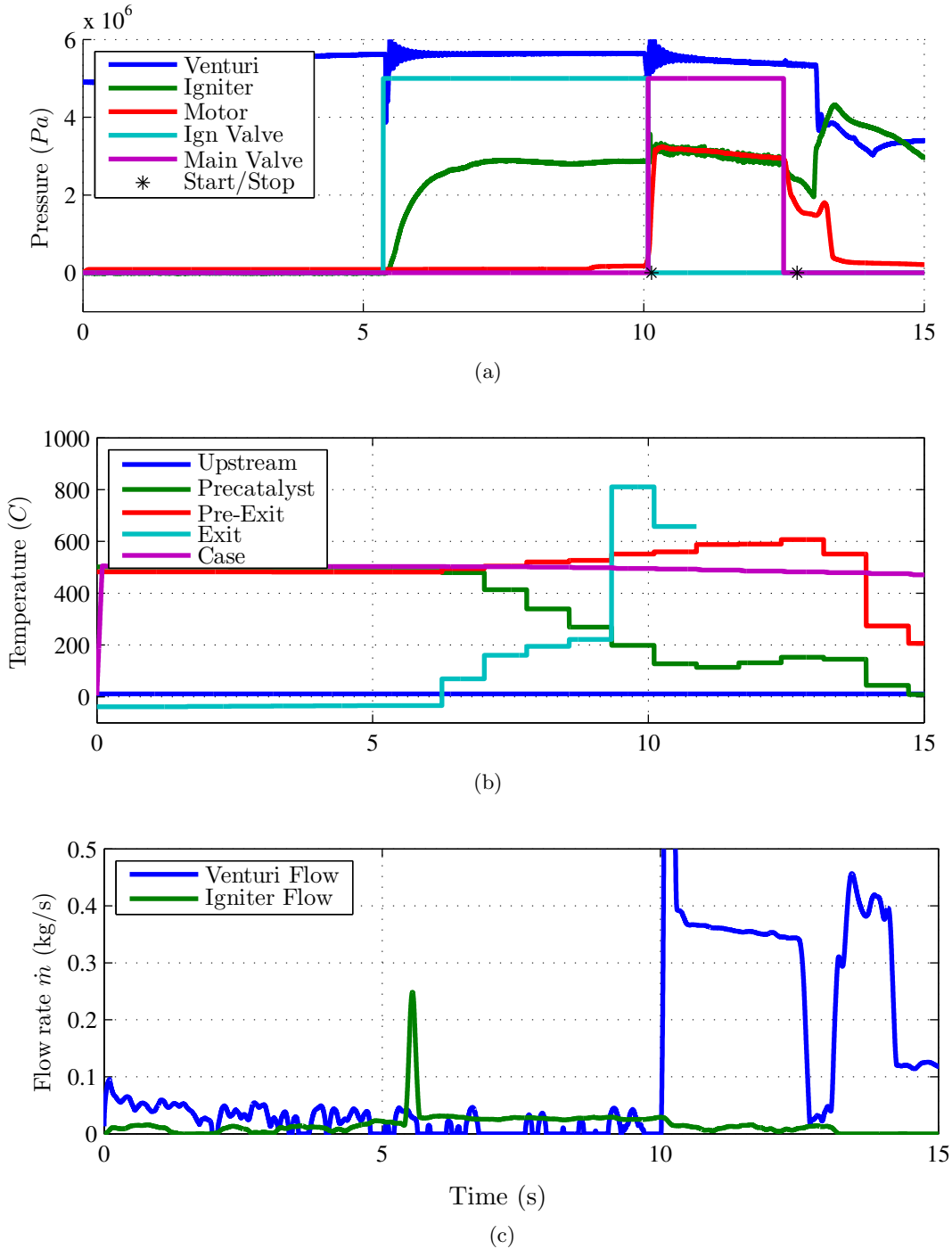

Fig. 5.26: Temperatures, pressures, and mass flow rates for the final hybrid motor ignition

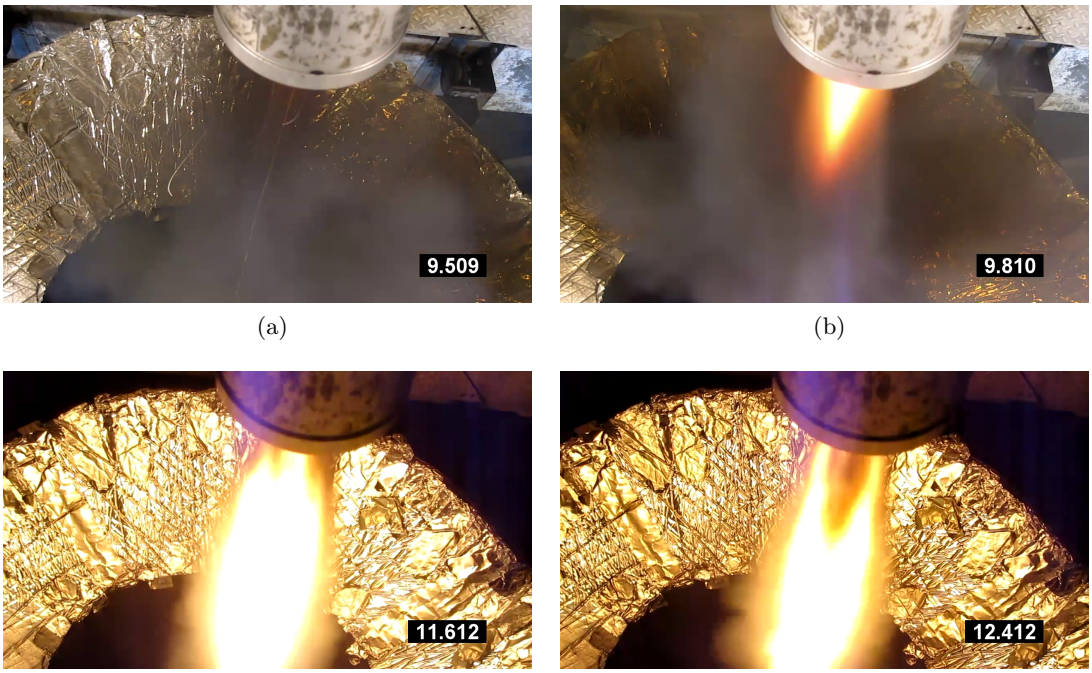

(a) (b)

(c) (d)

Fig. 5.27: Screen captures from the final hybrid ignition test.

careful viewing of the test video, this is the region of time where the motor exit products are smoke, but no visible flame is present. From the time of commanded oxidizer start, the motor burn via decomposition ignition experiences pressure ramp up a full 0.25 seconds before the traditionally lit motor. A much larger initial overpressure is present in the decomposition-lit hybrid motor, possibly as a result of the very fuel-rich pyrolysis products already filling the combustion chamber. However, within ~ 0.1 seconds, both motors take on a similar pressure profile, indicating that the decomposition ignition process only affects the ignition transient as expected.

The catalytic decomposition ignition test was deemed to be successful, with the ignition of the hybrid motor clearly demonstrated. Pressure profiles and mass flow rates were within expected ranges, and the

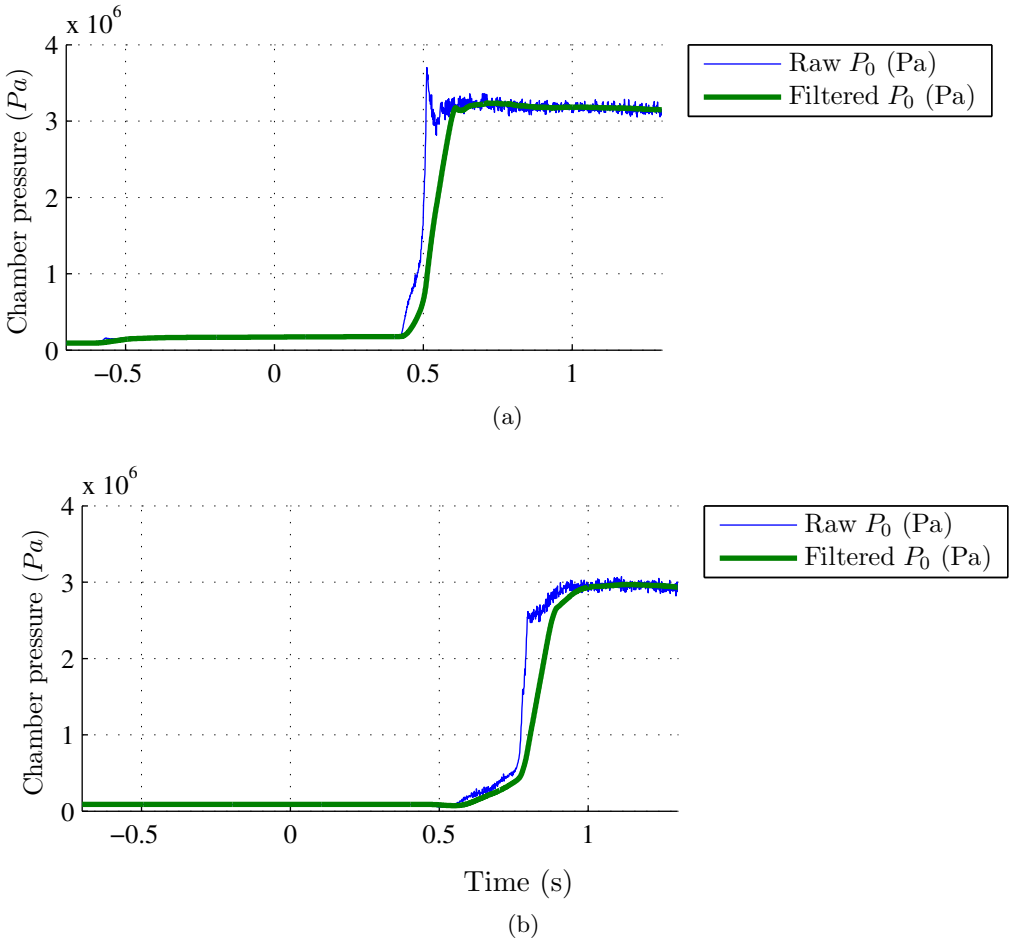

Fig. 5.28: Comparison of start-up transients for Chimaera motors lit (a) via decomposition igniter, and (b) via Estes igniter.

CHAPTER 6
CONCLUSIONS

With the increasing commercial and private interests in space access, the future of space propulsion technology lies with options that are less complex, less expensive and less hazardous to manufacture and operate. Technologies that can produce propulsion systems that fit these criteria are already receiving interest, and will continue to do so. The catalytic decomposition of nitrous oxide has been proposed as a "green" alternative ignition source that complies with these new guidelines. Such an ignition system would be practical for liquid bipropellant and hybrid systems that already use nitrous oxide as the oxidizing fluid.

The primary objective of the research has been to directly demonstrate the feasibility of a N_2O decomposition igniter by using an ignition system to light a hybrid motor. A hybrid motor system previously developed at Utah State University was used as a test article for the new ignition system. An ignition system has been designed and built, and a hybrid motor has been lit via the hot decomposition products. To the author's knowledge, this is the first time the success of such a system has been demonstrated.

6.1 Research Activity

Previous research into catalysts was studied for the objective of choosing a proper nitrous oxide decomposition catalyst. The industry-standard S-405 catalyst for hydrazine was considered, as were modern catalyst formulations, including hexa-aluminates. A comprehensive trade study led to a commercially-available catalyst composed of ruthenium deposited on alumina pellets as the final catalyst material used. The catalyst was evaluated at a range of temperatures and pressures to determine the decomposition properties, as well as the minimum and maximum useable temperature of the catalyst.

A one-dimensional simulation of an igniter system has been completed, consisting of a MATLAB implementation of a thermal model developed for the research. The algorithm

has been applied to the catalytic igniter design, assisting in the designing and sizing of the final ignition system. Using this tool, several prototype igniters have been built and tested. Each system provided valuable information on the key characteristics a functional igniter must have, and the culmination of the prototype testing phase was an igniter design capable of igniting a hybrid motor safely and consistently.

Finally, the newly developed ignition system was integrated into a pre-existing hybrid rocket motor system. Further tests were performed to ensure that the nitrous oxide decomposition reactor could be used safely and reliably, with no additional risk to the motor system. The possible hazards of the decomposition igniter were considered, and the risks associated with the decomposition igniter were mitigated as best as possible. Only after these steps were completed, the decomposition igniter was used to successfully ignite a hybrid motor.

The hybrid motor performance was shown to be minimally affected by the new ignition system, and the ignition process via N_2O decomposition has been shown to be a safe and effective method of initiating combustion.

6.2 Future Research

This research has investigated the possibility of using the catalytic decomposition of nitrous oxide as a method to ignite a liquid or hybrid bipropellant system that already uses N_2O as the oxidizer. The ignition of a hybrid motor using this method has been achieved, and demonstrates the feasibility of the approach. However, this research has also identified areas of supporting technology that are lacking, and suitable solutions will need to be found in order to make this method truly feasible. The areas of this design that are particularly in need of further study are:

- Catalyst development, focusing on a catalyst that has a higher heat tolerance than the Ruthenium/Alumina pellets used. Other characteristics, including lower activation temperatures and better packing densities, would also be beneficial.

- Application of more advanced manufacturing methods, to correctly balance the heat

transfer rate from the catalyst chamber into the preheater section. For this research, budget constraints limited the experiments to systems that could be easily built and iterated; future work that is not hindered by such constraints could utilize methods such as micromachining and powder sintering to produce more efficient igniters.

Combining both catalyst and advanced manufacturing, a feasible igniter can be built. Design goals should be to make a fully reusable igniter, with little to negligible deterioration for each firing, and to make an igniter with a low thermal mass and thermal dissipation, to minimize the necessary input power for preheating the combustion chamber.

6.3 Research Conclusions

This paper has investigated the application of nitrous oxide, an inexpensive, non- explosive, safe-handling, and readily available propellant, as an ignition fluid for liquid and hybrid rocket systems that use nitrous oxide as the primary oxidizer. The concept of hybrid rocket motor ignition using nitrous oxide decomposition is introduced, to fulfill the growing need for a hybrid ignition system that is reusable and indefinitely storable. A variety of possible catalysts have been considered, and a commercially available rhodium/alumina catalyst was chosen for a demonstration igniter. Catalyst activity tests were performed to study the properties of the rhodium/alumina catalyst, and MATLAB algorithm was written to study the thermodynamics of a regenerative igniter. Using the knowledge learned from the catalyst tests and the numerical model, a nitrous oxide decomposition igniter has been built and tested. Finally, the experimentally-validated igniter was used to successfully ignite a 98 mm hybrid motor. Nitrous oxide catalysis as a method for rocket motor ignition has been experimentally shown to be feasible.

REFERENCES

[1] Haeseler, D., Bombelli, V., Vuillermoz, P., Lo, R., Marée, T., and Caramelli, F., "Green Propellant Propulsion Concepts for Space Transportation and Technology Development Needs," *Proceedings of the 2nd International Conference on Green Propellants for Space Propulsion*, No. ESA SP-557, Cagliari, Sardinia, Italy, June 2004, p. p.4.1.

[2] Bombelli, V., "Economic Benefits for the Use of Non-toxic Monopropellants for Spacecraft Applications," *39th AIAA/ASME/SAE/ASEE Joint Propulsion Conference and Exhibit*, No. AIAA-2003-4783, Huntsville, AL, July 2003.

[3] Anon., "Department of Defense Interface Standard, Eletromagnetic Environmental Effects requirements for Systems, MIL-STD-464," October 2012.

[4] Bonanos, A. M., Schetz, J. A., O'Brien, W. F., and Goyne, C. P., "Dual-Mode Combustion Experiments with an Integrated Aeroramp-Injector/Plasma-Torch Igniter," *Journal of Propulsion and Power*, Vol. 24, No. 2, March - April 2008, pp. 267–273.

[5] Anon., "SpaceX, Updates: February 2005-May 2005," October 2012.

[6] Traxler, J. J., "Saturn IB/Centaur Propulsion Systems Compatibility Study," Tech. Rep. TN-AE-65-106, Chrysler Space Division, New Orleans LA, August 1965.

[7] Rudman, T. J., and Austad, K. L., "The Centaur Upper Stage Vehicle," *Proceedings of the 4th International Conference on Launcher Technology "Space Launcher Liquid Propulsion"*, Liege Belgium, December 2002.

[8] Anon., "Occupational Safety and Health Guideline for Nitrous Oxide," March 2012.

[9] Rhodes, G. W., "Investigation of Decomposition Characteristics of Gaseous and Liquid Nitrous Oxide," Tech. Rep. AD-784 602, Air Force Weapons Laboratory, Kirtland AFB, New Mexico, July 1974.

[10] Lide, D., *CRC Handbook of Chemistry and Physics*, CRC Press, Boca Raton, 76th ed., 1995.

[11] Zakirov, V., Sweeting, M., Goeman, V., and Lawrence, T., "Surrey Research on Nitrous Oxide Catalytic Decomposition for Space Applications," *14th AIAA/USU Conference on Small Satellites*, No. SSC00-XI-6, Logan, UT, August 2000.

[12] Nagamachi, M. Y., Oliveira, J. I., Kawamoto, A. M., and Dutra, R. C., "ADN - The New Oxidizer Around the Corner for an Environmentally Friendly Smokeless Propellant," *Journal of Aerospace Technology Management*, Vol. 1, No. 2, December 2009, pp. 153–160.

[13] Venkatachalam, S., Santhosh, G., and Ninan, K. N., "An Overview on the Synthetic Routes and Properties of Ammonium Dinitramide (ADN) and other Dinitramide Salts," *Journal of Propellants, Explosives, Pyrotechnics*, Vol. 29, No. 3, March 2004, pp. 178–187.

[14] Pembridge, J. R., and Stedman, G., "Kinetics, Mechanism, and Stoicheiometry of the Oxidation of Hydroxylamine by Nitric Acid," *Journal of Chemical Society, Dalton Transactions*, Vol. 11, 1979, pp. 1657–1663.

[15] Rheingold, A. L., Cronin, J. T., Brill, T. B., and Ross, F. K., "Structure of Hydroxylammonium Nitrate (HAN) and the Deuterium Homolog," *Acta Crystallographica*, Vol. 43, No. 1, 1987, pp. 402–404.

[16] Atkins, P. W., and Jones, L. L., *Chemistry: Molecules, Matter, and Change*, W. H. Freeman and Company, New York, 1997.

[17] Hunter, E., "The Thermal Decomposition of Nitrous Oxide at Pressures up to Forty Atmospheres," *Proceedings of the Royal Society*, Vol. 144, No. 1, 1934, pp. 386–412.

[18] Altman, D., "Hybrid Rocket Development History," *27th AIAA, SAE, ASME, and ASEE, Joint Propulsion Conference*, 1991.

[19] Schmidt, E. W., *Hydrazine and its Derivatives: Preparation, Properties, Applications, Second Edition*, Vol. 2, Wiley-Interscience, New York, 2nd ed., 2001.

[20] Sutton, G. P., and Biblarz, O., *Rocket Propulsion Elements*, Wiley, New York, 7th ed., 2001.

[21] Choudhary, G., IIansen, H., Donkin, S., and Kirman, C., "Toxicological Profile for Hydrazines," Tech. Rep., US Department of Health and Human Services Public Health Service Agency for Toxic Substances and Disease Registry (ATSDR), Atlanta, GA, 1997, pp. 1-224.

[22] Schmidt, E. W., *Hydrazine and its Derivatives: Preparation, Properties, Applications*, Vol. 1, Wiley-Interscience, New York, 2nd ed., 2001.

[23] Zilliac, G., and Karabeyoglu, M. A., "Modeling of Propellant Tank Pressurization," *41st AIAA/ASME/SAE/ASEE Joint Propulsion Conference & Exhibit*, No. AIAA-2005-3549, Tucson, AZ, July 2005.

[24] Wernimont, E. J., "System Trade Parameter Comparison of Monopropellants: Hydrogen Peroxide vs Hydrazine and Others," *42nd AIAA/ASME/SAE/ASEE Joint Propulsion Conference & Exhibit*, No. AIAA-2006-5235, Sacramento, CA, July 2006.

[25] Anon., "Occupational Health Guidelines for Hydrogen Peroxide," US Department of Health and Human Services Bulletin 0335 [online], http://www.cdc.gov/niosh/docs/81-123/pdfs/0335.pdf, [retrieved 15 November 2012].

[26] Janovsky, R. S., "HAN-Based Monopropellant Assessment for Spacecraft," Tech. Rep. TM-107287, National Aeronautics and Space Administration, July 1996.

[27] Anon., "ECAPS, Moog and ATK Announce Partnership to Bring High Performance Green Propulsion (HPGP) Technology to the US Space Propulsion Market," A-ZET.org [online], http://www.a-zet.org/aerospace-industry-and-business-news/market-monitor/393-ecaps-moog-and-atk-announce-partnership-to-bring-high-performance-green-propulsion-hpgp-technology-to-the-us-space-propulsion-market.html [retrieved 12 September 2012].

[28] Goldstein, E., "The Greening of Satellite Propulsion," *Aerospace America*, February 2012, pp. 26–28.

[29] Pokrupa, N., Anglo, K., and Svensson, O., "Spacecraft System Level Design with Regards to Incorporation of a New Green Propulsion System," *46th AIAA/ASME/SAE/ASEE Joint Propulsion Conference and Exhibit*, No. AIAA-2011- 6129, San Diego, CA, July - August 2011.

[30] Persson, M., Anflo, K., and Dinardi, A., "A Family of Thrusters For ADN-Based Monopropellant LMP-103S," *48th AIAA/ASME/SAE/ASEE Joint Propulsion Conference & Exhibit*, No. AIAA-2012-3815, Atlanta, GA, July - August 2012.

[31] Klein, N., and Stiefel, L., "Liquid Propellants for Use in Guns," *Gun Propulsion Technology, Progress in Astronautics and Aeronautics*, Vol. 109, 1988.

[32] Anon., "Liquid Propellant 1846 Handbook," Tech. Rep., Jet Propulsion Laboratory, U.S. Department of the Army, ARDEC, Picatinny Arsenal, July 1994.

[33] Freedman, E., and Stiefel, L., "Thermodynamic Properties of Military Gun Propellants," *Gun Propulsion Technology, Progress in Astronautics and Aeronautic*, Vol. 109, 1988.

[34] Decker, M., N., K., Freedman, E., Leveritt, C., and Wojciechowski, J., "HAN-Based Liquid Gun Propellants: Physical Properties," Tech. Rep. BRL-TR-2864, U.S. Army Ballistic Research Laboratory, Aberdeen Proving Ground, MD, 1987.

[35] Meinhart, D., "Selection of Alternate Fuels for HAN-BASED Monopropellants," *27th JANAFF PDCS and 16th S&EPS Joint Meeting, CPIA Pibl. 674*, Vol. 1, April 1998, pp. 143–147.

[36] Hurlbert, E., Applewhite, J., Nguyen, T., Reed, B., Zhang, B., and Wang, Y., "Nontoxic Orbital Maneuvering and Reaction Control Systems for Reusable Spacecraft," *Journal of Propulsion and Power*, Vol. 14, No. 5, 1998, pp. 676–687.

[37] Haeseler, D., Gotz, A., and Frohlich, A., "Non-Toxic Propellants for Future Advanced Launcher Propulsion Systems," *36th AIAA/ASME/SAE/ASEE Joint Propulsion Converence and Exhibit, July 2000*.

[38] Bombelli, V., Simon, D., Maree, T., and Moerel, J.-L., "Economic Benefits of the use of Non-Toxic Mono-Propellants for Spacecraft Applications," *39th Joint Propulsion Conference, Huntsville, Ala. July 2003*.

[39] Anon., "Space Shuttle Solid Rocket Boosters," February 2013.

[40] Anon., "Hazard Analysis of Commercial Space Transportation; Vol. 1: Operations, Vol. 2: Hazards, Vol. 3: Risk Analysis," *U.S. DOT, PB93-199040, Accession No. 00620693*, 1988.

[41] Dougherty, Jr., N. S., and Rafferty, C. A., "Altitude Developmental Testing of the J-2 Rocket Engine in Propulsion Engine Test Cell (J-4)," Tech. Rep. AEDC Interim Report, Accession Number AD0848188, February 1969, url: http://handle.dtic.mil/100.2/AD0848188 [retrieved 28 January 2013].

[42] Dumoulin, J., "Solid Rocket Boosters," NASA Kennedy Space Center [online], url: http://science.ksc.nasa.gov/shuttle/technology/sts-newsref/srb.html [retrieved 2 February 2013].

[43] Campbell, P. B., (To Lockheed Aircraft Corporation), "Starter for Rocket Motor," U.S. Patent 3,116,599, January 7, 1964.

[44] Bradford, J. N., and Jones, R. A., (To The United States Air Force), "Hybrid Rocket Motor Ignition System," U.S. Patent 3,518,828, July 7, 1970.

[45] Holtzmann, A. L., (To United Aircraft Corporation), "Hybrid Demonstrator," U.S. Patent 3,156,092, November 10, 1964.

[46] Rosenfield, G. C., (To Aerotech, Inc.), "Pyrotechnic Valve, Igniter, and Combustion Preheater for Hybrid Rocket Motors," U.S. Patent 5,579,636, December 3, 1996.

[47] Kannan, S., and Swamy, C. S., "Catalytic Decomposition of Nitrous Oxide on In Situ Generated Thermally Calcined Hydrotalcites," *Applied Catalyst B: Environmental*, Vol. 3, 1994, pp. 109–116.

[48] Kapteijn, F., Rodriguez-Mirasol, J., and Moulijn, J. A., "Heterogeneous catalytic decomposition of nitrous oxide," *Applied Catalysis B: Environmental*, Vol. 9, 1996, pp. 25–64.

[49] Kawi, S., Liu, S. Y., and Shen, S.-C., "Catalytic decomposition and reduction of N2O on Ru/MCM-41 catalyst," *Catalysis Today*, Vol. 68, 2001, pp. 237–244.

[50] Yuzaki, K., Yarimizu, T., Ito, S., and Kunimori, K., "Catalytic Decomposition of N2O Over Supported Rhodium Catalysts: High Activities of Rh/USY and Rh/Al2O3 and the Effect of Rh Precursors," *Catalysis Letters*, Vol. 47, 1997, pp. 173–174.

[51] Zeng, H. C., and Pang, X. Y., "Catalytic Decomposition of Nitrous Oxide on Alumina-Supported Ruthenium Catalysts Ru/Al203," *Applied Catalysis B: Environmental*, Vol. 13, 1997, pp. 113–122.

[52] Santiago, M., and Perez-Ramirez, J., "Decomposition of N2O over Hexaaluminate Catalysts," *Environmental Science and Technology*, Vol. 41, 2007, pp. 1704–1709.

[53] Zakirov, V., Lawrence, T. J., Sellers, J. J., and Sweeting, M. N., "Nitrous Oxide as a Rocket Propellant for Small Satellites," *Proceedings of the 5th International Symposium on Small Satellite Systems and Services*, France, 2000, pp. 19–23.

[54] Zakirov, V., Richardson, G., and Sweeting, M., "Surrey Research Update on Nitrous Oxide Catalytic Decomposition for Space Applications," *37th AIAA/ASME/-SAW/ASEE Joint Propulsion Conference*, No. AIAA-2001-3922, 2001, pp. 8–11.

[55] King, S. M., Marx, P. C., and Taylor, D., "The Aerospace Corporation Shell 405 Catalyst Evaluation Program, Volume I: Physical and Catalytic Properties," Tech. Rep. Aerospace Report No. TR-066 (5210-10)-4, Vol. 1, USAF Report No. SAMO-TR-271, Vol. I, August 1969.

[56] McRight, P., Popp, C., Pierce, C., Turpin, A., Urbanchock, W., and Wilson, M., "Confidence Testing of Shell 405 and S-405 Catalysts in a Monopropellant Hydrazine Thruster," *41st AIAA/ASME/SAE/ASEE Joint Propulsion Conference*, No. AIAA 2005-0205-849, Tucson, AZ, July 2005.

[57] Anon., "Total Propulsion Solutions," Tech. Rep. 2006-H-3391, AeroJet, Redmond Operations, June 2007.

[58] Baker, A. M., and Gibbon, D., "Catalytic Decomposition of Nitrous Oxide," Tech. Rep. SPDB-38569-03, Surrey Satellite Technology, Ltd., European Office of Aerospace Research & Development (EOARD), June 2003.

[59] Wickham, D. T., Hitch, B. D., and Logsdon, B. W., "Development and Testing of a High Temperature N20 Decomposition Catalyst," *AIAA 2010-7128*, 2010.

[60] Hitch, B. D., and Wickham, D. T., "Design of a Catalytic Nitrous Oxide Decomposition Reactor," *AIAA 2010-7129*, 2010.

[61] Zhu, S., Wang, X., Wang, A., and Zhang, T., "Superior Performance of Ir-Substituted Hexaaluminate Catalysts for N2O Decomposition," *Catalysis Today*, Vol. 131, 2008, pp. 339–346.

[62] Anon., "Hydroxyl Terminated Polybutadiene Resins and Derivatives," *Sartomer Product Bulletin*, March 2006.

[63] Anon., "PAPI 94 Product Information," *Dow Plastics Form No. 109-00707-801XQRP*, August 2001.

[64] Brown, M. E., and Rugunanan, R. A., "A Temperature-Profile Study of the Combustion of Black Powder and Its Constituent Binary Mixtures," *Propellants, Explosives, Pyrotechnics*, Vol. 14, No. 2, April 1989, pp. 69–75.

[65] Dyer, J., Doran, E., Dunn, Z., Lohner, K., Zilliac, G., and Cantwell, B., "Modeling Feed System Flow Physics for Self Pressurizing Propellants," *AIAA 2007-5702*, 2007.

[66] Lemmon, E. W., and Span, R., "Short Fundamental Equations of State for 20 Industrial Fluids," *Journal of Chemical Engineering Data*, Vol. 51, 2006, pp. 785–850.

[67] Span, R., and Wagner, W., "Equations of State for Technical Applications. I. Simultaneously Optimized Functional Forms for Nonpolar and Polar Fluids," *International Journal of Thermophysics*, Vol. 24, No. 1, 2003, pp. 1–39.

[68] Span, R., and Wagner, W., "Equations of State for Technical Applications. III. Results for Polar Fluids," *International Journal of Thermophysics*, Vol. 24, No. 1, 2003, pp. 111–162.

APPENDICES

Appendix A
THERMODYNAMIC CALCULATION

A.1 Algorithm

The numerical algorithm was written to implement the mathematical models developed in section 5.2.2 into a MATLAB script, for the purpose of determining orifice sizes, mass flow rates, and operating parameters for proper igniter function.

From the initial properties, including the initial nitrous oxide porperties, the desire chamber pressure and outlet pressure, and the fass flow rate through the system, the properties of the nitrous oxide flow at each key point in Fig, A.1 are found. The solver proceeds down the flow path, using the properties from the previous point, and the known changes, to find the flow properties for the next point. The key points, and the calculations to progress, are:

1. The nitrous oxide inlet. At least two of the thermodynamic properties of the flow here must be given, to fully define the nitrous oxide state. In addition, the mass flow rate through the reactor is defined, as well as the chamber pressure and exit pressure.

2. Using the NHNE model, the mass flux necessary through the orifice is calculated, given the upstream properties and the downstream pressure. Independently, the properties downstream of the orifice are calculated using isenthalpic relations. It is important to note that although the flow relation between (1) and (2) is isenthalpic, the flow is assumed to be isentropic from inlet to the minimum area of the orifice. From the mass flux, the desired area of the upstream orifice is calculated.

3. The post-catalyst properties are then determined, modeling the decomposition process as a pure enthalpy increase, as well as a small specified pressure drop, estimated to be 3 kPa based upon the characterization tests. The minor point (2.5) is not explicitly calculated from the heat transfer rates; instead a necessary temperature for

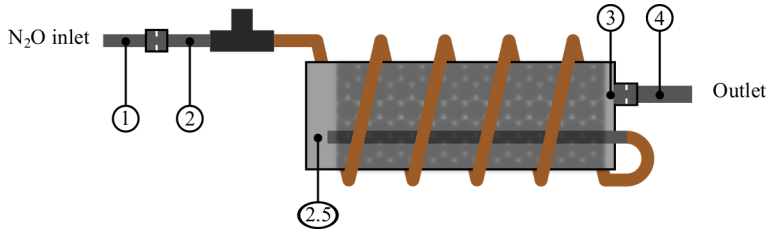

Fig. A.1: Diagram of the system analyzed by the numerical algorithm, showing key flow points.

catalyzation is assumed, and the heating power required to reach this temperature is calculated. The exit gas is no longer a pure gas at this point, being instead comprised of molecular oxygen, nitrogen, and any non-catalyzed nitrous oxide remaining. The flow properties are approximated by the molar-weighted average of the individual gas properties.

4. The flow beyond the exit orifice is calculated, using the same calculation methods as for step (2). The NHNE model for a pure gas is identical to the standard choking flow rate calculations, so the NHNE model was used to calculate this mass flux rate, and thus the orifice area.

The files `N2OProps.m`, `O2Props.m`, and `N2Props.m` that implement the Helmholtz property models are not included, as the algorithm code is detailed in the original papers by Lemmon and Span [66] and Span and Wagner [67, 68].

A.2 MATLAB Code

`IgniterSizing.m`

```
close all
clear all
clc

psi2MPa=6.89475729E-3;
```

```
in2m=0.0254;

Pdown = 12*psi2MPa;
mdotArr = zeros(1,length(Pdown));
cmdot = mdotArr;
A = 1E-5;

% ====== INPUTS
  ============================================================

T1 = 293.15; %K
rho1 = 778; %kg/m^3
% rho1 = 157.9;
Pv=812*psi2MPa;
P2=500*psi2MPa;
T25 = 673.15;

% mdot=0.015; kg/s
W = 7000; %Watts

T_STP = 293.15;
P_STP = 0.101325;

P4 = Pdown;

Cd=0.85;
% Cd = 1.0;

y_n2o = .1;
MW_N2O = 44.00774;
MW_O2 = 31.99886;
MW_N2 = 28.01344;
hf = 82.05*1000/MW_N2O; % ~1800 kJ/kg

opts = optimset('Display','off','TolX',1E-10);
```

```
40 % opts = optimset('TolX',1E-10);
41
42 % ====== FIRST ORIFICE
     ====================================================
43 TR1 = [T1;rho1];
44
45 [Props1] = N2OProps(TR1);
46
47 G1 = Cd*MassFlux(@N2OProps,Props1,P2);
48 % Props2 = PSsolver(@N2OProps,P2,Props1.s,TR1);
49 Props2 = PHsolver(@N2OProps,P2,Props1.h,TR1);
50 TR2 = [Props2.T;Props2.rho];
51
52 Props25 = TPsolver(@N2OProps,T25,Props2.P,40);
53
54 % ====== REACTOR FLOW
     ====================================================
55
56 mf_O = (.5*MW_O2/(.5*MW_O2+MW_N2))*(1-y_n2o);
57 mf_N = (MW_N2/(.5*MW_O2+MW_N2))*(1-y_n2o);
58 mf_NO = y_n2o;
59 ExitProps = @(x)gasMixer(x,y_n2o);
60
61 P3 = P2-0.3;
62 h3 = Props2.h + hf*(1-y_n2o);
63 Props3 = PHsolver(ExitProps, P3, h3, TR2);
64 TR3 = [Props3.T;Props3.rho];
65
66 % ====== SECOND ORIFICE
     ====================================================
67 G2 = Cd*MassFlux(ExitProps,Props3,P4);
68 % Props4 = PSsolver(ExitProps,P4,Props3.s,TR3);
69 Props4 = PHsolver(ExitProps,P4,Props3.h,TR3);
70
```

```
71 % ====== MASS FLOW RATE
     ==================================================
72 rho_STP=lsqnonlin(@(rho) (P_STP-getfield(gasMixer([T_STP;rho],y_n2o),'P'))
     /P_STP,1.0,0, inf, opts)
73 [PropsSTP] = gasMixer([T_STP;rho_STP],y_n2o)
74 mdot = W/(Props4.h-PropsSTP.h)/1E3
75 % W = mdot*(Props4.h-PropsSTP.h)*1E3
76 Wpre = mdot*(Props25.h-Props2.h)*1E3
77 Wdec = mdot*hf*1E3
78
79 % ====== AREA CALCS
     ==========================================================
80 Aexp1=mdot/G1;
81 Dexp1=sqrt(4*(Aexp1)/pi)
82 Dexp1in=Dexp1/in2m
83
84 Aexp2=mdot/G2;
85 Dexp2=sqrt(4*(Aexp2)/pi)
86 Dexp2in=Dexp2/in2m
87
88 mdotArr(iP) = G2*A;
89 g = 1.398;
90 cmdot(iP) = A*sqrt(P3*1E6*TR3(2))*sqrt(g)*((g+1)/2)^-(.5*(g+1)/(g-1));
91
92 % plot(Pdown/psi2MPa,mdotArr,Pdown/psi2MPa,cmdot)
93
94 [Props1.T Props2.T Props3.T Props4.T]-273.15
95 [Props1.P Props2.P Props3.P Props4.P]/psi2MPa
96 [Props1.h Props2.h Props3.h Props4.h]
```

MassFlux.m

```
function [GTOT] = MassFlux(eqn,Props1,P2)
dp = 1E-8;
err = 1E-9;
[GTOT a b] = MFpure(Props1,PSsolver(eqn, P2,    Props1.s, [Props1.T;
  Props1.rho]));
GTOT2= MFpure(Props1,PSsolver(eqn, P2+dp, Props1.s, [Props1.T; Props1.rho
  ]));
GTOT3= MFpure(Props1,PSsolver(eqn, P2-dp, Props1.s, [Props1.T; Props1.rho
  ]));
   if GTOT2> GTOT3% ||1==1
        %Perform Golden search method to find choking flow
        Ps=P2;
        Pf=Props1.P;
         l=(sqrt(5)-1)/2;
        Pm2=l*(Pf-Ps)+Ps;
        Pm1=Pf-l*(Pf-Ps);
        GTOTm1=MFpure(Props1,PSsolver(eqn, Pm1, Props1.s, [Props1.T;
          Props1.rho]));
        GTOTm2=MFpure(Props1,PSsolver(eqn, Pm2, Props1.s, [Props1.T;
          Props1.rho]));

        while abs(GTOTm2-GTOTm1)>=err

            if GTOTm2>GTOTm1
                Ps=Pm1;
                GTOTm1=GTOTm2;
                Pm2=l*(Pf-Ps)+Ps;
                GTOTm2=MFpure(Props1,PSsolver(eqn, Pm2, Props1.s, [Props1.
                  T; Props1.rho]));
            else
                GTOTm2=GTOTm1;
                Pf=Pm2;
                Pm1=Pf-l*(Pf-Ps);
```

```
28                  GTOTm1=MFpure(Props1,PSsolver(eqn, Pm1, Props1.s, [Props1.
                      T; Props1.rho]));
29              end
30          end
31          GTOT=max([GTOTm2 GTOTm1 GTOT]);
32      end
33
34  end
35
36  function [GTOT GHEM GSPI]=MFpure(Props1,Props2)
37
38
39  GHEM=Props2.rho*sqrt(2*(Props1.h-Props2.h)*1000);
40  GSPI=sqrt(2*Props1.rho*(Props1.P-Props2.P)*10^6);
41
42
43  if Props2.X >0 && Props2.X<1 && Props1.X <1
44      %Fluid is saturated
45  %       Props1Sat=N2OProps(Props1.T,Props1.rho/2);
46  %       Pv=Props1Sat.P*10^6;
47
48      k=sqrt((Props1.P-Props2.P)/(Props1.Pv-Props2.P));
49      GTOT=(1/(1+k)*GHEM+(1-1/(1+k))*GSPI);
50  elseif Props2.X==0 && Props1.X <1
51      %Fluid is liquid
52      GTOT=GSPI;
53
54  else
55      %Fluid is a gas
56      GTOT=GHEM;
57  end
58  end
```

BiasCalc.m

```
T0_bc = 298; %K
P0_bc = 0.1; %Mpa

opts = optimset('Display','off','TolX',1E-10);
rho0_bc = 1; % Guess value
rho0_N2O = lsqnonlin(@(r) (P0_bc-getfield(N2OProps([T0_bc;r]),'P'))/P0_bc,
  rho0_bc, 0, inf, opts);
rho0_N2 = lsqnonlin(@(r) (P0_bc-getfield(N2Props([T0_bc;r]),'P'))/P0_bc,
  rho0_bc, 0, inf, opts);
rho0_O2 = lsqnonlin(@(r) (P0_bc-getfield(O2Props([T0_bc;r]),'P'))/P0_bc,
  rho0_bc, 0, inf, opts);
STP_N2O = N2OProps([T0_bc; rho0_N2O]);
STP_O2 = O2Props([T0_bc; rho0_O2]);
STP_N2 = N2Props([T0_bc; rho0_N2]);

O2bias_h = STP_N2O.h-STP_O2.h;
N2bias_h = STP_N2O.h-STP_N2.h;
O2bias_s = STP_N2O.s-STP_O2.s;
N2bias_s = STP_N2O.s-STP_N2.s;
O2bias_u = STP_N2O.u-STP_O2.u;
N2bias_u = STP_N2O.u-STP_N2.u;

clear T0_bc P0_bc rho0_bc rho0_N2O rho0_N2 rho0_O2 STP_N2O STP_O2 STP_N2s
```

TPSolver.m

```
function [State,err]= TPsolver(eqn,T2,P2,rhog)

opts = optimset('Display','off','TolX',1E-10);

if nargin <4
    rhog=100;
end

ef=0;
[X2 err] = lsqnonlin(@(X) (P2 - getfield(eqn([T2;X]),'P'))/P2,...
                             rhog,0,inf,opts);

if err>0.000001
    rhog=1100;
    [X2 err] = lsqnonlin(@(X) (P2 - getfield(eqn([T2;X]),'P'))/P2,...
                                 rhog,0,inf,opts);
end
State=eqn([T2;X2]);

end
```

PHsolver.m

```
function [State]= PHsolver(eqn,P2,h2,Xg)

opts = optimset('Display','off','TolX',1E-10);

if nargin <4
    Tg = 200;
    rhog = 1000;
else
    Tg = Xg(1);
    rhog = Xg(2);
end

ef=0;
[X2 err] = lsqnonlin(@(X) ([P2;h2] - [getfield(eqn(X),'P');
                                      getfield(eqn(X),'h')])./[P2;h2],...
                        [Tg;rhog],[0;0],[inf inf],opts);

if err>0.000001
    Tg = 200;
    rhog = 10;
    X2 = lsqnonlin(@(X) ([P2;h2] - [getfield(eqn(X),'P');
                            getfield(eqn(X),'h')])./[P2;h2],...
                            [Tg;rhog],[0;0],[inf inf],opts);
end
State=eqn(X2);

end
```

PSsolver.m

```
function [State]= PSsolver(eqn,P2,s2,Xg)

opts = optimset('Display','off','TolX',1E-10);

if nargin <4
    Tg=max(200+800/2.5*s2,200);
    rhog=max((1200-500*s2),100);
else
    Tg = Xg(1);
    rhog = Xg(2);
end

ef=0;
[X2 err] = lsqnonlin(@(X) ([P2;s2] - [getfield(eqn(X),'P');
                            getfield(eqn(X),'s')])./[P2;s2],...
                            [Tg;rhog],[0;0],[inf inf],opts);

if err>0.000001
    Tg=max(200+800/2.5*s2,200);
    rhog=max((900-500*s2),100);
    X2 = lsqnonlin(@(X) ([P2;s2] - [getfield(eqn(X),'P');
                          getfield(eqn(X),'s')])./[P2;s2],...
                          [Tg;rhog],[0;0],[inf inf],opts);
end
State=eqn(X2);

end
```

gasMixer.m

```
function [state] = gasMixer(X1, y)
% y is mass fraction of N2O, NOT decomposition fraction


MW_N2O = 44.00774;
MW_O2 = 31.99886;
MW_N2 = 28.01344;
BiasCalc


mf_O = (.5*MW_O2/(.5*MW_O2+MW_N2))*(1-y);
mf_N = (MW_N2/(.5*MW_O2+MW_N2))*(1-y);
mf_NO = y;

NO = N2OProps([X1(1);X1(2)*mf_NO]);
N = N2Props([X1(1);X1(2)*mf_N]);
O = O2Props([X1(1);X1(2)*mf_O]);

if (mf_NO <= 0)
    names = fieldnames(NO);
    for i = 1:numel(names)
        NO.(names{i}) = 0;
    end
end
if (mf_N <= 0)
    names = fieldnames(N);
    for i = 1:numel(names)
        N.(names{i}) = 0;
    end
end
if (mf_O <= 0)
    names = fieldnames(O);
    for i = 1:numel(names)
        O.(names{i}) = 0;
```

```
35      end
36  end
37
38  state.T = X1(1);
39  state.rho = X1(2);
40  state.P = NO.P + N.P + O.P;
41  state.X = 1;
42  state.state = 2;
43  state.s  = mf_NO*NO.s  + mf_O*(O.s + O2bias_s)  + mf_N*(N.s+N2bias_s);
44  state.u  = mf_NO*NO.u  + mf_O*(O.u + O2bias_u)  + mf_N*(N.u+N2bias_u);
45  state.cv = mf_NO*NO.cv + mf_O*O.cv + mf_N*N.cv;
46  state.cp = mf_NO*NO.cp + mf_O*O.cp + mf_N*N.cp;
47  state.h  = mf_NO*NO.h  + mf_O*(O.h+O2bias_h)  + mf_N*(N.h+ N2bias_h);
48  state.c  = mf_NO*NO.c  + mf_O*O.c  + mf_N*N.c;
```

Appendix B

PROCEDURAL CHECKLISTS

The checklists followed during the catalyst activity tests, reactor prototype tests, and the final hybrid ignition test, are included here. Each checklist covers the assembly of the test article, the installation of the article onto the appropriate testing system, and the procedures for the test itself.

B.1 Catalyst Activity Test

Catalyst Activity Testing Checklist
Test Location:_____
Date:
_____
Additional Notes:_____
_____

	Pre- Movement Inspection
	Ensure that preheater tube, catalyst tube, and TC-Tees are assembled, wrapped in heat tape, and insulated: This is the catalyst section
	Ensure that catalyst section is securely attached to utility cart
	Ensure that 5 gallon bucket, Teflon Tubing, and temperature control box are on utility cart
	Ensure that necessary wrenches and tools are on cart for plumbing change
	Ensure that protective caps are screwed onto the H2, Ar, and N2O cylinders
	Cart and Tank Movement
	Use SPL's handcart to carry over H2, Ar, and N2O tanks to test cell; secure against wall with strap
	Wheel over Utility cart
	Pre-Reduction Preparation
	Ensure that H2/Ar Needle valve and Tee assembly is securely attached to catalyst section inlet
	Ensure that Teflon tubing is attached to catalyst section outlet, and leads to 5 gallon bucket
	Fill 5 gallon bucket 1/2-7/8 full of water.
	Unscrew protective cap on H2 and Ar cylinders, attach H2 and Ar regulators
	Connect red welding hose from H2 regulator to the needle valve side of the T-assembly
	Connect black tube from Ar regulator to other side of the T-assembly
	Pre-reduction
	Ensure that all nonessential personnel are removed from test cell, all essential personnel should put on eye protection
	Ensure that H2 regulator adjustment handle is fully unscrewed (fully closed), and Ar flow regulator is fully tightened (fully closed)
	Slowly open H2 cylinder valve, check for leaks
	slowly tighten H2 regulator handle until very slight pressure increase downstream, check for leaks
	Slowly open needle valve as little as possible, until bubbles appear from the teflon tube submerged in the bucket of water. Bubbles should be distinct, with a period of several seconds between each bubble
	mark location of needle valve, close needle valve.
	Ensure that Ar flow regulator is fully off.
	Open Ar cylinder valve, check for leaks
	Slowly open Ar flow regulator, until bubbles appear from the teflon tube in the 5 gal bucket. Criteria are similar to H2 setup, although a higher flow rate is acceptable. Mark location of Ar flow regulator
	When Ar flow is steady, ensure that heater coil is NOT plugged into temperature controller box, and the tube TC IS plugged into the Temp controller
	Turn on Temperature Controller box. Verify settings on the TC3YT: K-type TC, Desired Temp at 400 C.
	Ensure that tube temp is reasonable.
	Plug hand-held TC reader into first Yor-Lok'd TC (flow TC)
	Plug heater coil into TC box, ensure temperature on both tube TC and flow TC is rising
	Wait until Temperatures reach steady state
	Adjust desired temp on TC box until flow TC reads ~ 400 C steady state
	slowly turn off Ar flow, and slowly turn H2 needle valve to marked position. Ensure that bubble flow rate is still slow, and that there are no leaks.

- [ ] Begin 4 hour timer. Everyone should evacuate test cell at this time, although the setup should not be left unattended. Periodically the system should be checked to ensure H2 flow has not increased, and that the flow temperature is ~400C
- [ ] After 4 hours, slowly shut H2 needle valve, and slowly re-open Ar flow regulator to marked position.
- [ ] Unplug Heater coil from TC box, ensure temperatures begin to drop
- [ ] Close hydrogen cylinder.
- [ ] Maintain Ar flow until catalyst section is near room temperature.
- [ ] close Ar cylinder, allow line pressures to return to ambient.
- [ ] Open H2 needle valve to marked position, allow line pressures to return to ambient.

- [ ] **Pre-reduction to Activity Plumbing Change**
- [ ] Unscrew H2 and Ar regulators from cylinders, Screw on protective cylinder caps.
- [ ] Unscrew red welding hose from H2 regulator and T section; unscrew tubing from Ar regulator
- [ ] Unthread H2/Ar T section from catalyst section; unthread teflon tubing from catalyst section
- [ ] Thread N2O needle valve arrangement onto catalyst section inlet
- [ ] Thread plug section into catalyst section outlet
- [ ] Unscrew protective cap from N2O cylinder; attach N2O regulator.
- [ ] Attach green welding hose from N2O regulator to N2O needle valve.

- [ ] **Software Check**
- [ ] Start ActivityTest.vi
- [ ] Run ActivityTest to ensure wiring is setup correctly

- [ ] **Test Checklist**
- [ ] Ensure that all plumbing is tight and assembled
- [ ] Ensure that software is working and reading temps
- [ ] Ensure that Solenoid valve is working, and can be controlled from inside test cell
- [ ] Remove all nonessential personnel from test cell, essential personnel should have safety glasses
- [ ] Ensure the N2O regulator is fully closed
- [ ] Slowly open N2O cylinder, check for leaks
- [ ] Slowly open N2O regulator as small as possible, check for leaks
- [ ] Slowly open needle valve as little as possible, check for leaks
- [ ] Flow rate is not significantly important, catalytic decomposition as a function of length is independent of velocity. Less flow is safer
- [ ] Pulse solenoid valve, ensure that limited flow escapes
- [ ] Ensure heater coil is not plugged into TC box, plug in TC box and set temperature to 400C (catalyst is theoretically active at 350 C; more will ensure reaction)
- [ ] Ensure software is reading both flow TCS
- [ ] Plug in heater coil, evacuate test cell, ensure the digital reading on the TC box is visible from the test window
- [ ] Wait until system has reached 400 C
- [ ] Remotely open solenoid valve, watch TC box and flow TC readings carefully. Temperature of exit flow should begin to increase
- [ ] Once exit flow has been shown to increase, close solenoid valve.
- [ ] Enter test cell, unplug heater coil from TC box.
- [ ] Close N2O cylinder
- [ ] Wait for system to return to room temperature

- [ ] Open solenoid valve, allow system to depressurize.
- [ ] Disassemble regulator, welding hose, put cap on N2O bottle.
- [ ]
- [ ] **Alternative Test:**
- [ ] Similar to regular test, with the exception that nitrous oxide flow is turned on and the test cell is evacuated while the catalyst section is heating up. This allows for a rough estimation of Temp necessary for activation

B.2 Catalytic Reactor Test

Catalytic Igniter Hot Fire Checklist 9-19-12

Date:_____

Notes:_____

	Motor Assembly and Preparation
	Check inlet and outlet orifices for roundness, clogs, etc.
	Thread outlet orifice into bottom reactor cap, being sure to not use excessive pipe tape (to prevent orifice clogging)
	Use rutland fire cement around orifice disc
	Insert mesh into bottom reactor cap, being sure that the 1/4" stainless steel tubing passes through the hole
	Thread reactor body onto bottom reactor cap, tighten with pipe wrench
	slide copper tubing over outside of reactor, attach to reactor bottom via yor-lok fittings
	fill reactor with catalyst pellets to top of body, vibrate to ensure good packing.
	Record catalyst pellet weight here: _____
	thread on top reactor cap, tighten with pipe wrench. If desired, be sure secondary temp probe hole lines up with internal SS pipe
	Attach thermocouple probe, pressure transducer pipe
	Attach inlet orifice system
	Wrap with heating element
	Wrap with insulation

	Pre- Movement Inspection
	Ensure that all N2O tanks are fully closed and secured tightly to MoNSTeR Cart
	Ensure that all N2 tanks are fully closed and secured tightly to NiBBleR Cart
	Ensure that all cables, hoses, straps, etc are secured and will not inhibit cart movement
	Ensure that the NiBBleR and MoNSTeR cart toolboxes contain
	-1 1/4 wrench
	-large cresent wrench
	- electrical tape
	- volt meter
	- Cordless drill with socket for hose clamps
	- 1 each #2 Phillips and flat head screwdrivers
	- 3 sets of safety glasses
	- Various zip ties
	Ensure that the MoNSTeR cam and MoNSTeR cam power adapter are on the MoNSTeR cart or NiBBleR cart

	Test Cell Setup
	Locate the CO2 deluge switch on the instrument panel in the control room. DO NOT TOUCH THESE SWITCHES
	Turn on cell 115 VAC switch on the instrument panel

	MoNSTeR Cart Assembly
	Position MoNSTeR Cart in test cell.
	Ensure that the manual high voltage power switch is in the off position
	Connect extension cord to main power cord on MoNSTeR Cart
	Power on MoNSTeR Cart UPS
	Connect USB cables from cDAQ to USB extendenders
	secure USB connections with electrical tape
	Ensure that motor is still firmly connected to the test stand.
	Ensure that the nitrous flow fitting and CO2 purge fittings are attached and tight
	Ensure that all 4 TC's are securely attached and electrical connections made
	Ensure that all Pressure Transducers are securely attached and electrical connection made

- [ ] Ensure that 120V heater(s) are plugged in to their receptacle

Bottle Connections

- [ ] Ensure that CGA fitting on small CO2 pneumatic pressure supply bottle is securely connected and the valve is fully closed
- [ ] Ensure that CGA fitting on all three nitrous oxide supply bottles are securely connected and all valves are fully closed
- [ ] Ensure that all gauges on both carts read zero PSI. Check the Nitrous Manifold, Nitrogen Manifold, CO2 manifold

Computer Setup

- [ ] Plug in and power on main test computer
- [ ] If computer was already on, restart computer
- [ ] plug cDAQ USB extender cable into main test computer
- [ ] Ensure that team viewer and any other programs are closed

VI Setup

- [ ] Power on national instruments DAQ and ensure cDAQ is connected to main test computer
- [ ] Ensure that the manual high voltage power switch is in the "off" position
- [ ] Open most recent VI "MoNSTeR_Igniter_#.#" in "MoNSTeRViandData" folder on the desktop
- [ ] Ensure that the filename path on the Vi frontpanel is correct
- [ ] Ensure that error handling in file->vi Properties ->execution (on the dropdown list) is set to automatic error handling (radio button on right hand side should be checked) Turn off Allow Debugging option.
- [ ] Start VI
- [ ] Verify that everything in the VI is working properly and the tab control is set to "safe"
- [ ] Set the igniter mode as "Decomposition"
- [ ] Pulse igniter valve on then off and ensure valve is working by listening for valve to click using the following sequence: Set the main operating mode to manual, click run valves, then click igniter valve on the off (igniter pane).
- [ ] Turn off run valves button and set tab control to "safe"
- [ ] Set the timing values for igniter valve actuation in the main test computer vi. Record values
  Valve Start:_____ Valve End:_____
  Oxidizer open:_____ Burn Length:_____
  shutoffT:_____ RegulatedT:_____

Instrumentation Checkout

- [ ] Check voltage/pressure range on each pressure transducer
- [ ] Check voltage range on each thermocouple and make sure the "bad thermocouple" button is not on
- [ ] Check excitation voltage range on VI..it should be within about 0.005 V to 10V
- [ ] Ensure value of millisecond timer is low enough (it resets at 2^32, button turns red ~14 hours before that)

CO2 Pneumatic System Pressurization

- [ ] Ensure that all personnel are wearing eye protection
- [ ] Close test cell bay doors
- [ ] Ensure that vent valve on the pneumatic supply manifold is closed
- [ ] Slowly turn on valve on the small 20lb pneumatic pressure supply bottle.
- [ ] Ensure that gauge downstream of CO2 regulator is set to 100psi
- [ ] Listen and feel for leaks around push to connect fittings
- [ ] Ensure that igniter valve is closed
- [ ] Close CO2 Cylinder (procedure for leaky igniter valve)

Pre- Pressurization Inspection

- [ ] Ensure that motor assembly is tight and is secured to test stand
- [ ] Ensure that cart is free of loose debris
- [ ] Ensure that all fittings on igniter are tight
- [ ] Ensure that igniter heater is plugged in to local plug
- [ ] Turn on servo valve switch, ensure servo valve moves to closed position
- [ ] Ensure that mSEc and mSec L2 manual valves are closed, and liquid bypass manual valve is open

Valve Test And Pressure Zeroes

- [ ] Change filename to "PressureCal" and the date
- [ ] Set the tab control in the vi to "manual" and turn on run valves button
- [ ] Open and leave open each Pneumatic ball valve with the labview VI, ensure that each one opens
- [ ] -1- Nitrous / Fill Valve
- [ ] -2- Nitrogen Purge Valve
- [ ] -3- Top Pressure Valve
- [ ] -4- Vent Valve
- [ ] -5- Motor Valve
- [ ] -6- Tank Valve
- [ ] -7- Motor Bypass Valve
- [ ] -8- CO2 Purge Valve
- [ ] Servo Valve
- [ ] Listen for leaks
- [ ] hit save data button, wait 3 seconds and turn off save data button
- [ ] turn run valves button to off and change tab control to "safe"

Heating checklist

- [ ] Ensure that heater is plugged into socket, and that all TCs are properly aligned
- [ ] Ensure igniter is securely fastened and insulated
- [ ] Ensure GFCI is not tripped
- [ ] Make sure everyone in the test cell has protective gear, open CO2 liquid bottle and evacuate chamber
- [ ] Set desired temperature in VI, turn on heaters button.
- [ ] Ensure temperature is rising
- [ ] Occasionally, CO2 can be pulsed using the CO2 purge valve, motor valve, and igniter valve

NO2 Pressurization Checklist

- [ ] Ensure that the "nitrous valve" pneumatic ball valve is fully closed (The red markings on the top of the valve should be perpendicular with the pipe direction)
- [ ] Ensure that CO2 pneumatic ball valve is fully closed
- [ ] Ensure that nitrous manifold reads 0 psi
- [ ] Ensure that the manual nitrous valve is closed
- [ ] Partially open the valve of one of the nitrous oxide cylinders, allowing a small amount of gas to flow into the nitrous manifold
- [ ] Allow pressure to equalize
- [ ] Listen for any obvious leaks
- [ ] Slowly open the manual valve until pressure starts to bleed through to the pneumatic valve.
- [ ] Once sure that flow is not passing the pneumatic valve, fully open manual valve
- [ ] Fully open the valves on all N2O cylinders
- [ ] Record Pressure on Nitrous Manifold Gauge_____
- [ ] Verify that MonsterCam is set to movie mode and sd card is locked
- [ ] Attach cords and position MonsterCam in MonsterCam box
- [ ] Power on MonsterCam
- [ ] Verify that MonsterCam remote control is working
- [ ] Start any cameras that must be manually started in test cell. Note time cameras are started

	Evacuate Test cell, ensure everyone is out.
	Set tab control to manual; click run valves, and open the N2O fill valve. Allow pressures to equalize
	Set tab control to safe

RUN Checklist

	Ensure that reactor is up to the desired temperature
	Change VI data filename to test name and date
	Check decomp control vi settings
	Check valve timing in the main control vi
	Ensure all personnel are out of test cell and close test cell door.
	Ask for silence in control room
	Tell audience to not touch any switches on the control panel unless directed to do so by the test director
	Station someone near the 115 volt AC power switch and tell them to turn switch off if directed to do so by the test director
	If igniter failure, turn off run valves button
	Stop and then restart VI
	Ensure that VI is working
	Switch Igniter Mode to "Decomp Igniter"
	Switch main Tab Control to "Test igniter"
	Notify test controller that if motor does not ignite when motor valve opens or other issue is apparent to immediately turn off run valves button and proceed to depressurization checklist.
	If motor is on fire or explodes, operator should turn off "run valves button" and switch the main tab control to safe. 115V switch operator should turn off 115V power to test cell. Wait for fire to extinguish then proceed to depressurization checklist.
	Start Test Cell fans
	Start MoNSTeR Cam
	Perform 5 second countdown and then press "Run Valves" button, notify any visitors that test will start x seconds after countdown ends
	(firing)
	Stop MoNSTeRCam
	Verify that run valves button is off
	Verify that tab control is set to "Safe"
	Verify that "Save Data" button is off

Depressurize

	Ensure that all personnel are wearing safety glasses
	Enter Test Cell
	Ensure that manual high voltage switch is in the off position
	Close N2O and CO2 cylinder(s)
	Ensure all personnel are out of test cell and close test cell door.
	Switch Tab Control to manual, press "run valves" button
	Open and leave open all valves, starting with motor bypass
	Switch Tab Control to "safe"
	Ensure that personnel in test area are wearing eye protection.
	Enter Test Cell
	Close liquid bypass Manual Valve
	Close 20lbm CO2 tank
	Vent 20 lbm CO2 tank via manual valve on pneumatic valve manifold
	Disconnect USB cables and store box on MoNSTeR Cart
	Disconnect ethernet cable from MoNSTeR Cart and secure all cables
	Disconnect power cord from cart
	Turn off the UPS

Post Test

	Update MoNSTeR Test Summary with all post test values
	Add test video to MoNSTeR Cart Data svn folder.
	take photographs of inside and outside of fuel grain, nozzle exit and inlet
	add photographs to test pictures folder in MoNSTeR cart data folder, in folder created for pre-test pictures
	add new data, images, and video to SVN and commit
	Add this checklist to the checklist drawer.

Emergency Procedures

	switch tab control to "safe"
	turn "run valves" button to off
	ensure that all personnel are out of test cell and close test cell door
	Turn off 110V power to test cell
	follow de-pressurization checklist

B.3 Hybrid Ignition Test

Hot fire Catalytic Ignition Checklist 12-10-12

Date:_____

Notes:_____

	Igniter Assembly and Preparation
	Check inlet and outlet orifices for roundness, clogs, etc.
	Thread outlet orifice into bottom reactor cap, being sure to not use excessive pipe tape (to prevent orifice clogging)
	Use rutland fire cement around orifice disc
	Insert mesh into bottom reactor cap, being sure that the 1/4" stainless steel tubing passes through the hole
	Thread reactor body onto bottom reactor cap, tighten with pipe wrench
	slide copper tubing over outside of reactor, attach to reactor bottom via yor-lok fittings
	fill reactor with catalyst pellets to top of body, vibrate to ensure good packing.
	Record catalyst pellet weight here: _____
	thread on top reactor cap, tighten with pipe wrench. If desired, be sure secondary temp probe hole lines up with internal SS pipe
	Attach thermocouple probe, pressure transducer pipe
	Attach inlet orifice system
	Wrap with heating element
	Wrap with insulation
	Motor Assembly and Preparation
	Fuel Grain Name: _____
	Weigh Fuel grain and record weight on MonsterCartTestSummary sheet
	Inspect fuel grain for de-laminated sections, cuts, channels or other anomalies
	Inspect phenolic liner for burns, cracks or anomalies
	Inspect graphite inserts for cracks or anomalies
	Measure nozzle throat diameter in two axes, average result and record in TestSummary sheet
	Inspect all four orings for cuts, burs, burns or anomalies, clean if necessary
	take photographs of inside and outside of fuel grain, nozzle exit and inlet, and graphite liners
	add photographs to test pictures folder in monster cart data folder, label a seperate folder for these images and add folder name to test summary spreadsheet
	Insert Injector into motor cap, ensure that injector is tight and pipe tape will not clog orifice
	Test continuity of igniters with volt meter
	install estes motors and igniters in forward enclosure.
	Test continuity of igniters with volt meter from outer electrical connection
	Inspect the orings on the estes motor caps for cuts or breaks, replace if required. Lubricate orings
	Ensure that the estes motor tube caps are tight
	ensure that the graphite nozzle and insert are secure in the nozzle retaining ring
	Coat the orings on the nozzle holder ring with water based lubricant
	Install orings on the nozzle holder ring
	apply a thin (less than 1/8 in) bead of RTV to the slot for the phenolic liner on the nozzle retaining ring
	release RTV caulk gun pressure
	slide the nozzle and retaining ring most of the way into the aft end of the motor casing (the end with the band on it)
	use the plywood tool to shove the nozzle retaining ring into the motor casing such that about 1/4 in of threads show past the retaining ring
	tighten the retaining ring until it presses tightly against the nozzle ring
	liberally coat the outside of the phenolic liner with water based lubricant
	slide the phenolic liner into the motor casing until seated against the nozzle retaining ring

- [ ] verify that the phenolic liner is seated properly
- [ ] apply a thin bead of RTV to the bottom edges of the fuel grain
- [ ] liberally apply a coat of water based lubricant to the outside of the fuel grain
- [ ] gently slide (do not drop) the fuel grain into the motor casing such that the mixing inset faces aft (flat end should still be visible)
- [ ] liberally apply water based lubricant on o rings on forward enclosure.
- [ ] install orings on forward enclosure
- [ ] ensure that graphite insert is secured in forward enclosure
- [ ] apply a thin bead of RTV to the slot for the phenolic liner on the forward enclosure
- [ ] apply a thin bead of RTV to the spot for the fuel grain on the forward enclosure
- [ ] slide the forward enclosure into the motor casing onto until it contacts the phenolic liner, use the plywood tool to press against the aft end of the motor casing
- [ ] twist forward enclosure a half turn
- [ ] tighten the forward retaining ring until tightened against the forward enclosure or threads are bottomed out
- [ ] Connect union for oxidizer feed and tighten
- [ ] Secure motor casing to test stand with hose clamps such that the forward enclosure is about 1/3 of an inch from the hard stop so that the forward end cap and move out.
- [ ] tighten the threads on the aft retaining ring until tight. Verify that retaining ring is snug against the aft enclosure and ignition wires are not pinched between the motor and stand
- [ ] Loosen the hose clamps, push motor up against hard stop and re-tighten
- [ ] Ensure that motor is secure on test stand and firmly pressed against hard stop on end of test stand. Check level if necessary
- [ ] Connect tubing for motor pressure transducer, ensure that it is tight
- [ ] Do NOT connect electrical connections for igniters to bananna plugs
- [ ] Ensure that igniter switches are in the off position
- [ ] electrical tape motor TC to aft end of motor casing, near the ring on the end of motor
- [ ] Place plastic motor cap on end of motor
- [ ] Ensure that tools are stowed back in box on monster and nibbler carts

Pre- Movement Inspection

- [ ] Ensure that all N2O tanks are fully closed and secured tightly to MoNSTeR Cart
- [ ] Ensure that all N2 tanks are fully closed and secured tightly to NiBBleR Cart
- [ ] Ensure that all cables, hoses, straps, etc are secured and will not inhibit cart movement
- [ ] Ensure that the NiBBleR and MoNSTeR cart toolboxes contain
- [ ] -1 1/4 wrench
- [ ] -large cresent wrench
- [ ] - electrical tape
- [ ] - volt meter
- [ ] - Cordless drill with socket for hose clamps
- [ ] - 1 each #2 Phillips and flat head screwdrivers
- [ ] - 3 sets of safety glasses
- [ ] - Various zip ties
- [ ] Ensure that the MoNSTeR cam and MoNSTeR cam power adapter are on the MoNSTeR cart or NiBBleR cart

Test Cell Setup

- [ ] Locate the CO2 deluge switch on the instrument panel in the control room. DO NOT TOUCH THESE SWITCHES
- [ ] Turn on cell 115 VAC switch on the instrument panel
- [ ] Secure foam cover to conical exhaust inlet in test cell with tape.
- [ ] Ensure that foam acoustic cover is secure

MoNSTeR Cart Assembly

- [ ] Secure MoNSTeR Cart to I-beam in test cell.
- [ ] Ensure that the manual high voltage power switch is in the off position

	Connect extension cord to main power cord on MoNSTeR Cart
	Power on MoNSTER Cart UPS and Heaters (if necessary)
	Close MoNSTER Cart Shower Curtains (if necessary)
	Check Nitrogen Supply Line connection for debris and then connect quick-connect between Nibbler cart and MoNSTeR Cart
	Connect wire connection for nitrogen manifold thermocouple
	Connect USB cables from cDAQ to USB extendenders
	secure USB connections with electrical tape
	Ensure that motor is still firmly connected to the test stand.
	Ensure that the nitrous flow fitting and CO2 purge fittings are attached and tight
	Ensure that all 4 TC's are securely attached and electrical connections made
	Ensure that all Pressure Transducers are securely attached and electrical connection made
	Ensure that 120V heater(s) are plugged in to their receptacle
	Remove plastic motor cap from end of motor
	Connect hose from faucet in test cell to bottom of igniter plumbing cooler
	Run hose from exit of cooler to as close to drain as possible
	Ensure that clear tubing extends up, and exits facing away from the monster cart.

Bottle Connections

	Ensure that CGA fitting on small CO2 pneumatic pressure supply bottle is securely connected and the valve is fully closed
	Ensure that CGA fitting on all three nitrous oxide supply bottles are securely connected and all valves are fully closed
	Ensure that CGA fitting on all four nitrogen supply bottles are securely connected and all valves are fully closed
	Ensure that all gauges on both carts read zero PSI. Check the Nitrous Manifold, Nitrogen Manifold, CO2 manifold

Computer Setup

	Plug in and power on main test computer
	If computer was already on, restart computer
	plug cDAQ USB extender cable into main test computer
	Ensure that team viewer and any other programs are closed
	Plug in and Power on ToughBook
	Plug USB extender for webcam into toughbook

VI Setup

	Power on national instruments DAQ and ensure cDAQ is connected to main test computer
	Ensure that the manual high voltage power switch is in the "off" position
	Open most recent VI "MoNSTeR_Igniter_#.#" in "MoNSTeRViandData" folder on the desktop
	Ensure that the filename path on the Vi frontpanel is correct
	Ensure that error handling in file->vi Properties ->execution (on the dropdown list) is set to automatic error handling (radio button on right hand side should be checked) Turn off Allow Debugging option.
	Start VI
	Verify that everything in the VI is working properly and the tab control is set to "safe"
	Set the igniter mode as "Decomposition"
	Pulse igniter valve on then off and ensure valve is working by listening for valve to click using the following sequence: Set the main operating mode to manual, click run valves, then click igniter valve on the off (igniter pane).
	Turn off run valves button and set tab control to "safe"
	Set the timing values for igniter valve actuation in the main test computer vi. Record values.

- [ ] **Ensure that Valve End is 0. For TC igniton, ensure that Valve Start is acceptably long, and that the Shutoff T is very high. Also ensure that Ignition T is set correctly**
- [ ] Ign Start:_____ Ign End:_____
- [ ] Valve Start:_____ Burn Length:_____
- [ ] shutoffT:_____ RegulatedT:_____

Fieldpoint and Servo Valve Setup

- [ ] Ensure that NI fieldpoint is powered on
- [ ] After it has had time to boot, ensure that LED A on the Fieldpoint is blinking, indicating that valve program is running
- [ ] Ensure that servo bracket screws are tight and servo is rigidly connected
- [ ] Flip servo power switch to on position, verfiy that white LED is lit
- [ ] Check voltage level on Servo battery
- [ ] Turn servo valve off by turning off both "fieldpoint com" buttons in monster VI
- [ ] Ensure valve closes
- [ ] Open servo valve by turning on both "fieldpoint com" buttons in monster VI
- [ ] Ensure valve opens

Instrumentation Checkout

- [ ] Exercise each load cell on the run tank assembly and verify output in VI
- [ ] Exercise each load cell on the thrust stand and verify output in VI
- [ ] Check voltage/pressure range on each pressure transducer
- [ ] Check voltage range on each thermocouple and make sure the "bad thermocouple" button is not on
- [ ] Check excitation voltage range on VI..it should be within about 0.005 V to 10V
- [ ] Ensure value of millisecond timer is low enough (it resets at 2^32, button turns red ~14 hours before that)

CO2 Pneumatic System Pressurization

- [ ] Ensure that all personnel are wearing eye protection
- [ ] Close test cell bay doors
- [ ] Ensure that vent valve on the pneumatic supply manifold is closed
- [ ] Slowly turn on valve on the small 20lb pneumatic pressure supply bottle.
- [ ] Ensure that gauge downstream of CO2 regulator is set to 100psi
- [ ] Listen and feel for leaks around push to connect fittings
- [ ] Ensure that igniter valve is closed
- [ ] Close CO2 Cylinder (procedure for leaky igniter valve)
- [ ] Ensure that MUPHyN main flow manual valve is closed

Pre- Pressurization Inspection

- [ ] Ensure that motor assembly is tight and is secured to test stand
- [ ] Ensure that cart is free of loose debris
- [ ] Ensure that all fittings on igniter are tight
- [ ] Ensure that igniter heater is plugged in to local plug
- [ ] Turn on servo valve switch, ensure servo valve moves to closed position
- [ ] Ensure that mSEc and mSec L2 manual valves are closed, and liquid bypass manual valve is open

Valve Test And Pressure Zeroes

- [ ] Change filename to "PressureCal" and the date
- [ ] Set the tab control in the vi to "manual" and turn on run valves button
- [ ] Open and leave open each Pneumatic ball valve with the labview VI, ensure that each one opens
- [ ] -1- Nitrous / Fill Valve
- [ ] -2- Nitrogen Purge Valve
- [ ] -3- Top Pressure Valve

- [ ] -4- Vent Valve
- [ ] -5- Motor Valve
- [ ] -6- Tank Valve
- [ ] -7- Motor Bypass Valve
- [ ] -8- CO2 Purge Valve
- [ ] Servo Valve
- [ ] Listen for leaks
- [ ] hit save data button, wait 3 seconds and turn off save data button
- [ ] turn run valves button to off and change tab control to "safe"

Heating checklist

- [ ] Ensure that heater is plugged into socket, and that all TCs are properly aligned
- [ ] Ensure igniter is securely fastened and insulated
- [ ] Ensure GFCI is not tripped
- [ ] Open water faucet main valve (located inside control room, opposite the faucet) and the faucet valve to desired water flow
- [ ] Make sure everyone in the test cell has protective gear, open CO2 liquid bottle and evacuate chamber
- [ ] Set desired temperature in VI, turn on heaters button.
- [ ] Ensure temperature is rising
- [ ] Occasionally, CO2 can be pulsed using the CO2 purge valve, motor valve, and igniter valve

Pre- Pressurization Inspection

- [ ] Ensure that motor assembly is tight and is secured to test stand
- [ ] Ensure that cart is free of loose debris
- [ ] Ensure that the needle valve is on the desired setting (about 3 bands)
- [ ] Unscrew Nitrogen regulator one full turn
- [ ] Place foam cover on the monster box, ensuring velcro straps are secure

N2 Pressurization Checklist

- [ ] Open and secure shower curtains on MoNSTeR cart
- [ ] Verify that plastic top cover is secure in areas where gas will be venting nearby
- [ ] Clear area of all non-essential personnel
- [ ] Ensure that personnel in test area are wearing eye protection.
- [ ] Ensure all pneumatic valves are closed and VI is in safe position. (The red markings on the top of the valves should be perpendicular with the pipe direction)
- [ ] Ensure that vent valve on nitrogen manifold is fully closed
- [ ] Open manual nitrogen valve
- [ ] Ensure hydraulic line is securely connected between the Nibbler and Monster carts
- [ ] Slowly open one of the nitrogen bottles until flow just barely starts to bleed into the manifold. Monitor gauge downstream of nitrogen regulator, shut off nitrogen bottle immediately if gauge reads over 820 psi or if nitrogen is flowing past any pneumatic valves.
- [ ] Once sure that nitrogen regulator is set for 820 psi, fully pressurize manifold
- [ ] Fully open valves on all nitrogen cylinders
- [ ] Record pressure on nitrogen manifold gauge: _____

N2O Pressurization Checklist

- [ ] Ensure that the "nitrous valve" pneumatic ball valve is fully closed (The red markings on the top of the valve should be perpendicular with the pipe direction)
- [ ] Ensure that CO2 pneumatic ball valve is fully closed
- [ ] Ensure that nitrous manifold reads 0 psi
- [ ] Ensure that the manual nitrous valve is closed
- [ ] Partially open the valve of one of the nitrous oxide cylinders, allowing a small amount of gas to flow into the nitrous manifold
- [ ] Allow pressure to equalize

- [ ] Listen for any obvious leaks
- [ ] Slowly open the manual valve until pressure starts to bleed through to the pneumatic valve.
- [ ] Once sure that flow is not passing the pneumatic valve, fully open manual valve
- [ ] Fully open the valves on all N2O cylinders
- [ ] Record Pressure on Nitrous Manifold Gauge_____
- [ ] Verify that MonsterCam is set to movie mode and sd card is locked
- [ ] Attach cords and position MonsterCam in MonsterCam box
- [ ] Power on MonsterCam
- [ ] Verify that MonsterCam remote control is working
- [ ] Start any cameras that must be manually started in test cell. Note time cameras are started
- [ ] Ensure that faucet flow rate is as desired.
- [ ] Evacuate Test cell, ensure everyone is out.
- [ ]

Nitrogen pressurization checklist

- [ ] Ensure all personnel are out of test cell and close test cell door.
- [ ] Change Tab control in VI to "manual" and turn on run valves button
- [ ] Open and leave open the following valves in series, pause after each valve and look through window for venting gas
- [ ] -Nitrogen Fill/Purge Valve (Verify Venturi Pressure)
- [ ] -Top Pressure Valve
- [ ] -Tank Valve (Verify Tank Pressure)
- [ ] Wait for pressure to equalize
- [ ] Hit save data button to record pressures, wait 4 seconds and then turn off save data button
- [ ] Turn off "Run Valves" button
- [ ] Switch Tab Control to "safe"

RUN Checklist

- [ ] Ensure that reactor is up to the desired temperature
- [ ] Change VI data filename to test name and date
- [ ] Check decomp control vi settings
- [ ] Ensure TC Ignition is selected
- [ ] **Ensure Valve Start has been reset**
- [ ] Check valve timing in the main control vi
- [ ] Ensure all personnel are out of test cell and close test cell door.
- [ ] Ask for silence in control room
- [ ] Tell audience to not touch any switches on the control panel unless directed to do so by the test director
- [ ] Station someone near the 115 volt AC power switch and tell them to turn switch off if directed to do so by the test director
  Station someone to watch the motor exit; when fire begins the watcher should instruct the test controller to manually fire the motor.
- [ ] If igniter failure, turn off run valves button
- [ ] Ensure that "run valves" button is off
- [ ] turn on and then off "tare tank" button
- [ ] Enter desired fill level in lbm in "Desired Fill Level" control. Load about 1 lbm of nitrous per second of test fire
- [ ] Change supercharge pressure lower to a pressure 10 psi above the initial pressure of the nitrous oxide.
- [ ] change nitrous supercharge pressure upper to a pressure 30 psi lower than the regulator pressure
- [ ] Switch Tab Control to "Fill with Supercharge"
- [ ] Hit "Run Valves Button"
- [ ] Monitor tank weight, if tank weight goes beyond desired fill level, hit "run valves" button and return tab select to "safe" _____
- [ ] Stop and then restart VI
- [ ] Ensure that VI is working

- [ ] Switch Tab Control to "Manual"
- [ ] hit "Run Valves Button"
- [ ] open and leave open Tank Valve
- [ ] Open servo valve by turning on fiedpoint com A and B
- [ ] quickly pulse (about 1/2 s) the motor valve button
- [ ] turn off run valves button
- [ ] Ensure that servo valve is in desired operating mode
- [ ] Switch Igniter Mode to "Decomp Igniter"
- [ ] Notify test controller that if motor does not ignite when motor valve opens or other issue is apparent to immediately turn off run valves button and proceed to depressurization checklist.
- [ ] If motor is on fire or explodes, operator should turn off "run valves button" and switch the main tab control to safe. 115V switch operator should turn off 115V power to test cell. Wait for fire to extinguish then proceed to depressurization checklist.
- [ ] Start Test Cell fans
- [ ] Start MoNSTeR Cam
- [ ] Ensure that run valves button is off
- [ ] Ensure that Exit TC on decomposition settings is reasonable, and below the trigger temperature
- [ ] Switch Tab Control to "Run"
- [ ] Perform 5 second countdown and then press "Run Valves" button, notify any visitors that test will start x seconds after countdown ends
- [ ] (firing)
- [ ] Stop MoNSTeRCam
- [ ] Verify that run valves button is off
- [ ] Verify that tab control is set to "Safe"
- [ ] Verify that "Save Data" button is off
- [ ] Start 5 minute timer for test cell to clear.

Depressurize

- [ ] Switch tab control to "manual"
- [ ] turn on "run valves" button
- [ ] Open and leave open the following valves in series
- [ ] -Vent Valve
- [ ] -Tank Valve
- [ ] -Motor bypass Valve
- [ ] Wait for tank to depressurize
- [ ] Hit "run valves" button
- [ ] Switch tab control to "safe"
- [ ] Ensure that all personnel are wearing safety glasses
- [ ] Enter Test Cell
- [ ] Ensure that manual high voltage switch is in the off position
- [ ] Close N2O, N2 and CO2 cylinder(s)
- [ ] Ensure all personnel are out of test cell and close test cell door.
- [ ] Switch Tab Control to manual, press "run valves" button
- [ ] Open and leave open all valves, starting with motor bypass
- [ ] Switch Tab Control to "safe"
- [ ] Ensure that personnel in test area are wearing eye protection.
- [ ] Enter Test Cell
- [ ] Close liquid bypass Manual Valve
- [ ] Close Nitrous Manual Valve
- [ ] Close Nitrogen Manual Valve
- [ ] Switch servo power and isolator switches to off
- [ ] Ensure nitrogen manifold is fully vented by opening manual valve on nitrogen manifold
- [ ] Close manual valve on nitrogen manifold
- [ ] Disconnect quick connect nitrogen line

- [ ] Replace balloons on both ends of nitrogen quick connect
- [ ] Close 20lbm CO_2 tank
- [ ] Vent 20 lbm CO_2 tank via manual valve on pneumatic valve manifold
- [ ] Disconnect N_2 TC
- [ ] Disconnect USB cables and store box on MoNSTeR Cart
- [ ] Disconnect ethernet cable from MoNSTeR Cart and secure all cables
- [ ] Disconnect power cord from cart
- [ ] Turn off the UPS

Post Test

- [ ] Update MoNSTeR Test Summary with all post test values
- [ ] Add test video to MoNSTeR Cart Data svn folder.
- [ ] take photographs of inside and outside of fuel grain, nozzle exit and inlet
- [ ] add photographs to test pictures folder in MoNSTeR cart data folder, in folder created for pre-test pictures
- [ ] add new data, images, and video to SVN and commit
- [ ] Add this checklist to the checklist drawer.

Emergency Procedures

- [ ] switch tab control to "safe"
- [ ] turn "run valves" button to off
- [ ] ensure that all personnel are out of test cell and close test cell door
- [ ] Turn off 110V power to test cell
- [ ] follow de-pressurization checklist